SCHOOL OF ENGINEERING

Energy Storage and Electric Vehicles as a means of Mitigating Uncertainty in Urban Microgrids

A THESIS PRESENTED FOR THE DEGREE OF

DOCTOR OF PHILOSOPHY

Andrew Martin Jenkins

February 2019

Abstract

The United Kingdom (UK) government intends to end the sale of new conventional petrol and diesel cars by 2040, and Electric Vehicles (EVs) could emerge as the replacement. This is likely to increase the load on electrical distribution networks, while uncontrolled EV charging could increase load forecast uncertainty. Utilising sufficient Energy Storage System (ESS) power to maintain the networks within their power flow and voltage limits without needing to reinforce the network, while not over using the storage despite the uncertainty, remains a challenge. Similarly, the EVs themselves have been suggested as a flexible load however realising this flexibility also remains a challenge. This Thesis researches the ability of ESSs and EVs to mitigate load and generation uncertainty within urban microgrids.

Initially, the technical and economic impacts of uncontrolled EV charging on distribution networks is investigated by combining an extensive real world dataset of EV charging events and domestic household load. It is found that distribution transformer power flow limits will be the first operational limit to be breached when EV penetration reaches 40%. The resulting reinforcement cost that Ofgem would allow Distribution Network Operators (DNOs) to recover from consumers is estimated at £60.81bn - £74.27bn up to 2040.

A methodology is then proposed to forecast future uncontrolled EV charging load based on the ‘here and now’ load experienced on the network. In addition, a methodology is proposed to aggregate a number of smart charging EVs to form a Virtual Energy Storage System (VESS) able to deliver services to the distribution network with a high degree of controllability (~99%), while also guaranteeing the energy required by the EVs for their primary purpose of transportation. The VESS is combined with other forms of flexibility to deliver an Enhanced Frequency Response (EFR) service where a fuzzy logic control methodology is proposed to maximise power availability.

Finally, a Robust Optimisation (RO) formulation is developed that balances the trade-off between the cost of protecting network operational limits from load and generation uncertainty, against the cost of failing to protect network operational limits. RO requires a linear representation of the power system, and the errors introduced through linearization via sensitivity factors are calculated as up to 1.6% when there is no load and generation uncertainty, and up to 4.0% when there is load and generation uncertainty.

Acknowledgement

I wish to thank my academic supervisors; Prof Phil Taylor, Prof Phil Blythe, Dr Haris Patsios and Dr Neal Wade. The research presented in this Thesis would not have been possible without their support, expertise, advice, harsh honesty, challenging debate and unwavering faith in what could be possible.

I would like to thank the Engineering and Physical Sciences Research Council (EPSRC) Siemens for the financial support that made the research possible.

I wish to thank my colleagues for their encouragement, support, interesting discussions and sharing their expertise. In particular from industry I wish to thank Dr Vincent Thornley, Ola Olabisi, Ian Lloyd, Dr Pádraig Lyons, Dale Geach and Steve Ingram, and in particular from academia I wish to thank Dr Jialiang Yi, Dr David Greenwood, Dr Pete Davison, Dr Chris Mullen, Dr Jonathan Powell, Dr Sara Walker, Myriam Neaimeh, Nikolas Spiliopoulos, Ilias Sarantakos, Luke Burl and Laura Brown.

I would like to thank my PhD examiners; Dr Liana Cipcigan, Prof Elisabetta Cherchi and Dr Paul Ezhichelvan, who provided a stimulating academic discussion during the oral examination. Their suggested amendments have resulted in a much improved final version of the Thesis.

The School of Engineering IT Team; Ian Pitcher, Dr Ian Clark, Carol Booth and Norbert Wojciak, are thanked for their innovative thinking and the huge efforts made beyond the call of duty to make possible the computing power required during the course of the research. At one point, a total of 57 computers were assigned to the research from across the Newcastle University campus accessible via remote login from a single machine.

Most importantly, I wish to thank my family for their continuous and unwavering love, support and encouragement regardless of what challenges are put before me, or what course of action I initially take.

List of publications

Journal papers

- **A. M. Jenkins**, C. Patsios, P. Taylor, O. Olabisi, N. Wade, P. Blythe, (2017), "Creating virtual energy storage systems from aggregated smart charging electric vehicles", CIRED – Open Access Proceedings Journal, Volume 2017, Issue 1, p. 1664-1668. DOI: https://dx.doi.org/10.1049/oap-cired.2017.0937
- M. Neaimeh, R. Wardle, **A. M. Jenkins**, J. Yi, G. Hill, P. Lyons, Y. Hübner, P. Blythe, P. Taylor, (2015). "A probabilistic approach to combining smart meter and electric vehicle charging data to investigate distribution network impacts", Applied Energy 157(0): 688-698. DOI: https://dx.doi.org/10.1016/j.apenergy.2015.01.144

Conference papers

- **A. M. Jenkins**, C. Patsios, P. Taylor, A. Khayrullina, V. Chirkin, "Optimising virtual power plant response to grid service requests at Newcastle Science Central by coordinating multiple flexible assets", CIRED workshop 2016, Helsinki. DOI: https://dx.doi.org/10.1049/cp.2016.0812
- **A. M. Jenkins**, J. Duncan and C. A. Lynch, "Impact of steam turbine valve closure on a synchronous machine and its reverse power protection," *12th IET International Conference on Developments in Power System Protection (DPSP 2014)*, Copenhagen, 2014, pp. 1-6. DOI: https://dx.doi.org/10.1049/cp.2014.0075
- **A. M. Jenkins**, M. Scutariu and K. S. Smith, "Offshore wind farm inter-array cable layout," 2013 IEEE Powertech Conference, Grenoble, 2013, pp. 1-6. DOI: https://dx.doi.org/10.1109/PTC.2013.6652477

Acronyms

Acronym	Definition
A	Amperes
AC	Alternating current
ADMD	After Diversity Maximum Demand
BAU	Business As Usual
bn	Billion
BoU	Budget of Uncertainty
CESI	The national Centre for Energy Systems Integration
CHP	Combined Heat and Power
CIRED	International Conference and Exhibition on Electricity Distribution
CLNR	Customer Led Network Revolution
CO_2	Carbon Dioxide
CYC	Charge Your Car
DC	Direct Current
°C	Degrees Celsius
DNO	Distribution Network Operator
DSO	Distribution System Operator
DSR	Demand Side Response
DUoS	Distribution Use of System
EFR	Enhanced Frequency Response
EHV	Extra High Voltage ($\geq$ 33 kV)

EMS	Energy Management System
ENA	Energy Networks Association
EOBoU	Economically Optimal Budget of Uncertainty
EOPoS	Economically Optimal Probability of Success
EPSRC	Engineering and Physical Sciences Research Council
ESCos	Energy Service Companies
ESS	Energy Storage System
EV	Electric Vehicle
FFR	Firm Frequency Response
G2V	Grid-to-Vehicle
GB	Great Britain
GB	Giga Bytes
GW	Giga Watts
HV	High Voltage (0.4 kV > HV > 33 kV)
HVAC	Heating, Ventilation, and Air Conditioning
IC	Internal Combustion
IEEE	Institute of Electrical and Electronic Engineers
IET	Institute of Engineering and Technology
k	thousand
km	kilo-metres
kV	kilo Volts
kVA	kilo Volt Amperes
kW	kilo Watt

kWh	kilo Watt hours
LCT	Low Carbon Technologies
LP	Linear Programming
LV	Low Voltage (0.4 kV)
m	million
MCS	Monte Carlo Simulation
MEAV	Modern Equivalent Asset Value
MILP	Mixed Integer Linear Programming
mm	millimetres
MVA	Mega Volt Amperes
NP-hard	Non-deterministic Polynomial time hard
OLTC	On-Load Tap Changers
ONS	Office for National Statistics
ONSPD	Office for National Statistics Postcode Directory
OPF	Optimal Power Flow
PDF	Probability Distribution Function
PoS	Probability of Success
PV	photovoltaic
RAM	Random Access Memory
RO	Robust Optimisation
RTTR	Real Time Thermal Ratings
s	seconds
SoC	State of Charge

STOR	Short Term Operating Reserve
TSO	Transmission System Operator
TV	Television
UCC	Utility Controlled Charging
UI	Uncertainty Interval
UK	United Kingdom
UMIST	University of Manchester Institute of Science and Technology
USB	Urban Sciences Building
V2G	Vehicle-to-Grid
V2V	Vehicle-to-Vehicle
VESS	Virtual Energy Storage System
VoLL	Value of Lost Load
VPP	Virtual Power Plant
VSoC	Virtual State of Charge
Ω	Ohms

Nomenclature

Symbol	Definition	Unit
$V_{unbalance}$	Voltage unbalance	%
$C_{reinforcement}$	Allowable network reinforcement cost to the consumer	£m
G	Growth in maximum demand	MVA
H	Historic cost of the network based upon the MEAV	£m/MVA
α	Allowable ratio of capacity to be upgraded relative to the growth in maximum demand	-
β	Allowable ratio of expected upgrade costs relative to the historical network cost	-
$\Delta L_{t,j}$	Difference in uncontrolled EV charging load between settlement period t and settlement period t+j.	kW
L_t	Uncontrolled EV charging load at settlement period t	kW
L_{t+j}	Uncontrolled EV charging load at j settlement periods ahead of settlement period t	kW
j	Number of settlement periods looking ahead	Settlement periods
t	'Here and now' settlement period of the day	Settlement periods
$P_{t,j}^{forecast}$	Expected uncontrolled EV charging aggregated load range at t, looking forward by j	kW
$D_{t,t+j}$	Difference between the longer term diurnal expected uncontrolled charging load at settlement period t and settlement period t+j	kW
n_j	Short term forecast UI of aggregated uncontrolled EV charging load as a proportion of the diurnal UI for a forecast horizon of j settlement periods	%

$W_{t+j}^{diurnal}$	Three times the standard deviation of the longer term expected diurnal aggregated uncontrolled EV charging load at settlement period t+j	kW
$\boldsymbol{c}$	The vector of coefficients for the cost function	-
$\boldsymbol{c}'$	The inverse of $\boldsymbol{c}$	-
$\boldsymbol{x}$	The array of decision variables or control variables	-
$\boldsymbol{A}$	The matrix of constants for constraints	-
$\boldsymbol{b}$	The right hand side vector of constraints	-
$\boldsymbol{D}$	The matrix of coefficients for equality constraints	-
$\boldsymbol{e}$	The right hand side vector of equality constraints	-
$\boldsymbol{l}$	The lower limit of decision variables	-
$\boldsymbol{u}$	The upper limit of decision variables	-
$\boldsymbol{w}$	The maximum of the cost function	-
d	Control variable with fixed value of 1.0	-
$\boldsymbol{A}'$	Revised $\boldsymbol{A}$ matrix when it also includes the $\boldsymbol{b}$, $\boldsymbol{D}$, $\boldsymbol{e}$, $\boldsymbol{l}$ and $\boldsymbol{u}$ vectors and matrices	-
$\widetilde{\boldsymbol{A}}$	The $\boldsymbol{A}$ matrix when its elements are subject to uncertainty	-
a_{ij}	The nominal value of one element within the matrix $\boldsymbol{A}$	-
$\tilde{a}_{ij}$	The real value of a_{ij}	-
$\hat{a}_{ij}$	The maximum variation of a_{ij}	-
z	Robust optimisation control variable	-
p	Robust optimisation control variable	-
y	Robust optimisation control variable	-

Γ	Budget of uncertainty (Number of uncertain coefficients that the constraints are protected against)	-
φ_{db}	Power flow sensitivity factor between decision variable, d, and branch (cable or transformer), b	kVA/kW
S_b	Apparent power through the branch (cable or transformer), b	kVA
P_d	Real power of the decision variable, d	kW
b	Branch (cable or transformer) identifier	-
d	Decision variable identifier	-
$\boldsymbol{R}$	Array of calibration values	kVA
$\boldsymbol{S}$	Array of apparent power flow through each branch (cable or transformer)	kVA
$\boldsymbol{\varphi'}$	Inverse of the matrix of power flow sensitivity factors	kVA/kW
γ	Constraint derating value	per unit
$\hat{\varphi}_{db}$	Maximum variation of $\varphi_{db}$to model the maximum uncertain variation of $\hat{x}_d$within the constraints matrix	kVA/kW
$\hat{x}_d$	Maximum variation of x_d	kW
c_d	Network operating cost associated with the controllable decision variable, d	£/kW
D_d	Degradation cost associated with using the storage	£/kW
K_t	Cost associated with replacing transformer, t	£
K_f	Cost associated with replacing cable, f	£
K_e	Value of energy	£/kWh
T	Number of transformers in the network	Transformers

F	Number of cables in the network	Cables
ϑ_{dt}	Loss of life sensitivity factor between transformer, t, and controllable decision variable, d.	% life/kW
θ_{df}	Loss of life sensitivity factor between cable, f, and controllable decision variable, d.	% life/kW
ϵ_{dt}	Electrical losses sensitivity factor between transformer, t, and controllable decision variable, d.	kWh/kW
ϵ_{df}	Electrical losses sensitivity factor between cable, f, and controllable decision variable, d.	kWh/kW
L_f	Life expectancy of cable, f	years
p_f	Loading of cable, f	per unit
ζ_0	Coefficient constant, -32.854	-
ζ_1	Coefficient constant, 2.2737×10^{-13}	-
ζ_2	Coefficient constant, 50.028	-
τ	Time duration the constraint violation is experienced	hours

Table of contents

Table of figures

List of tables

Chapter 1 Introduction

1.1 Background

There is a global desire to reduce greenhouse gas emissions from human activity to lower the risks and impacts of climate change. The Paris Agreement sets out the responsibilities of each nation state in order for global average temperatures to remain below 2°C above pre-industrial levels [1]. Greenhouse gas emissions from within the United Kingdom (UK) are dominated (81%) by carbon dioxide (CO_2) [2] and the country has a target of reducing carbon emissions to 80% of 1990 levels by 2050 [3]. In 2015, 24% of UK CO_2 emissions came from transportation [2] however the UK government intends to end the sale of new conventional petrol and diesel cars by 2040 [4]. Electric Vehicles (EVs), which typically have emissions approximately 50% of an Internal Combustion (IC) vehicle when considering all energy conversion processes from oil-well to wheel [5], may replace IC and shift the transportation emissions onto the power system which itself represented 29% of all UK emissions in 2015 [2]. In preparation for this shift the UK government has passed the Automated and Electric Vehicles Act 2018, giving the Department for Transport powers to create regulations surrounding the compatibility, availability and technical requirements of EV charging [6].

To achieve the UK's carbon reduction targets, the carbon intensity of electricity needs to be below 50 gCO_2/kWh by 2030 [7]. Achieving a low carbon solution is not the only consideration however. Energy must also be delivered economically with a high security of supply, leading to the idea of the energy trilemma [8]. Achieving any two elements of the trilemma is not difficult, however ignoring any one element of the trilemma is unsustainable [8].

Inspection of the range of carbon intensity and associated levelised cost of energy for a number of generating technologies [9] suggests that a significant proportion of the future low carbon generation mix is to come from technologies that are intermittent by nature and connected to the distribution network. Traditionally, generation has been centralised and connected at higher voltages. One technology likely to be connected to urban distribution networks, where 81.5% of the English and Welsh population resides according to the UK 2011 census [10], is solar Photovoltaic (PV) which has experienced significant growth in recent years [11].

1.2 Future distribution network challenges and solutions

The challenges for future distribution networks to achieve the required power system decarbonisation are introduced in Section 1.2.1. The technologies that are seen as potential solutions to these challenges are introduced in Section 1.2.2.

1.2.1 Challenges for future distribution networks

The challenges associated with voltage control, power flow management, and the uncertainty surrounding load and generation forecasts within future distribution networks are introduced in Section 1.2.1.1, Section 1.2.1.2 and Section 1.2.1.3 respectively.

1.2.1.1 Voltage control

In the UK, the voltage in all locations within the network must remain within +10% and -6% of nominal for Low Voltage (LV) networks, and ±6% for voltages between 1 kV and 132 kV [12]. The voltage varies within the network dependent upon the load, or generation, and the network impedance. It has been estimated that when around 30% of houses in urban networks have a 2 kW solar array installed, the distribution network will experience unacceptable voltage rise and require network reinforcement [13]. The traditional approach to maintaining voltages within the limits is through network reinforcement to change the impedance, or to utilise locally controlled On-Load Tap Changers (OLTC) at primary substations. The reinforcement approach requires a high capital expenditure, while the OLTC approach applies the voltage to all feeders supplied by the primary substation. It is possible in future scenarios that one feeder might be heavily loaded with a cluster of EVs resulting in an under voltage, while another feeder is supplied by a cluster of solar PV resulting in an over voltage, thus the OLTC is unable to solve both voltage limit excursions concurrently. A smart solution to this scenario is utilising an Energy Storage System (ESS) [14], which also has significant cost associated with it.

1.2.1.2 Power flow management

Components in the power system, such as transformers and cables, all have a thermal rating. If the current passing through the component exceeds the rating, there is risk of overheating and reducing the life of the component [15]. It has been estimated that when EV deployment reaches 15%, rural distribution networks will experience thermal overloads and need reinforcing. Urban networks will need reinforcing when EV deployment reaches 60% [16]. The traditional approach to alleviate power flow overload is to reinforce the network, requiring significant capital expenditure. A smart solution utilising an ESS could also be

implemented such as limiting the power flow through a network component to its Real Time Thermal Rating (RTTR) [17], with an associated cost.

1.2.1.3 Load and generation forecast uncertainty

There is significant uncertainty in the load of individual houses on a domestic level that becomes increasingly predictable with increasing numbers of properties considered together due to their diversity [18]. Traditionally, the distribution network has been designed to the worst case extremes of operation, and thermal generation plants follow the load at transmission level with good forecasts available. In comparison, distributed renewable generation can be connected at distribution level with its output uncertain with the uncertainty of weather forecasts [19, 20]. Similarly, there is significant uncertainty over the arrival and departure times [21] and the initial State of Charge (SoC) [16] of individual EVs and their resulting load on the distribution network. This load is dependent on the rating of the EV charge point, summarised in Table 1-1, which is significant when compared to the existing UK domestic After Diversity Maximum Demand (ADMD) of 1.57 kW (for 100 customers) [18].

Table 1-1 Electric vehicle charge points [22]

Charger	Power rating
Standard	Up to 3 kW
Fast	7-22 kW
Rapid AC	43 kW
Rapid DC	Up to 50 kW

Any smart solution responding to the needs of the network must appropriately take into account the load and generation uncertainty to ensure the robustness of the network with respect to its operational limits.

1.2.2 Potential solutions to future distribution network challenges

A number of technologies have been suggested as potential solutions to future distribution network challenges. These include microgrids and Virtual Power Plants (VPPs) introduced in Section 1.2.2.1, ESS introduced in Section 1.2.2.2, smart charging EVs introduced in Section 1.2.2.3 and Demand Side Response (DSR) introduced in Section 1.2.2.4. This Thesis builds on these technologies to provide economically effective voltage control and power flow

management through utilising ESS and smart charging EVs when the distribution network is operated as a microgrid and subjected to load and generation uncertainty.

1.2.2.1 Microgrids & Virtual Power Plants

A microgrid consists of a combination of electrical or heat generation and load controlled in a single system [23]. To enable some flexibility in operational control to ensure the network remains within its operational limits despite the generation and load uncertainty, a form of ESS is often included in a modern microgrid [24].

A VPP is similar to a microgrid, however there are some key differences [25]:

- Microgrids can be grid-connected, or islanded, or able to disconnect and reconnect as required. VPPs however are always grid tied.
- Microgrids normally include some kind of storage. In VPPs, storage is possible but not always required.
- Microgrids encompass resources within a limited geographical area. VPPs can coordinate multiple resources over larger geographical areas.

1.2.2.2 Energy storage

An ESS can act as both a load and a generator in a controllable manner. It is a time limited resource dependent upon its SoC and thus must be controlled carefully to ensure it is available when required by the distribution network.

There are two main components to an ESS; an energy storage medium and a power interface between the storage and the grid.

There are numerous storage technologies, including vanadium redox flow batteries, super-capacitors, lead acid batteries, sodium-ion batteries, sodium-sulphur batteries, pumped hydro storage, lithium-ion, compressed air storage, thermal storage, nickel based, flywheels, and hybrid systems. Each technology has different characteristics such as cost, power and energy density, round-trip efficiency, self-discharge rate, response time and lifetime making them suitable, or unsuitable, for a particular application. In a distribution network, an ESS can support location critical services such as power-flow management and voltage control [14, 17].

1.2.2.3 Vehicle-to-grid and Smart Charging of Electric Vehicles

EVs are typically parked around 96% of the time and could provide a valuable secondary function as a responsive charging load [26]. Further support to the grid can also be provided by exporting power from the battery of the vehicles to the grid [27]. Similarly to ESS, this is a

time limited resource requiring careful control, and sufficient energy also needs to be in the vehicle for its primary purpose of travel at the time of departure.

1.2.2.4 Demand side response

Customers can be encouraged to change their load pattern and reduce demand when needed by the distribution network. Such requests are Demand Side Response (DSR) calls, and one trial showed that nine out of 13 calls were successfully delivered by the customer [28]. Industrial and commercial loads with DSR potential include Heating, Ventilation, and Air Conditioning (HVAC), hot water, refrigeration, lighting, and water pumping. Domestic loads with DSR potential include electric resistive storage heating, heat pumps, wet appliances, and cold appliances [29].

1.3 Research objectives

Urban microgrids with high penetrations of EVs and subjected to load and generation uncertainty is researched. The main objectives of the Thesis are:

- To quantify the likely technical and economic impacts of wide scale uncontrolled EV charging within distribution networks.
- To develop a methodology to forecast aggregated uncontrolled EV charging load on distribution networks and the uncertainty surrounding the forecast.
- To investigate the available flexibility to control EV charging load.
- To develop methods to balance the risk of failing to protect microgrids operating under load and generation uncertainty from exceeding power flow and voltage limits, against the cost of over protection through over use of ESS and the flexibility of smart charging EVs.

1.4 Contributions to knowledge, publications and awards

The main contributions to knowledge are summarised as follows:

- A comprehensive study is undertaken to quantify the percentage uptake of EVs that is likely to cause distribution networks to exceed transformer power flow, under voltage and voltage unbalance limits. This is the first such study to utilise real EV charging load data rather than statistical distributions or assume that EVs would be utilised in a similar way to existing IC vehicles.
- A study, taking into account the networks of all Distribution Network Operators (DNOs), is undertaken to estimate the expected network reinforcement cost that DNOs could expect to recover from consumers under a high EV uptake scenario.

- A methodology is developed to forecast future uncontrolled EV charging load and the uncertainty surrounding that forecast, based on the 'here and now' uncontrolled EV charging load experienced on the network.
- A methodology is developed for smart charging EVs to appear to the grid in aggregate like traditional ESS with a high degree of controllability while ensuring the energy needed on departure for transportation, thus allowing EVs to be integrated into storage scheduling and control algorithms.
- A methodology using fuzzy logic is developed to combine any number of flexible loads and through effective energy management coordination to maximise total power availability to deliver an Enhanced Frequency Response (EFR) service to the macrogrid.
- Using a Robust Optimisation (RO) technique and the Budget of Uncertainty (BoU) to control the conservatism of ESS power set-points against load and generation uncertainty, a methodology is developed to balance the risk of failing to protect microgrids from exceeding power flow and voltage limits, against the cost of over protection.

A number of journal and international conference papers have been published as a result of the work in this Thesis, and are listed below:

- **A. M. Jenkins**, C. Patsios, P. Taylor, O. Olabisi, N. Wade, P. Blythe, (2017), "Creating virtual energy storage systems from aggregated smart charging electric vehicles", CIRED – Open Access Proceedings Journal, Volume 2017, Issue 1, p. 1664-1668. DOI: https://dx.doi.org/10.1049/oap-cired.2017.0937
- **A. M. Jenkins**, C. Patsios, P. Taylor, A. Khayrullina, V. Chirkin, "Optimising virtual power plant response to grid service requests at Newcastle Science Central by coordinating multiple flexible assets", CIRED workshop 2016, Helsinki. DOI: https://dx.doi.org/10.1049/cp.2016.0812
- M. Neaimeh, R. Wardle, **A. M. Jenkins**, J. Yi, G. Hill, P. Lyons, Y. Hübner, P. Blythe, P. Taylor, (2015). "A probabilistic approach to combining smart meter and electric vehicle charging data to investigate distribution network impacts", Applied Energy 157(0): 688-698. DOI: https://dx.doi.org/10.1016/j.apenergy.2015.01.144

A number of oral presentations have been made about the work presented in this Thesis, some of which are available to watch online, as listed below:

- **A.M. Jenkins**, D. Greenwood, "Preparing the GB distribution system for the mass uptake of electric vehicles", Institution of Mechanical Engineers, 11 October 2017
- P. Agese, R. Fowler, V. Oldenbroek, **A. M. Jenkins**, I. Muller, "NEETS: What is Vehicle-to-Grid (V2G) and why should we care?", NEETS live webinar 26 July 2017. Available to watch on YouTube online: https://www.youtube.com/watch?v=t3mvOkHb2Ns&t=3374s
- **A. M. Jenkins**, "Creating virtual energy storage systems from aggregated smart charging electric vehicles", CIRED conference 13 June 2017, Glasgow. Available to watch on IET TV online: https://tv.theiet.org/?videoid=10399

A number of academic awards have been made during the study period, as listed below:

- **First place** for 'Best Presentation' in the Electrical Power research group at the Newcastle University School of Electrical and Electronic Engineering Annual Research Conference 2017.
- **First place** for 'Best Paper' in the Electrical Power research group at the Newcastle University School of Electrical and Electronic Engineering Annual Research Conference 2016.

1.5 Thesis outline

The Thesis outline is summarised in Figure 1-1, and structured as follows:

Chapter 1 – This chapter.

Chapter 2 – Literature review to identify the specific areas where a contribution to knowledge can be achieved and inform the research direction.

Chapter 3 – An investigation into uncontrolled EV charging. First the technical impacts are investigated, followed by estimating the economic cost to upgrade the domestic distribution networks if uncontrolled charging becomes the norm. Finally, an uncontrolled EV charging load forecasting methodology is developed.

Chapter 4 – A methodology is developed for smart charging EVs to appear to the grid in aggregate like more traditional ESSs, allowing EVs to be integrated into storage scheduling and control algorithms. The methodology is then used within a microgrid alongside other forms of flexibility and storage to deliver an Enhanced Frequency Response (EFR) service. A

fuzzy control algorithm is developed to maximise power availability through intelligent energy management.

Chapter 5 – A Robust Optimisation (RO) formulation is developed and used to balance the trade-off between the cost of protecting network operational limits from load and generation uncertainty, and the cost of failing to protect network operational limits. The algorithm requires a linear approximation to the non-linear power system equations, and the errors associated with linearization are quantified under both certain and uncertain load and generation scenarios.

Chapter 6 – A discussion of the ideas and results presented in this Thesis.

Chapter 7 – Conclusions and potential future research.

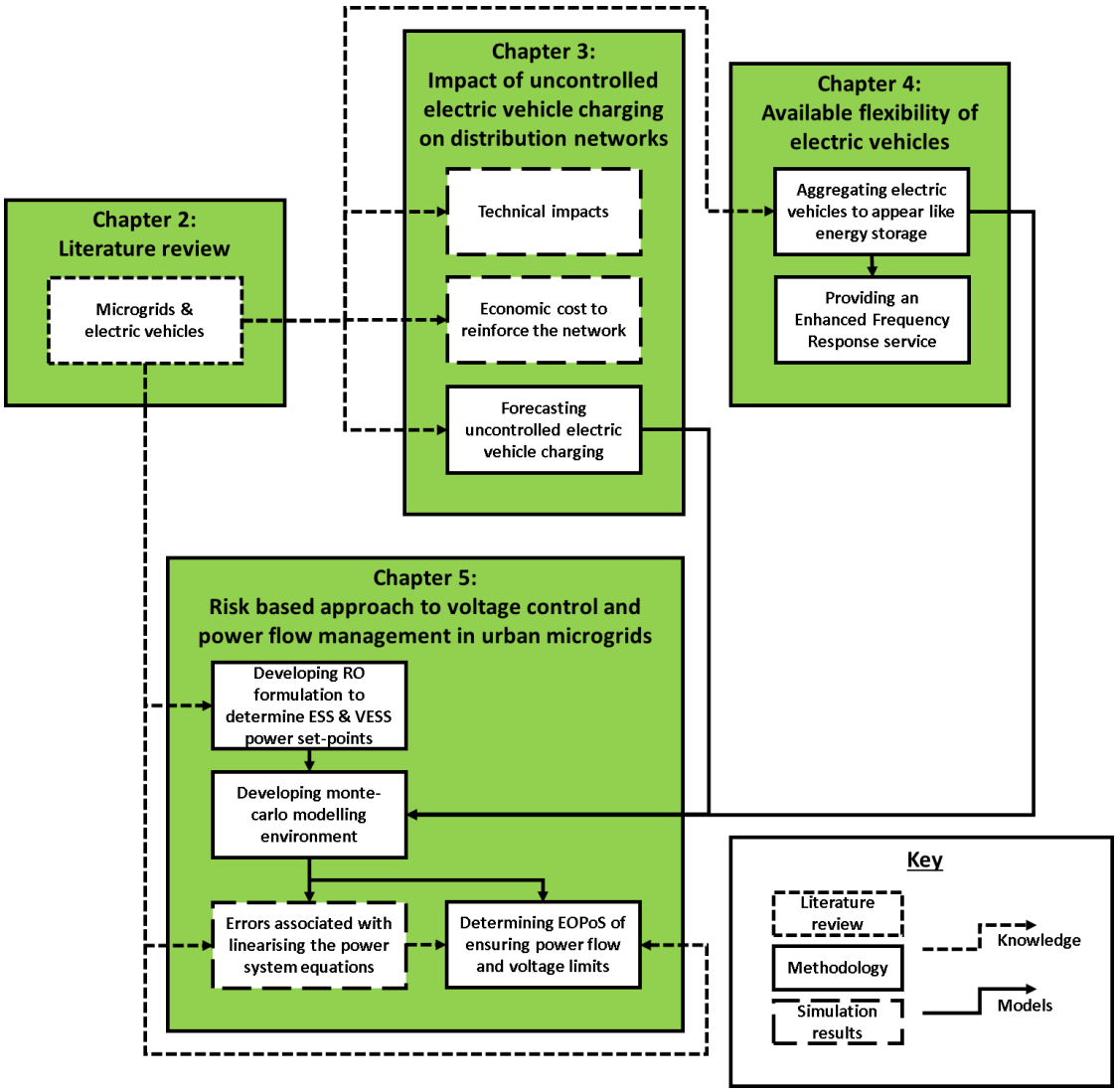

Figure 1-1 Thesis overview

Chapter 2 Literature review

2.1 Introduction

This Chapter presents a review of relevant literature to identify the specific areas where a contribution to knowledge can be achieved and informs the research direction for later Chapters. Chapter 3 presents research regarding the impact of uncontrolled EV charging on distribution networks, Chapter 4 presents a methodology to aggregate smart charging EVs into a Virtual Energy Storage System (VESS), and Chapter 5 presents a risk based approach to voltage control and power flow management in urban microgrids. The literature associated with microgrids is presented in Section 2.2 and the literature associated with EVs is presented in Section 2.3. The flow of models and knowledge between Chapters is summarised in Figure 2-1.

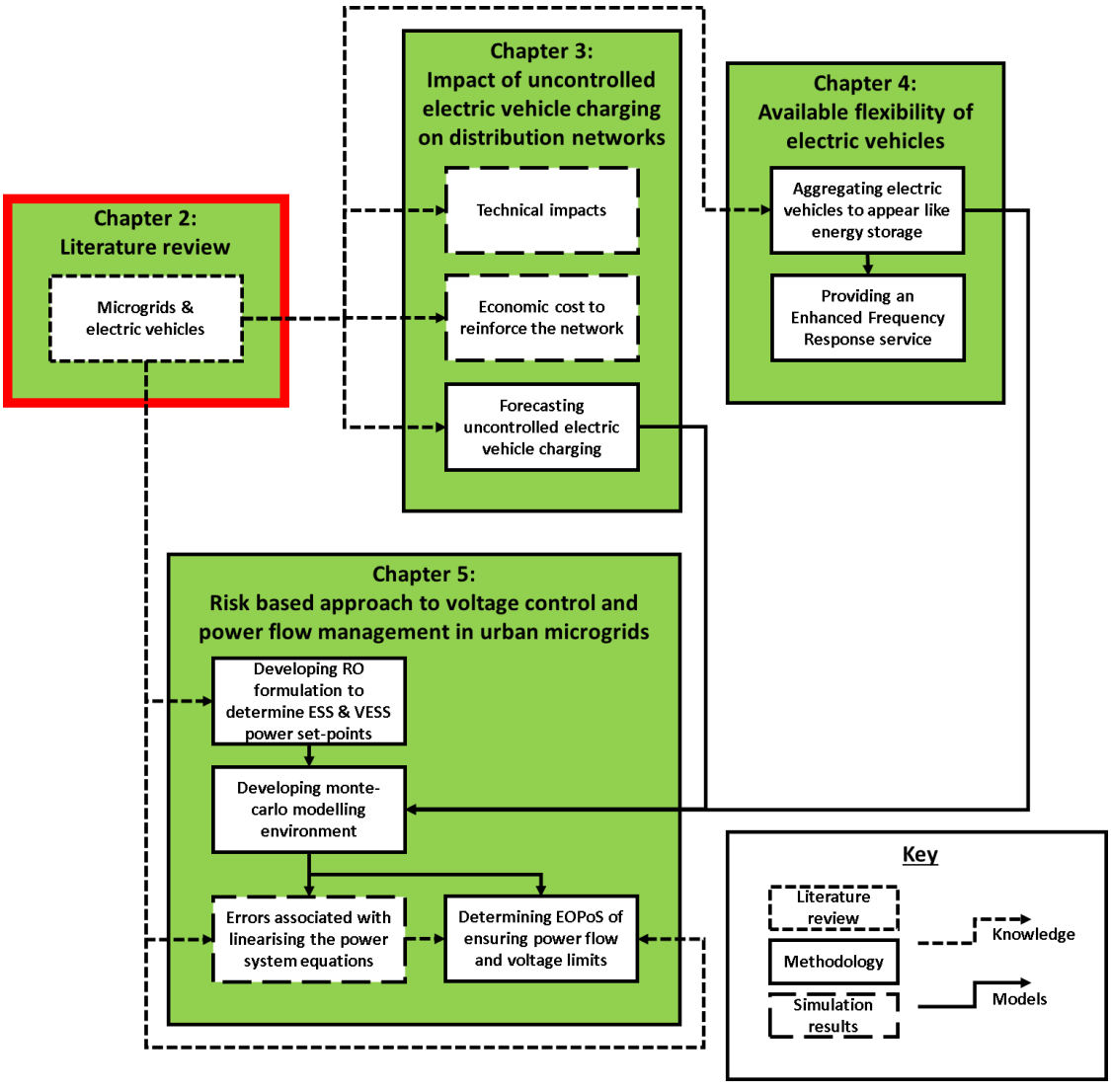

Figure 2-1 How Chapter 2 fits into the wider Thesis

2.2 Microgrids

The commercial market framework of microgrids is reviewed in Section 2.2.1 in order to give context for technological reviews. Section 2.2.2 reviews the different types of microgrid control that could be researched and how they interact with one another, before focusing on determining ESS power exchange with the network under load and generation uncertainty in Section 2.2.3.

2.2.1 Microgrid market framework

A review of microgrid demonstrators is included in [30]. All examples were either built by academic institutions demonstrating the technology, or developed when specific Low Carbon Technology (LCT) integration issues were encountered that could be solved through the deployment of a microgrid. In the UK, the majority of microgrids to date are owned and operated independent from a Distribution Network Operator (DNO) and there is a risk that the wide scale deployment of such microgrid systems could result in the duplication of the existing networks [31]. The existing network is a natural monopoly because it exhibits such strong economies of scale making it uneconomical to have active competition between numerous smaller networks [32]. Historically the winners of competing technologies are not necessarily the technologically superior, but the ones that are the more responsive to market conditions and requirements [33]. Therefore for the largescale deployment in the UK, microgrids must be retrofitted into existing networks by introducing microgrid control systems that operate within the existing market frameworks.

The UK electricity market is separated into four licensed areas; Generators, Transmission System Operator (TSO), DNOs, and Suppliers [34]. The suppliers sell energy on behalf of generators to customers. Use of system charges are paid by suppliers on behalf of customers, and by generators, for the use of networks. Suppliers and DNOs are not allowed to be the same entity [34], making it difficult for DNOs to utilise flexible loads and generators to facilitate the development of microgrids without procuring services from or through other entities. Despite this, any and all actors could be the commercial benefactors of microgrids [35].

It has been suggested by [35] that to achieve load flexibility the industry needs to move from being supplier-centric to being consumer-centric, in a similar way to mainframe computers becoming laptops, and conventional telephones became smart phones. However, only large consumers can influence the market giving rise to the need of aggregators to combine the services delivered by many small individual consumers to gain sufficient scale within the

market [36]. Similarly, Energy Service Companies (ESCos) sell energy services such as a warm home or illumination [37] and could develop to deliver this service while flexing their demand as procured by a DNO. To enable the power and energy load (or generation) flexibility, there needs to be high technological and social change, and thus it is expected that new innovative business models will emerge and develop [38].

On the generation side there have been some moves toward constrained connection offers in order to negate the need for network reinforcement. For one DNO the reduced cost of connection offers (and reinforcement) through constrained connections was £38m, or £32m when including the cost of the control system and generation curtailment [39]. Across the industry, smart technologies have been estimated to reduce the future required investment in distribution networks by 2050 from £46bn to £23bn-£27bn [40]. It is suggested in [41] that a trusted intermediary between DNO and generator is required to help facilitate constrained connections due to the commercial sensitivities involved. Commercially, the generator will maximise energy delivery up until the point where the marginal cost of energy equals the price offered by the DNO to curtail output [42].

Based on the literature reviewed, the author envisages that microgrids will be implemented in existing networks by DNOs transitioning into Distributed System Operators (DSOs) and procure services from third parties (generators, aggregators, ESCos, ESS providers amongst others) for a contracted fee. The DSO would procure these services in the most economical way for themselves while ensuring power flows and voltages remain within limits such that reinforcement is not required. The loads and generators would see a commercial benefit through the difference between what the DSO pays for a particular service, and what it costs that entity to provide the service. This view is supported by the UK government energy system flexibility plan published in July 2017, which stated that Ofgem will "ensure that network operators cannot directly operate storage" because "if a network company owns or operates storage it could impede the development of a competitive market for storage and flexibility services" [43]. It is this market framework that is assumed throughout this Thesis. It must be noted however that there is uncertainty regarding what market framework will develop for DSOs to operate within.

2.2.2 Microgrid control hierarchy

There are three main control levels associated with the power export or import of flexible assets within microgrids; primary, secondary and tertiary control [44]:

- *Primary control* – This provides the fastest response and is implemented locally. It takes the power set-points provided by the Secondary control and ensures that each asset reaches its required operating state.
- *Secondary control* – This controls the microgrid assets to ensure reliable and economical operation by determining the optimal unit commitment and dispatch of the flexible loads and generators. It is often referred to as the Energy Management System (EMS).
- *Tertiary control* – This controls the upstream interactions with the microgrid in question, scheduling and coordinating the interaction of multiple microgrids.

Microgrid secondary control is chosen to be the subject of this Thesis because of the challenges associated with load and generation uncertainty, and the time limited nature of the power and energy flexibility solutions available within urban microgrids. These challenges and solutions were discussed further in Section 1.2.

Secondary control can be implemented as a centralised or decentralised system, or a combination of the two [44]. The centralised approach allows all relevant information to be utilised to develop an optimised solution, but can require re-configuring when alterations are made to the network. In contrast, the decentralised system is much more amenable to plug-and-play, but can have difficulty in operating microgrids that require high levels of coordination. The decentralised system typically consists of some central control guiding local controllers [44]. This Thesis focuses predominantly on centralised systems due to considering future scenarios of high penetrations of EVs and the potential need for high levels of coordination to remain within distribution network operational limits for power flow (within thermal limits of cables and transformers) and voltage (LV: between -6% and +10% of nominal, 1 kV to 132 kV: ±6% of nominal).

2.2.3 Determining power set-points of ESS under load and generation uncertainty

A review of microgrid and VPP scheduling literature is given in [25]. In general the objective of the formulations is to minimise cost, or maximise profit, subject to various constraints. Linear Programming (LP) (after problem linearization) is advocated due to its simplicity and speed of calculation. The review, amongst other conclusions, found that greater emphasis has to date been placed on deterministic formulations that are not subject to uncertainty, rather than stochastic formulations that take into account the variability of the real world.

Scheduling procured power services from flexible load and generation to prevent power flows and voltages from exceeding limits when using a DC representation to approximate the AC

network is considered a Mixed Integer Linear Programming (MILP) problem. This is classified as NP-hard, and consequently there can be computational challenges [45]. The state of the network is based on the forecasted status of constituent components such as renewable generators and EVs which are subject to uncertainty. One way of considering the load uncertainty during the optimisation is to undertake a Monte Carlo Simulation (MCS) based on Probability Distribution Functions (PDFs). In a MCS [46], the PDFs are sampled to develop a representative scenario of the uncertain problem which can then be evaluated. Through evaluating a sufficiently large number of representative scenarios, a probabilistic understanding can be obtained of the complex interactions between the uncertain load and generation and its non-linear impact on power flows and voltages within distribution networks. The greater the number of representative scenarios modelled, the more accurate the MCS becomes however so does the computational challenge. Even after introduction of scenario reduction techniques, the consideration of load uncertainty increases the computational challenge relative to not considering uncertainty [47]. It is noted in [48] that the computational challenge increases with the number of time steps considered during the optimisation. There is sometimes a trade-off between solution quality and computational time [45]. In [49] and [50] the compromise for including uncertainty in the formulation was achieved by not considering the power flows and voltages relative to their respective limits. A multi-objective formulation to minimise operational cost and maximise the minimum reserve under load uncertainty in a day ahead context was modelled in [51] to find the pareto front however 42 computer cores were required in order to execute the model within 30 minutes. The model consisted of a 180-bus distribution network with 90-load points over 24-time steps, and considered 116 diesel generation units, 7 ESSs and 1000 EVs. In [52], the authors undertook a traditional worst case analysis to define critical nodes that had the potential to exceed operational limits. Such analysis could be used to minimise the number of constraints needing to be modelled in a microgrid scheduling optimisation thus minimising the calculation time.

Within the problem constraints, the optimisation is based upon the objective function formulation, which itself may be subject to uncertainty. A sensitivity analysis was undertaken in [45] where it was found that the energy value had the greatest impact on results. It was found in [53] that when the objective function was changed from minimising losses to maximising EV charging energy, the electrical losses increased by 19.5%. These electrical losses also have an economic value subject to uncertainty. Undertaking a new schedule on

every time-step was found in [50] to return an operational cost 8.6% lower than scheduling just once per day due to more accurate forecasts at the time of implementation.

In practice it is very difficult to calculate PDFs for the various uncertainties making the stochastic optimisation techniques unrealistic, however it is often possible to determine an Uncertainty Interval (UI) in which it could be expected all values to fall within [54]. RO is a technique based upon LP that finds solutions protected against the uncertain values falling anywhere within the UI. A parameter called Budget of Uncertainty (BoU) is used to adjust the level of conservatism in protecting against the full UI bounds. In this Thesis, the term 'robust' refers to the ability of a control system to maintain the distribution network within its safe operational limits for power flow (within thermal limits of cables and transformers) and voltage (LV: between -6% and +10% of nominal, 1 kV to 132 kV: ±6% of nominal), despite load and generation uncertainty.

The BoU was compared against the traditional unit outage criterion of reliability in [55], calculating the cost of robustly operating the network with different numbers of network components simultaneously out of service. A relationship between limit violation and BoU, allowing the calculation of optimal BoU for specified probabilistic risk, was proposed by [54]. The cost of operating the network and the number of constraint violations with and without RO was presented in [56] leading to the quantification of the cost to protect the network against each violation. No study found however has balanced this cost against the value of supply to the consumer and thus the cost penalty applied to the DNO. An adjustable interval was proposed by [57] to protect against changing uncertainties, however this was based upon the running of traditional generators on low loading and minimising the reserve cost which is not such a problem for ESS and EVs that can respond very quickly. The RO method was utilised by [45] to estimate the number of EVs that could be integrated into a Canadian network at differing levels of probabilistic risk of violating network constraints.

With RO based upon LP, it is possible that the problem presented to the solver is infeasible. It was noted in [58] that as the BoU is set increasingly conservative, it is increasingly likely that the LP problem will become infeasible. It has been suggested when optimising demand response, that the most practical approach to rectify infeasibility in real time is to consider load shedding [56].

It is possible that there could be some cross-correlation of uncertainties. This was considered by [59] however the computational complexity resulted in only one time step being considered by the formulation.

It has been shown that by utilising a DC representation of the electrical constraints within the optimisation formulation, power flow and voltage constraints can be exceeded when implemented on the AC system [60]. Therefore the full AC system representation is required, but needs to be linearised in order to utilise the RO technique. This has been undertaken in the literature in two different ways. In [61] it was achieved by using a number of piecewise linear functions when a MILP solver is available. It allows a single optimisation to be undertaken, but with an increase in the number of constraints. In contrast, [62] uses a linear representation based upon the operating state of the network, allowing a LP solver to be used, and is recalculated following a generation power decision leading to an iterative process that continues until a stable generation power decision is achieved.

2.3 Electric vehicles

The primary purpose of EVs is transportation, and the needs of EV owners to achieve their primary objective is considered in Section 2.3.1. The literature is reviewed in Section 2.3.2 to consider the impact of uncontrolled EV charging on distribution networks. Section 2.3.3 then considers the various methods of controlling EVs to realise power flexibility that could be utilised by the energy system to generate value.

2.3.1 Electric vehicle requirements

In 2014, 96% of all UK car journeys were shorter than 25 miles [63], well within the range of many EVs [64-66]. Despite this, both actual and perceived range limitations are seen as a barrier to adoption of EVs [67-69].

Rapid charge points are seen as more important than standard charging when a vehicle travels more than 240 km per day, which accounts for less than 2% of journeys [67]. The potential for queues to form at rapid charge points was investigated by [70], whereby the queue must be kept to a minimum in order to maintain the advantage of rapid charge points over slower, potentially cheaper, home standard charging. Queueing theory was utilised to propose reduced cost of rapid charging in exchange for a reduced time at the charge point and associated delivered energy. Such a business model would encourage utilising rapid charging only for the amount of energy required to get to a destination, where a standard charge point would then be used. This means there is little scope for energy system flexibility with regards to rapid charging.

The majority of daily driving energy needs can be met by standard charging at locations such as at home or at work [67]. With EVs stationary around 96% of the time, there is potential that some control could be exercised by the grid in determining when the vehicles are

delivered the energy [26]. This flexibility can only be realised however, if EV owners are willing to plug their vehicles into smart charging posts. The willingness of consumers to utilise smart charging, or Utility Controlled Charging (UCC), overnight in Canada was investigated by [71]. A total of 53% were open to enrolling without any benefit (financial or increased renewable penetrations) provided 100% SoC was ensured by morning. As the guaranteed SoC by morning decreases, the acceptance of users also decreases as shown in the reproduced graph of Figure 2-2. The potential battery degradation was not considered by the survey and has an impact on Vehicle-to-Grid (V2G) viability, representing a cost [72-74]. The survey noted that if the cost of the energy reduced by 20% then adoption would increase by 18 percentage points [71]. It follows therefore that if the cost of degradation is greater than the reduction in cost of energy, then the adoption of smart charging would be expected to reduce relative to that shown in Figure 2-2. Despite this, there is clearly potential for significant numbers of prosumers to partake in flexible charging.

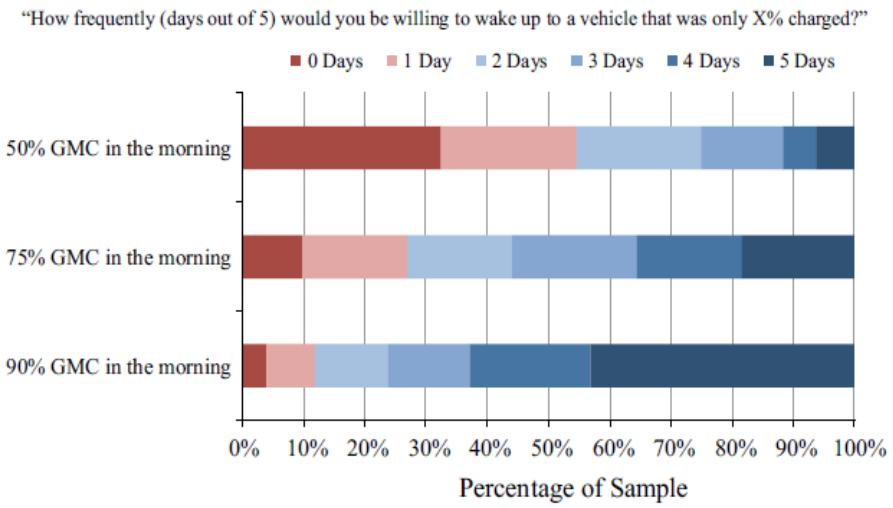

Figure 2-2 Respondent acceptance of guaranteed minimum charge assuming a pure EV with 240 km range. Early mainstream consumers only, m = 530 [71]

Many EV batteries are based on the Lithium-Ion chemistry [64-66, 75] whereby for a battery that is being utilized, cycling losses (from usage) are much more significant than calendar losses (from storage). Cycling losses are increased by [73, 74, 76-78]:

- Additional cycling
- Higher charge and discharge rates (through increased temperatures)
- Higher SoC

It has been suggested that V2G technology is best suited to high-value and time critical services [27] as opposed to generating value from energy trading [79] where algorithms

designed to extend battery life generate twice as much value [80]. Offering capacity as a back-up yet rarely utilising it also presents opportunities for EVs to earn additional revenue [81]. Every commercial EV battery has its own chemistry and resulting degradation characteristics which could impact on the suitability of each V2G revenue generating opportunity [72].

2.3.2 Electric vehicle impacts on the distribution network

Many of the studies investigating the impact of EVs on distribution networks did so as a baseline for proposing smart charging techniques. In this section, only the baseline studies are compared to understand the impact should uncontrolled charging become the norm. The majority of the studies focused on whether the charging would result in transformer or cable thermal overloads, or voltage limit excursions [26, 53, 68, 69, 82-97], some considered the impact on electrical losses [53, 68, 85, 87-90, 92, 93, 98], and a few studied the transformer life [85, 98] and voltage unbalance [68, 86, 93, 94]. The early studies made simple assumptions regarding the time when vehicles would all plug-in and charge at the same time [86, 89, 90, 95, 96]. Diversity was introduced by [87, 91] through implementing a couple of periods through the day that the vehicles would charge, and by [53, 69, 82, 85, 97] through making plug-in time statistical distribution assumptions. The diversity of charging was further improved through using travel surveys of conventional IC vehicles [26, 68, 83, 84, 88, 92-94, 98]. The resulting synthesised diversified EV load was checked to have a similar profile to that observed as the diversified load from a trial of 94 EVs in [94]. It was noted in [68] however, that always topping up with charge when stationary is a significant shift in driver behaviour whereby end users may restrict daily range rather than extensively using standard charging infrastructure. Similarly, a rapid charge takes significantly longer time than present refuelling practices [70]. Therefore there is uncertainty over consumer behaviour under a widespread EV uptake scenario resulting in uncertainty over how transferable the travel surveys are for modelling high penetrations of EV load on distribution networks.

Only one study was found to be based on data taken from EV usage trials [99]. This study used data mining and fuzzy logic to predict the risk to distribution networks based on the charging peak, growth of the peak over time, and weather predictability of the charging load. It looked only at geographical areas and did not consider the networks in those areas. Furthermore, it noted that there was no research to suggest what importance should be applied to the charging peak, growth of the peak, and weather predictability, to determine an appropriate risk factor.

The studies found, to varying degrees, that networks would need to be reinforced if uncontrolled changing would emerge as the norm while distribution losses would increase and transformer life decrease. All these impacts have a cost associated with them, which could indicate the potential financial value of smart charging. The cost of network reinforcement was only considered in two studies [68, 83]. It was estimated by [83] using representative networks from one DNO that the cost would be up to £36bn over 40 years, but could be reduced to £10bn with smart infrastructure. In comparison, [68] recognised that all networks have different levels of available capacity, making it difficult to extrapolate results. The authors assumed that 30% of UK distribution transformers would need reinforcing resulting in an estimated network upgrade cost of £2.6bn-£3.9bn.

2.3.3 Realising flexibility from electric vehicles

Price signals have been proposed to discourage charging at peak times, while still allowing consumers access to energy at all times if it is required. Setting two or three time periods during the day risks new peaks being formed by consumers delaying charging until a cheaper time period and all plugging in together [53, 88, 100]. More dynamic time of use tariffs have also been studied, allowing consumers to optimise their own charging locally with a greater diversity of charge time [84, 97, 100, 101]. Despite this, it was noted in [84] that as renewable penetration increases the method performs less favourably, and in [101] that greater economic value can be achieved through more centralised control approaches.

Ensuring the network is kept within its power flow and voltage constraints under scenarios of high EV penetrations can be achieved by simply curtailing charging when the limit is reached [75, 88], and when capacity becomes available prioritise the re-connection of the vehicles that were curtailed first [88]. A similar method was proposed by [92], however the vehicles curtailed were chosen based on SoC required at departure, the expected departure time and the location of the vehicle within the network relative to the constraint. Curtailment was also utilised by [100] after local vehicle scheduling of charging based on time of use tariffs. Although the curtailment method enables greater numbers of vehicles to connect to the network, it could have adverse impacts on consumers not being able to get the energy they need by the time they need it.

Both price signals and direct EV control is implemented in [95, 96, 102] via a hierarchical approach. Initially [95] undertakes an extensive search of possible charging schedules locally for each EV to determine its lowest cost acceptable charging schedule, [96] utilises price signals for EVs to determine via CPLEX their optimal charging profile locally, while a

microgrid auction is initially utilised in [102] to determine EV charging load based on the microgrid generation. If network limits are expected to be exceeded based on the reported charging plan, then the load is modified by a central agent in [95] based on a risk factor corresponding to the urgency of each EV to charge during the next time step, and in [96] based on a combination of network location and the number of idle charging hours within the schedule. If network limits are expected to be exceeded in [102] then the generation output is modified by an Optimal Power Flow (OPF). If network limits are still expected to be exceeded then the sensitivity of each EV within the system relative to the limit is established, and an iterative process is used to curtail or increase charging load as required to solve the network problem.

It was shown by [75] that the increase in load from EV charging can have significant impacts on distribution transformer life, and thus should be modelled in any network wide smart charging formulations along with other distribution network costs such as losses [98]. Minimisation of losses was the objective function of the smart charging game theory formulation in [87], whereby it was shown that the losses and voltage deviations increased relative to no EV charging but were significantly less than the uncoordinated charging scenario.

A non-linear solver within GAMS was used in [53] to control the charging load of each EV distributed throughout a network with four different objective functions, to investigate the value generation for consumers relative to the DNO:

- Minimising total energy drawn from a substation over a day – results in the highest cost for consumers
- Minimising total feeder losses over a day – results in a balanced cost for the DNO versus the consumer
- Minimising total cost of energy drawn from the external grid over a day – results in a balanced cost for the DNO versus the consumer
- Minimising total cost for each individual consumer assuming precise forecast of time of use pricing – results in increased losses and cost for the DNO

LP was utilised by [90, 93] to determine the charging load of individual EVs while maximising the energy delivered to the vehicles subject to the network limitations. The charging period was limited to between 10pm and 7am in [90], and a weighting factor based on SoC was proposed to prevent the method prioritising vehicles closest to the substation at the expense of those located further away. A LP formulation with individual EV charging

loads as the decision variables was proposed in [93] whereby linearization of the power flow and voltage constraints was achieved through a DC load flow because of a high power factor throughout the network. When the resulting decisions were implemented with the full AC power system equations, the maximum error observed for the transformer power flow constraints was 4.46% while the error for the voltage constraints was minimal.

A non-linear optimisation solver was utilised in [94] to centrally maximise EV charging load while maintaining voltage magnitude, voltage unbalance and power flow within the network operational limits. Due to the limitations of the solver used regarding the number of decision variables and constraints, an hourly resolution was initially utilised to determine network capacity in each location. A look-up table then interpolated these results to determine EV load despatch on a minutely basis.

It was noted in [97] that not all EVs would be willing to partake in controlled charging. The study considered a number of responsive and unresponsive EVs to charging cost differentials, finding that forecasting the demand from uncoordinated EV charging is critical to the optimal scheduling of smart charging EVs. A similar approach was taken in [69] dividing EVs into two groups, aware and unaware, when modelling both electrical and road network congestion. The unaware EVs were early adopters with little knowledge of geographical variations in charging cost and the road network congestion causing travel delays. The aware EVs had perfect knowledge of charging cost, road network congestion and had greater trust in the expected range of the vehicle allowing them more choice over when and where to re-charge and by how much. It was observed that the unaware EVs contributed to the distribution network peak load while the aware EVs displayed a valley filling characteristic. The aware EVs spread the charging load relatively evenly across the charging network, while the unaware EVs concentrated their load on the charging infrastructure in the centre of the traffic networks. Similar results were observed regarding road traffic congestion.

Whole system cost minimisation is achieved in [103] through a fuzzy logic approach to each vehicle choosing its driving route and associated charging locations, recognising that in a V2G world energy can be transported both by road and by electrical power systems. The study considered several large aggregations of EVs located electrically close to one another, separated by transmission lines and roads. The available upper and lower energy bounds of such a parking lot of 5000 EVs was calculated in [104] to optimise, via a MILP formulation, the day ahead system operation cost from the network operator perspective before the real time despatch of each individual vehicle. The formulation ensures that either all vehicles are

operating as V2G or G2V, without the ability to have some vehicles operating as V2G transferring energy to other G2V vehicles. With such a large number of vehicles aggregated, they are likely to be spread within the distribution network which could have limited capacity and was not considered in either of the studies [103, 104]. Similarly, [105] recognises a parking lot as potential storage, and optimises the individual EV schedules using CPLEX to maximise profit for the parking lot based on the energy value and reserve markets without consideration of distribution network impacts. The marginal cost of charging based on the cost of energy and the cost of parking is calculated for a parking lot with onside solar generation in [106] for each vehicle to make its own schedule using CPLEX. It was shown that rolling re-calculation of the formulation outperforms day-ahead schedules due to responding to new information regarding solar generation output and vehicle arrival and departure times. A fuzzy logic scheme was proposed by [107] for the internal energy management of the parking lot considering present SoC, SoC required on leaving, time remaining and the cost of energy, allowing the vehicles to charge with the lowest energy cost, resulting in valley filling and peak shaving. The parking lot algorithm proposed in [108] allowed vehicles to pass energy between one another via the grid to enable more flexibility but does not allow the aggregated vehicles to operate as V2G in a formulation that calculates virtual prices for each vehicle to determine its own charging schedule locally. The aggregator is responding to energy price signals, and the maximum power draw is limited as required by the capacity of the distribution network. Although this enables the parking lot aggregator to be integrated into the local distribution network, it does not enable the EV flexibility to be optimised in relation to other flexible elements of the power system, unless there is a major overhaul of the market framework whereby DNOs become responsible for setting the real-time price of energy.

In [109], a parking lot of EVs is considered as an uncertain storage medium where it's aggregated output is optimised in a microgrid alongside a Combined Heat and Power (CHP) unit and heat storage. Kirchhoff's law was used for the energy balance and thus no network modelling was undertaken, and the internal energy interaction of the parking lot between individual vehicles was not modelled; only the aggregated power and energy bounds were calculated via the total number of vehicles as an input to the wider microgrid optimisation. It is possible that if one vehicle has a low SoC and maximum V2G power is requested, then that vehicle may reach a zero SoC condition and thus the aggregated V2G available power becomes less than what the scheduler thinks is possible. An internal energy management scheme of the parking lot was proposed by [110] whereby a desired average SoC across the

whole EV fleet was calculated; those with a higher SoC discharged while those with a lower SoC charged. The method results in better internal energy management of the EV fleet, in terms of ensuring the maximum aggregate power that can be delivered, however also results in some EVs having a net energy loss over their time plugged in, conflicting with the needs of the users.

The location and sizing of smart charging parking lots was investigated by [111]. LP was used to determine the schedules of the parking lots, inside a genetic algorithm determining their size and location. It was found that land cost was the most influencing factor on the parking lot location. Therefore it must be expected that parking lots could be added to any part of the electrical network, rather than where is best electrically, and microgrid algorithms must utilise the flexibility optimally wherever it may be on the network relative to other flexible loads.

UCC has been implemented in the 'My Electric Avenue' trial [112], where a binary on-off decision is taken to ensure voltage and thermal limits are not exceeded on the feeders studied. This is being built upon with the "Electric Nation" project, running from January 2017 to December 2018, by expanding beyond one type of EV and managing the charging of 500-700 EVs [113]. By expanding beyond one type of EV the project will have to manage different battery sizes and charging rates.

The charging control model presented in [97] based on a virtual price enabling EVs to determine their charging schedule locally is being implemented at the Manchester Science Park, with the UKs first domestic V2G installed in May 2017 [114].

2.4 Chapter conclusions

The following gaps have been identified in the literature, giving scope to make a contribution to knowledge:

- Existing studies considering the technical impacts of uncontrolled EV charging make assumptions regarding charging times or assume that drivers would utilise EVs in a similar manor to conventional IC vehicles and charge whenever stationary. Chapter 3 improves on these studies by estimating network impacts using an extensive data set of real uncontrolled charging events coupled with an extensive smart meter data set available at Newcastle University.
- There is a large discrepancy between the two existing studies estimating UK network upgrade costs associated with largescale uptake of EVs. Chapter 3 estimates network upgrade costs considering the present network capacities of all UK DNOs.

- It has been found in the literature that understanding uncontrolled EV charging load is critical to the optimal scheduling of smart charging EVs, however no methodologies have been found to estimate aggregated uncontrolled EV charging load and the uncertainty surrounding the forecast. Chapter 3 develops a methodology to forecast uncontrolled EV charging load on distribution networks.
- Very large aggregations of EVs have been considered similar to energy storage previously to provide flexibility to the energy system on a transmission level, however EVs are expected to charge at distribution level in smaller aggregations with larger uncertainty surrounding the aggregate power and energy availability of the fleet. At distribution level, EVs have either been considered individual actors within optimisation formulations leading to scalability computational challenges, or when considered in aggregate the internal energy management of the fleet does not adequately take into account the needs of users with respect to delivering sufficient energy for the EV's primary purpose of transportation. Chapter 4 develops an EV charging aggregation algorithm, taking account of the uncertainty of when EVs will be connected and ensuring EVs have the energy needed on departure for transportation, such that the combined fleet of EVs can be used in coordination with other flexible loads to deliver services to the distribution system with a high degree of controllability.
- The literature has developed the RO technique to deterministically optimise the procurement of ESS power services under load and generation uncertainty, using the BoU to control the level of conservatism. Studies have considered how changing the BoU changes the probability of remaining within power flow and voltage constraints, however they have not determined what probability is economically optimal. A methodology to determine the Economically Optimal Probability of Success (EOPoS) of operating within power flow and voltage constraints is the subject of Chapter 5.
- Previous studies have quantified the errors associated with using a DC load flow within an optimisation formulation when implementing the resulting power set-points with the full AC load flow equations. Other studies have used sensitivity factors calculated based on the full AC load flow equations in order to achieve a linear representation of the network for use within optimisation formulations, however no study was found that quantified the errors arising from use of sensitivity factors. Chapter 5 investigates the magnitude of the errors introduced through linearization of the AC power system through sensitivity factors for use in RO algorithms operating under load and generation uncertainty.

Chapter 3 Impact of uncontrolled electric vehicle charging on distribution networks

3.1 Introduction

In this Chapter, the likely impact of wide scale adoption of EVs is investigated whereby consumers have full choice over when they plug in and charge their vehicles. The technical impacts are investigated in Section 3.2, and the associated reinforcement cost to enable the uptake while maintaining the network within safe operating limits is investigated in Section 3.3. Finally, a methodology to forecast uncontrolled EV charging is proposed in Section 3.4. The Chapter and how it fits within the Thesis as a whole is summarised in Figure 3-1.

The work presented in Section 3.2 has been published in an Applied Energy paper in 2015 [16]. The author took an existing PSCAD model of the test network and re-configured it to undertake the unbalanced analysis, and supported the preparation of the published paper manuscript. Others took the lead in the collection and preparation of load data.

The work presented in Section 3.3 was undertaken in collaboration with colleagues from the National Centre for Energy Systems Integration (CESI) at Newcastle University with input from every DNO in the UK. The author undertook the Ofgem Model analysis after having taken the output of the TRANSFORM model from others.

The methodology in Section 3.4 to forecast uncontrolled EV charging was developed by the author.

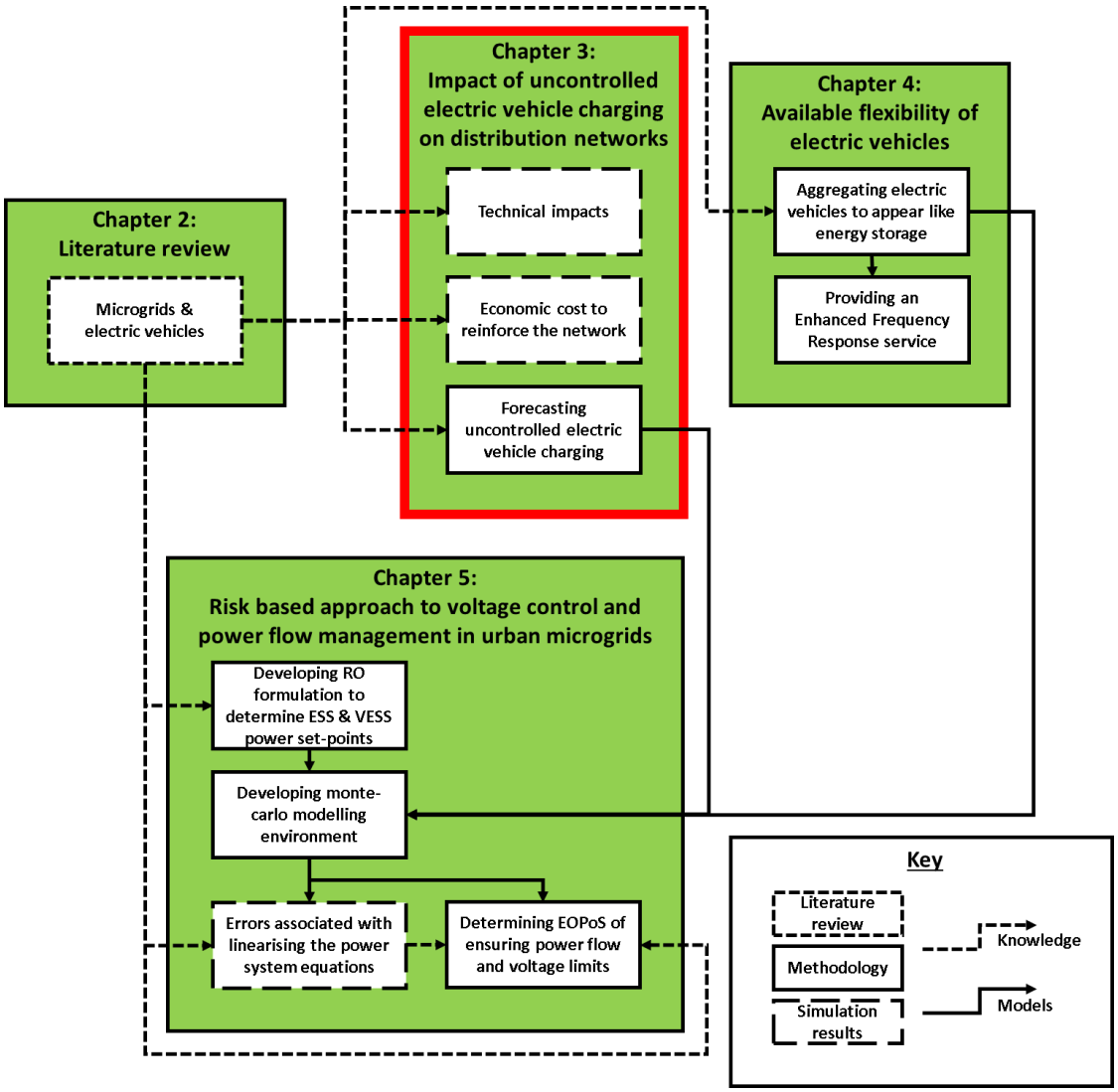

Figure 3-1 How Chapter 3 fits into the wider Thesis

3.2 Technical impacts of uncontrolled electric vehicle charging

In this section, the technical impacts of uncontrolled EV charging on domestic distribution networks is investigated. The technical impacts investigated include the distribution transformer power flow, feeder voltage drop and voltage unbalance. In this Thesis, uncontrolled EV charging refers to consumers having full choice over when and where they charge their EVs. The calculation methodology employed is described in Section 3.2.1 with the results presented in Section 3.2.2.

3.2.1 Calculation methodology

It was noted in Chapter 2 that there is uncertainty over the impact of EV charging on distribution networks, since no study has to date investigated the complex interactions between measured real world EV charging loads and measured real world domestic household loads for residential networks. Although computationally expensive, MCS can accurately handle complex uncertain variables [25] and have been used in this analysis. Non-residential

networks have not been studied because their loads are very industry, business-need and location specific [115] making it difficult to draw generalizable conclusions.

An overview of the calculation methodology is presented in Figure 3-2. The distribution network model and software used in the analysis are discussed in Section 3.2.1.1, and the sources of data for both domestic household load and future EV load are discussed in Sections 3.2.1.2 and 3.2.1.3 respectively

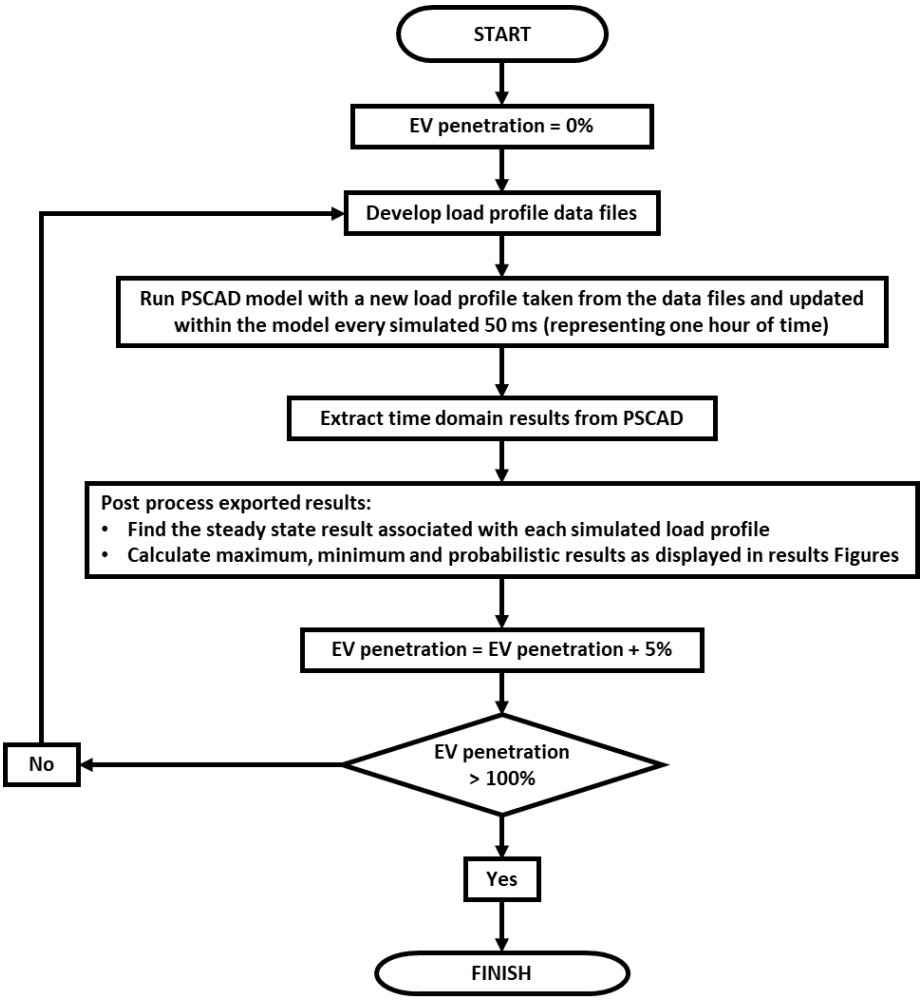

Figure 3-2 Overview of calculation methodology

3.2.1.1 Distribution network model and calculation method

A generic network, based on [116] and shown in Figure 3-3, has been used in this study in order to draw broad and generalizable conclusions across the UK distribution networks as a whole. This network has been deemed to be representative of a heavily loaded UK distribution network by all UK DNOs, who were involved in specifying and creating it. It has also been utilised by a number of authors for modelling a generic UK distribution network in order to draw broad and generalizable conclusions [52, 92, 94]. It consists of a 33 kV source feeding two 15 MVA 33/11 kV transformers. There are six 11 kV feeders, each of which have

eight 500 kVA 11/0.4 kV transformers equally spaced along 3 km of underground cable. Downstream of each 500 kVA transformer are 4 LV feeders of 300 m in length with 96 customers spaced equally along each feeder. The population parameters for the 386 customers under study on the generic network were assumed to be the same as that expected for an urban network as described in Table 3-1.

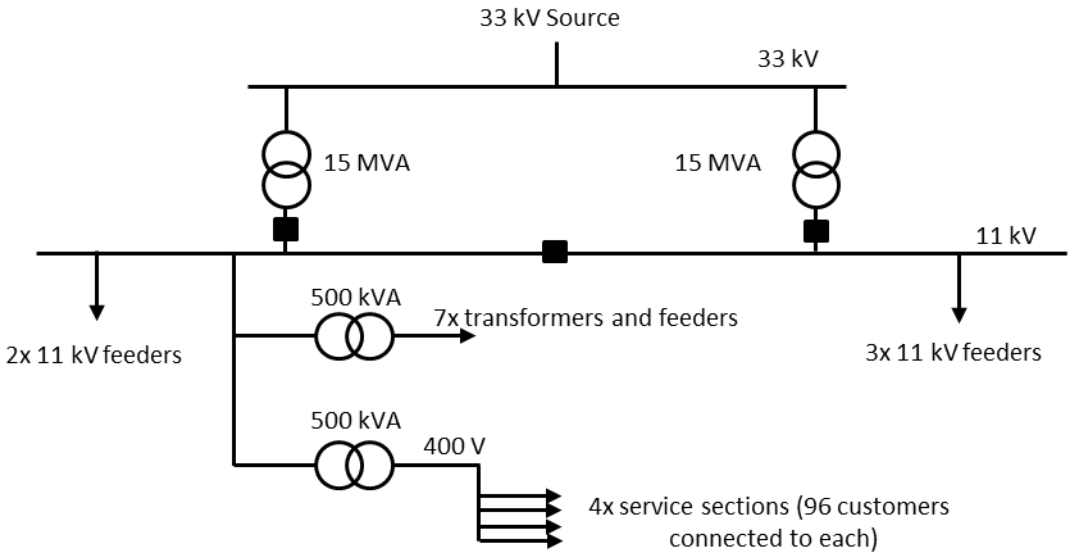

Figure 3-3 UK Generic distribution network model

The generic distribution network was modelled in PSCAD/EMTDC (See Appendix A for an image of the model), which is a commercial power systems analysis software package developed by the Manitoba HVDC Research Centre [117] and originally inspired by Dommel [118, 119]. It uses a time-domain based analysis (as opposed to frequency domain) and was used in this study primarily to allow the impact of unbalanced loads on the resultant voltages within the network to be determined. Due to a limitation on PSCAD model size, a number of load aggregations were made as shown in Figure 3-4 and described below:

- Five of the 11 kV feeders were lumped into three single phase loads; Load A.
- In the modelled 11 kV feeder, seven of the 11/0.4 kV transformers have their load lumped into three single phase loads, Load B.
- Below the eighth 11/0.4 kV transformer, three LV feeders have been lumped into three single phase loads, Load C.
- The most remote LV feeder has been modelled with 12 single phase loads each representing 8 customers (Loads D-O), separated by four modelled cables.

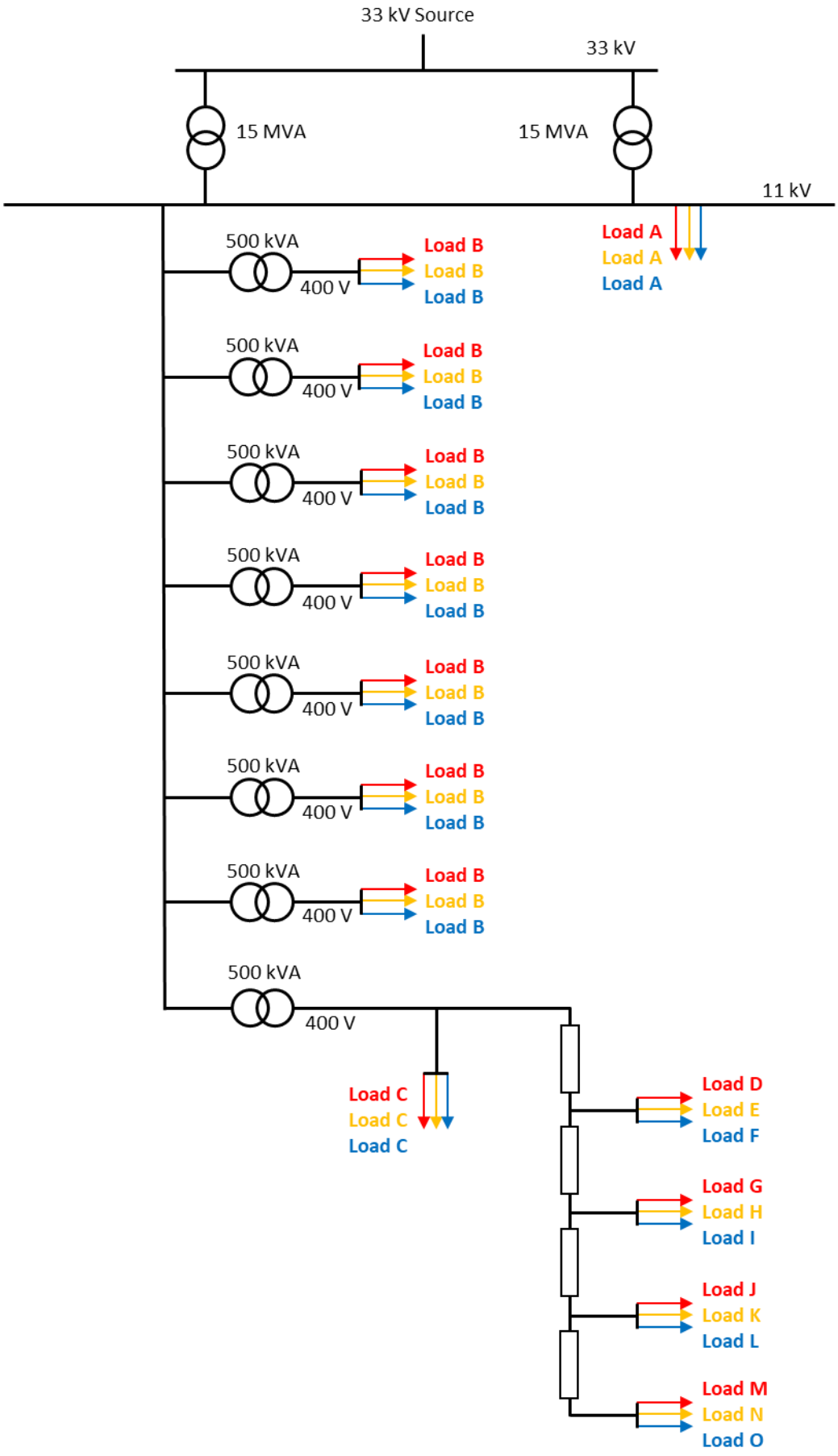

Figure 3-4 UK Generic distribution network modelled in PSCAD

Table 3-1 Summary of LV network and population parameters

	Urban network
Substation	6.6 kV/400 V 500 kVA
Feeders	4
Total LV customers	386
Vehicle ownership	86.0%
Number of vehicles in vehicle-owning households	1.7
ONS morphology code	1 (Urban)
Household thermal efficiency	Medium
Percentage of households with under 5s or over 65s	44%
Equivalent annual income (gross)	60%: > £30k 35%: £15-£30k 5%: < £15k
Tenure	Effective 100% home ownership
Household occupancy	97%

Peak consumption of electricity is in winter in the UK. In order to assess the additional impact of EVs during an existing peak loading event, a single peak load test day corresponding to the DNO's system peak load day in January is studied. MCS was used to build up a distribution of possible demands on the generic network as summarised in Figure 3-5. To reduce the computational burden in PSCAD, only the worst case hours of the peak day were assessed. This was 17:00-05:00 based upon a less computationally expensive frequency domain method calculated in IPSA2 and reproduced in Appendix B [16]. Load profiles for the simulation was produced by sampling the domestic load profile (discussed in Section 3.2.1.2) and EV charging profile (discussed in Section 3.2.1.3) populations. Individual households on the LV networks were randomly assigned load profiles in proportion to the local demographic makeup as defined in Table 3-1. A defined percentage of these users, corresponding to a level of EV penetration, were further assigned an EV load profile which was added to their base domestic profile. The EV penetration is defined as the ratio of EVs to the number of vehicle owning households.

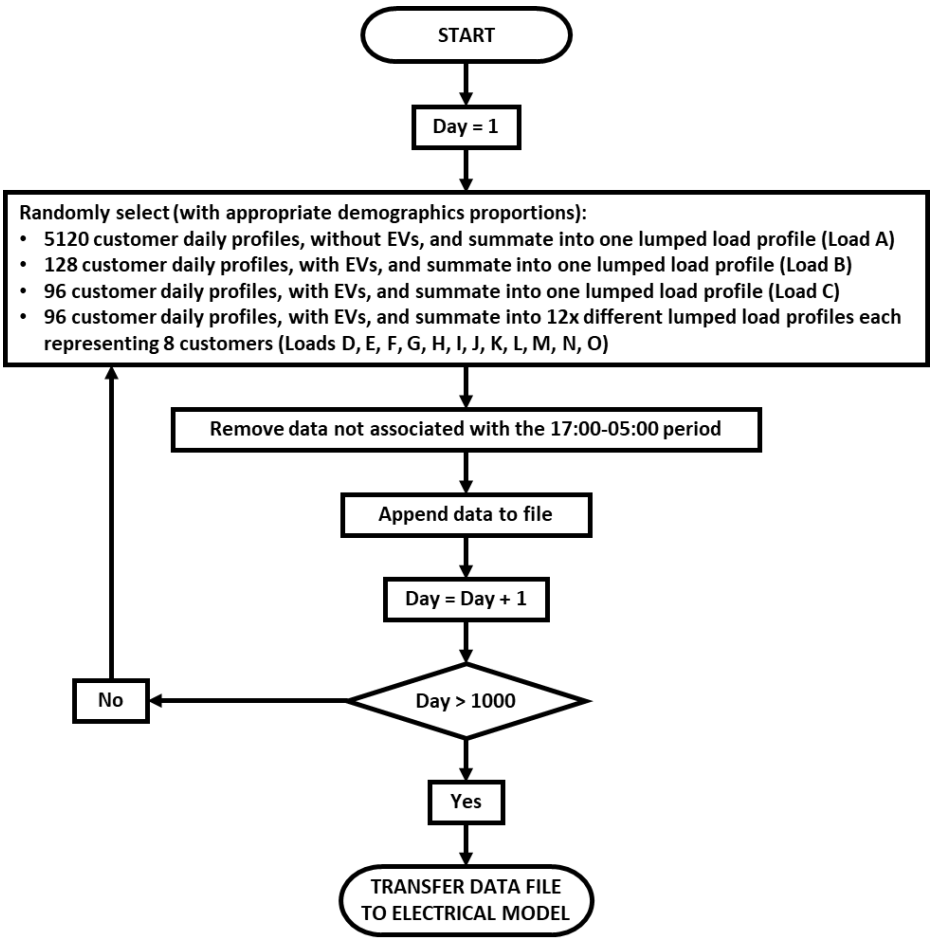

Figure 3-5 MCS sampling methodology to create load profiles for the PSCAD model

Each load profile for 1000 simulated peak days was used in PSCAD and the transformer power flow, voltage magnitude and voltage unbalance was assessed once each simulation reached a steady-state. This was undertaken for different EV penetration levels ranging from 0% to 100% in 5% steps. The voltage unbalance in a three-phase system is defined in Engineering Recommendation P29 [120] as the ratio (in per cent) between the rms value of the negative sequence component and the positive sequence component of the voltage. This can be approximated for the values of voltage unbalance of a few percent, as was the case for this study, as calculated by Equation (3.1):

$$V_{unbalance} = \frac{\left(\begin{matrix} Maximum\ deviation\ from\ the \\ average\ of\ the\ three\ phase\ voltages \end{matrix}\right)}{Average\ of\ the\ three\ phase\ voltages} \times 100\% \qquad (3.1)$$

1000 simulated peak days (i.e. 1000 simulation runs) were generated to ensure adequate variation of customer behaviour, EV charging profiles and customer location on the network. The generation of multiple random configurations naturally captures any spatial concentration of households with EVs (e.g. at the remote end of the longest feeder) which could cause additional voltage drops. This number of simulated days was deemed acceptable to produce stable and reliable estimates of simulated demand based on an analysis using the less computationally expensive IPSA2 in [16] and reproduced in Appendix B. For the Urban network with 60% EV penetration at 18.00 on the peak demand day, 1000 trials showed that the mean transformer demand had converged to a stable 385.8 kVA (standard error 0.29 kVA). The standard deviation of the distribution of transformer demand had also stabilised to 9.1 kVA.

3.2.1.2 Domestic load data population

The domestic household load is modelled based on the Customer Led Network Revolution (CLNR) project, which conducted a monitoring trial of over 9000 smart meters placed in residential locations in the UK. The smart meter dataset is classified by household income, presence of under 5 s or over 65 s, tenure, household thermal efficiency and area classification (urban/rural). UK Office for National Statistics (ONS) data was used to determine the characteristics of the study areas of this work, which are summarised in Table 3-1 along with the electricity network characteristics. Using the parameters in Table 3-1, a representative population of residential load profiles was extracted from the CLNR dataset representing the study areas.

3.2.1.3 Future EV load data population

The EV charging load is based on the SwitchEV project, which recruited different types of users (private and fleet drivers), who had access to an extensive charging infrastructure (home, work, public). The majority of vehicles used in the trial are production vehicles available on the market and were provided by Nissan (LEAF) and Peugeot (iOn). A total of 125 different users were recruited for the duration of the project [121]. The dataset included the diversity of charge event starting SoC as a result of variables such as temperature, driving behaviour of users (i.e. speed) and driving conditions such as the topography of the road network and network conditions (i.e. free flow or congested), all affecting the driving energy efficiency of the vehicle and the residual energy at the end of a driving event [122]. As a result, the data collected from the SwitchEV trial captured how people would use an electric car in a real-world context.

The SwitchEV trial is distinctive because it collaborated with Charge Your Car (North Ltd) (CYC), the operator of the North East of England's ''Plugged in Places'' project, which has provided one of the most extensive regional charging networks in Europe with more than 900 charging posts installed in public, work and home locations in the region during the SwitchEV trial. As a consequence, the participants were not limited to one charging location and they had real and varied options about when and where to charge. Their homes and work places could be equipped with charging units; they could access charging posts on-street and in commercial places and public car parks; and there were twelve accessible 50 kW DC rapid chargers installed at strategic locations in the region. The analysis of the dataset collected identified the charging locations used and the energy transferred at each of these locations, allowing the extraction of home charging events that were used for this study.

The EVs on the trial were leased as private and fleet cars. The charging profiles of private cars were used in this study. To determine the residence setting (i.e. urban vs rural) of the users on the SwitchEV trial, the Office for National Statistics Postcode Directory (ONSPD) was used. Postcodes on the ONSPD are assigned to urban or rural categories [123]. The postcode of the SwitchEV users were identified in the ONSPD and their residence setting was then determined. It was found that 70% of the SwitchEV users reside in urban areas while 30% reside in rural Areas.

3.2.2 Results

Figure 3-6 shows the average and maximum loading on the transformer, and the probability that it remains within the transformer's thermal limit, as EV penetration increases. The studies show that the maximum load is on the transformer thermal limit of this network prior to the addition of EVs, however due to the diversity between household load and EV charging the probability of remaining within the limit does not start to fall below 97.5% until an EV penetration of 40%. This is consistent with the frequency domain results calculated in IPSA2, reported in [16] and reproduced in Appendix B, and suggests that distribution networks in general are more robust than previous work has suggested because of the spatial, temporal and behavioural diversity of EV charging demand demonstrated in this study. Furthermore, the average demand remains well within the transformer thermal limit even at an EV penetration of 100%, suggesting that ESS, smart EV charging or V2G technology could potentially enable full electrification of the transport system without requiring traditional network reinforcement.

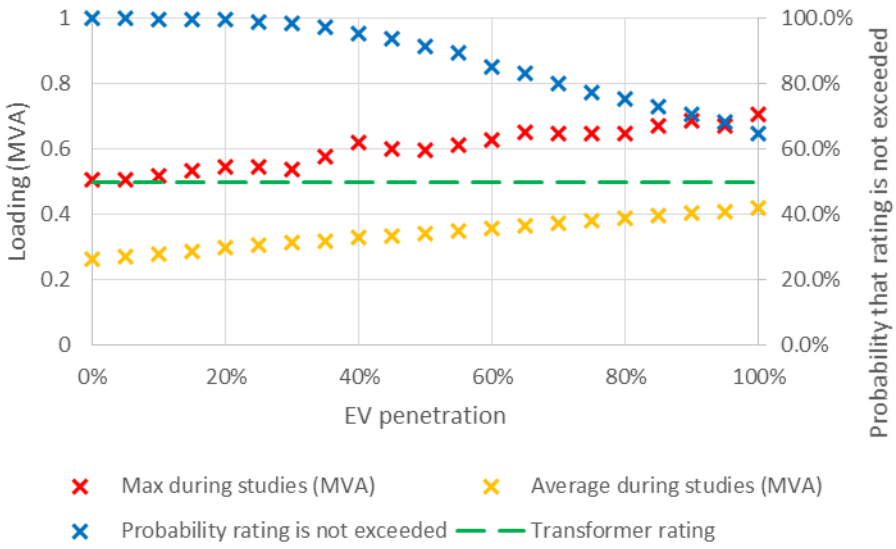

Figure 3-6 Maximum transformer loading magnitude observed for each EV penetration during all studies

The worst case for voltage drop is at the furthest end of the feeder, and therefore the voltage and its unbalance were measured at the end of the 400 V feeder. Industry planning regulations state that the voltage unbalance should not exceed 2% when assessed over any one minute period, and when sustained the voltage unbalance should not exceed 1.3% for systems with a nominal voltage below 33 kV [120]. The minimum voltage magnitude experienced for each EV penetration level during all the studies is shown in Figure 3-7 and the maximum voltage unbalance during all the studies is shown in Figure 3-8. The results for minimum voltage are consistent with the maximum loading condition of the frequency domain IPSA2 study [16] (reproduced in Appendix B). The PSCAD results show a marginally lower minimum voltage than IPSA2 results as the unbalance in load and EV connections across the LV network is modelled. As the penetration of EVs increases the load increases and the minimum voltage experienced reduces, although it does not cause a statutory limit violation even with 100% EV penetration.

Similarly an increase in charging load results in the unbalance of the network increasing. Using the 97.5% percentile, an EV penetration of 60% can be sustained on the generic network before the voltage unbalance would be considered an issue.

It has been noted that during the CLNR field trials, networks have been observed to exhibit a voltage unbalance that frequently approaches or exceeds the 1.3% limit with no EVs charging at all [16]. Therefore, the impact of high EV penetrations on unbalance should not be ignored, however the first limit expected to be encountered as EV uptake increases is transformer power flow.

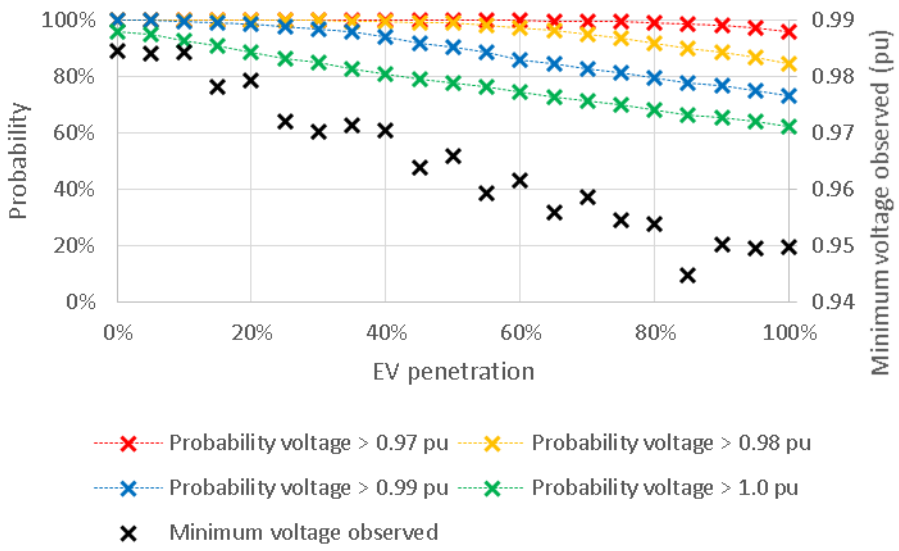

Figure 3-7 Minimum voltage magnitude observed for each EV penetration during all studies

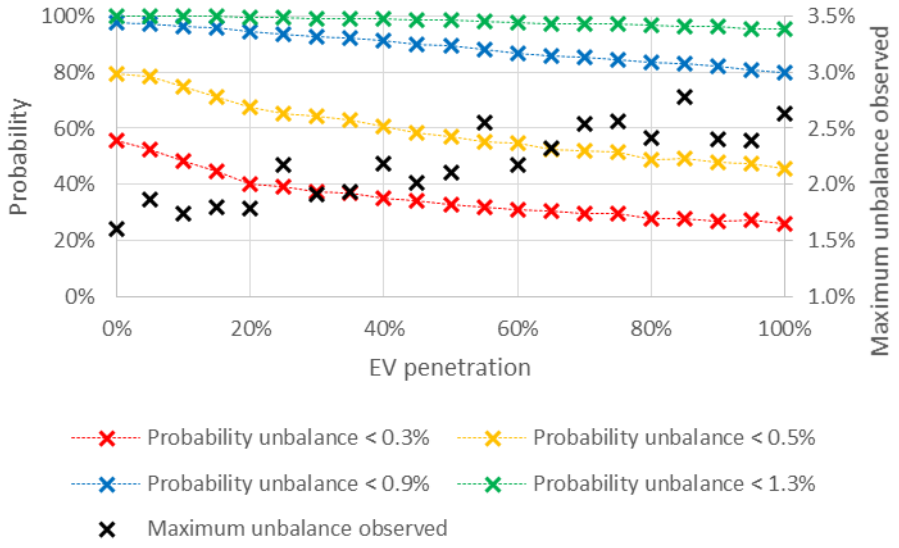

Figure 3-8 Maximum voltage unbalance observed for each EV penetration during all the studies

3.3 Reinforcement costs to enable wide scale uncontrolled electric vehicle charging

In this Section, the cost to reinforce the distribution networks to enable the largescale uptake of EVs is estimated. The uptake scenario studied, defined by industrial partners in 2016, is specified in Table 3-2. It should be noted that there is significant uncertainty surrounding the realised EV uptake relative to that forecast and defined in Table 3-2, since it is unknown what products and business models will be offered in a wide scale uptake scenario. Similarly, what is offered to consumers will depend on realised demand as the market develops.

The four stages of cost estimation that were used are shown in Figure 3-9.

Table 3-2 Uptake scenario of EV cars and vans defined by industrial partners in 2016

Year	Cumulative cars and vans Stock	Share of stock (private use)	Domestic off-street availability	Domestic Rapid charging share	Domestic Bidirectional share	Business Rapid share	Business bidirectional share
2020	470,000	50%	93%	1%	0%	5%	1%
2025	2,100,000	60%	87%	1%	2%	5%	5%
2030	8,200,000	70%	80%	1%	5%	5%	10%
2040	31,099,159	70%	80%	1%	5%	5%	10%

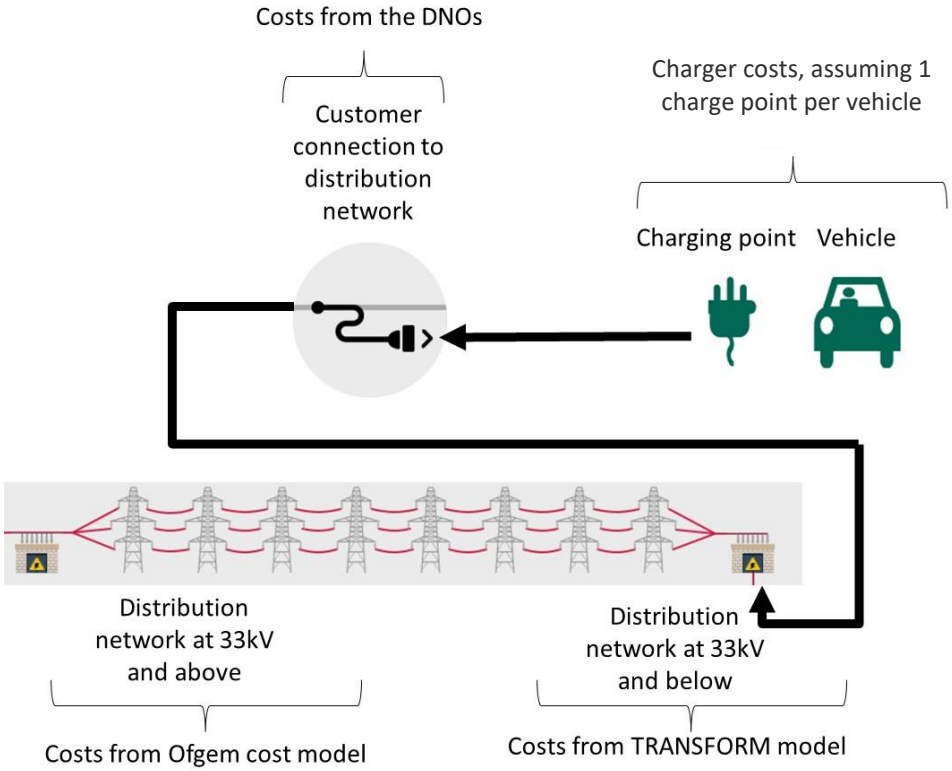

Figure 3-9 Stages of cost estimation for EV uptake

The author undertook the Ofgem model calculations presented in Section 3.3.3 within a Team, from CESI at Newcastle University with input from every DNO in the UK, that delivered the whole cost estimation. Since the Ofgem model's input is dependent upon the output of the TRANSFORM model, this is briefly described along with its input data in Section 3.3.2. The charging point and customer connection costs are also briefly described in

Sections 3.3.1. All costs are then brought together in Section 3.3.4. All values are calculated as of 2016.

3.3.1 Charger and customer connection costs

The charger costs for 2040 were extrapolated based on estimates until 2030, and the total capital cost is based on the uptake in Table 3-2 with an assumption of one charger per EV is shown in Table 3-3.

Table 3-3 Charger capital and installation cost estimate

	2030	2040
All chargers	£11.80bn	£26.62bn

Costs of single phase unbundling of looped connections and uprating some services to a three phase connection, to enable chargers to connect to the DNO networks were provided by industrial contacts within DNOs, and shown in Table 3-4. The costs do not include any protection or metering upgrades, or customer wiring.

Table 3-4 Service cost estimate

	2030	2040
All chargers	£0.74bn	£2.79bn

3.3.2 Distribution network at 33 kV and below (TRANSFORM model)

The TRANSFORM model is a tool which combines network design data and future LCT assumptions to predict where reinforcement is required, and then completes a cost benefit analysis of which network technologies (conventional and smart) could be applied to overcome the constraint most economically. There is a brief overview of the functionality of the TRANSFORM model in EA Technology's product brochure [124], and its modelling method and data are described in [125].

Only networks of 33kV and below are considered in the TRANSFORM model. For network modelling, load flow is not used due to the scale of the model and only a parametric model is used. Load diversity and different types of buildings are considered by the model, and all profiles for LCTs are fully diversified. The lack of diversity that can occur on LV networks is dealt with via scaling factors in line with accepted industry practice.

The EV uptake scenarios were based on that presented in Table 3-2. Highly diversified EV load profiles were based upon data taken from the SwitchEV project similar to that used in Section 3.2. A less diverse profile might be appropriate for earlier periods of the model, and thus costs might be underestimated for the period 2016-2030. Therefore a TRANSFORM scenario was created with load profiles increased by 50%, to (very roughly) reduce the diversity of the load profile. Since the TRANSFORM model looks forward for the most economical solution over time, an estimation of the number of EVs for 2050 was required for the TRANSFORM model. This was done through extrapolation as shown in Table 3-2 and as a result the number of EVs for 2050 is very large. Therefore the later costs for the period 2031-2050 could be an overestimation.

Two scenarios, namely Business As Usual (BAU) and incremental, were studied. The BAU approach includes only conventional network reinforcement and does not include smart grid solutions. On the other hand, the incremental approach considers smart grid solutions such as meshing radial networks, RTTR and ESS. All DNOs agreed the appropriate technology solutions to include in the incremental case, and the year from which they could be applied in the model.

A simplistic smart charging EV solution was implemented within TRANSFORM based on work done by the University of Manchester where they evaluated outputs from the My Electric Avenue project and assessed how much demand could successfully be constrained using smart charging [126]. These results were fed into the TRANSFORM model to provide an increase in capacity on those networks where the solution is applied, which is equal to the amount of demand that can be constrained. Therefore the maximum demand arising due to EV uptake is not altered in the TRANSFORM outputs, but the networks are assumed to have greater ability to cope with the demand levels. The maximum demand was then post processed to reduce it by the appropriate amount.

Maximum demand in the BAU scenario is shown in Figure 3-10, and is the input to the authors work utilising the Ofgem model in Section 3.3.3. The blue curve is the maximum demand and the dashed line is the maximum demand in 2016, which is approximately 56 GW. Despite the uptake of EVs, the peak demand decreases from 2016 to 2020 because the assumptions of improvements in energy efficiency outweigh the new EV load. Peak demand starts to increase from 2020. By 2025 and 2030, maximum demand is 56.8 GW and 62.4 GW, respectively.

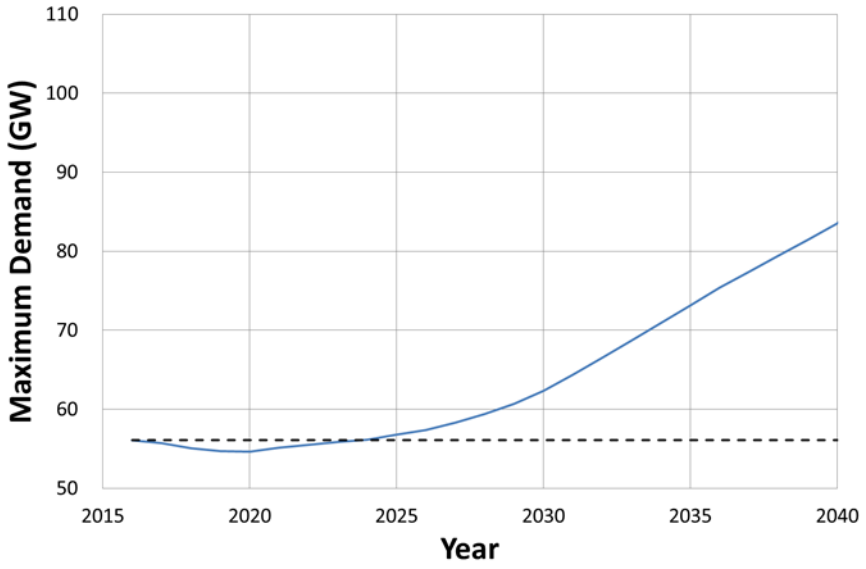

Figure 3-10 Maximum demand in BAU scenario from 2016 to 2040

The network reinforcement costs to facilitate the increased demand for the BAU scenario is shown in Figure 3-11 along with the cumulative number of EV cars and vans. By 2020, 2025 and 2030, cumulative gross total expenditure is £0.36bn, £1.01bn and £2.61bn, respectively. Cumulative Totex and cumulative vehicle stocks follows an approximate linear relationship in Figure 3-11.

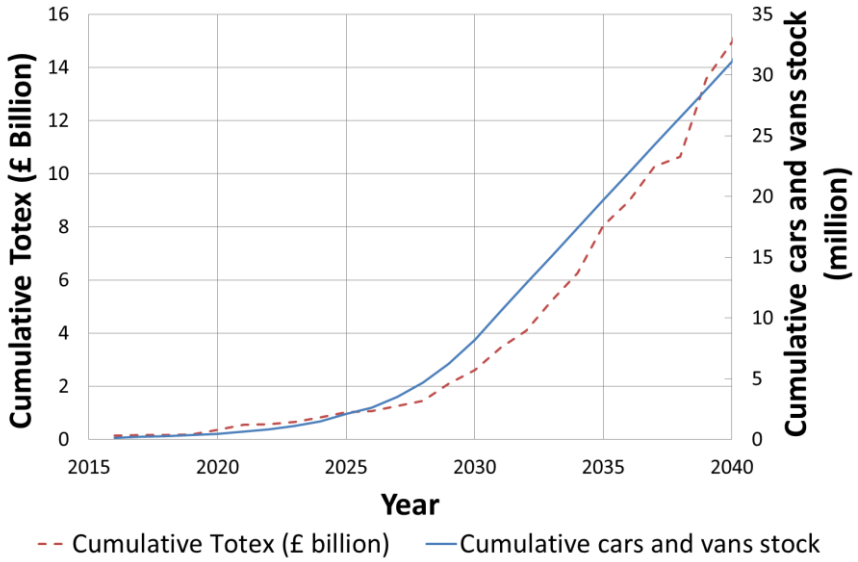

Figure 3-11 Cumulative BAU gross Totex and cumulative cars and vans stock from 2016 to 2040

In the incremental scenario, smart grid solutions such as RTTR and meshing radial networks are considered. It is found that the use of smart grid technologies can reduce the total expenditure for network reinforcement. In 2020, 2025 and 2030, the savings achieved by the

use of smart grid solutions is £0.14bn, £0.28bn and £0.86bn respectively, as illustrated in Figure 3-12.

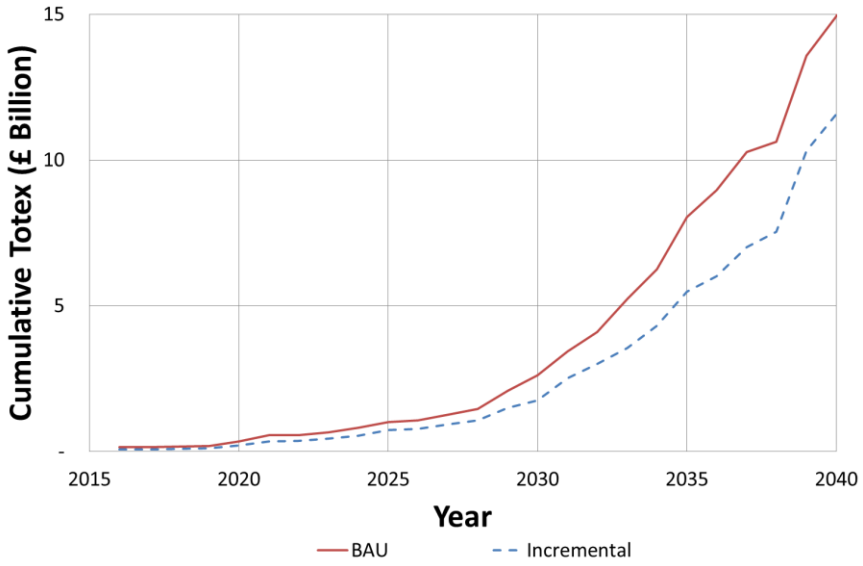

Figure 3-12 Cumulative gross Totex for BAU and incremental scenarios

A summary of the gross and discounted Totex between 2020 and 2040 is shown in Table 3-5, using a discount value of 3.5%.

Table 3-5 Summary of gross and discounted Totex between 2020 and 2040

Year	2020	2025	2030	2035	2040
Gross Totex					
Baseline, BAU	£0.36bn	£1.01bn	£2.61bn	£8.04bn	£14.94bn
Baseline, Incremental	£0.22bn	£0.74bn	£1.75bn	£5.49bn	£11.59bn
Reduced diversity, BAU	£0.36bn	£1.05bn	£3.71bn	£13.30bn	£23.28bn
Reduced diversity, Incremental	£0.22bn	£0.76bn	£2.81bn	£7.65bn	£16.53bn
Discounted Totex					
Baseline, BAU	£0.33bn	£0.85bn	£1.87bn	£4.86bn	£8.06bn
Baseline, Incremental	£0.20bn	£0.60bn	£1.26bn	£3.32bn	£6.14bn
Reduced diversity, BAU	£0.33bn	£0.88bn	£2.60bn	£7.94bn	£12.67bn
Reduced diversity, Incremental	£0.21bn	£0.63bn	£1.95bn	£4.66bn	£8.82bn

3.3.3 Distribution network at 33 kV and above (Ofgem model)

With advice provided by Iain Miller, Head of Innovation at NPg, the Ofgem model [127] is based upon the 33kV and above project specific upgrade costs that each DNO provided to Ofgem for the RIIO-ED1 price control. Ofgem compared these costs over a 13 year period

across all the 14 DNO license areas and specified, using the model, an acceptable upgrade cost level that can be passed onto the consumer.

The model is based upon two main criteria; the capacity by which to upgrade, and the cost of those upgrades. These are considered in Sections 3.3.3.1 and 3.3.3.2 respectively, before the model is brought together to calculate the allowable costs in Section 3.3.3.3 and the results presented in Section 3.3.3.4. The limitations of the Ofgem model are then discussed in Section 3.3.3.5.

3.3.3.1 Capacity by which to upgrade

When a circuit gets close to its maximum capacity, a small growth in maximum load will require a network upgrade. In order to allow for further future load growth without continually requiring expensive upgrades; some additional capacity is installed on top of that causing the upgrade to take place. The ratio of capacity added against maximum demand growth is used within the Ofgem model and labelled, α.

During the RIIO-ED1 review, each DNO specified what their expected maximum demand growth would be, and the resulting project specific upgrades required. This allowed for the α value to be calculated for each DNO. The cost that Ofgem allowed a DNO to pass onto consumers was based upon limiting α for each DNO by the median of all α values across the industry. By limiting the value, Ofgem ensured that excessive over-engineering is not taking place, while still allowing economically efficient network development over the long term.

The median α value was 7.69 across all DNOs. This is appropriate for the RIIO-ED1 period for BAU with small changes in maximum demand in isolated locations. With the large scale deployment of EVs adding significant maximum load growth over a short period of time, this may not be appropriate.

With a large change in demand, it may be more appropriate for the consumer to fund the upgrades that would leave the network in the same overall state of utilisation that they are presently in. This could be defined as the same over capacity in MVA regardless of maximum demand, or the utilisation could be defined as a multiple of the maximum demand. The latter would result in a growth in spare capacity proportional to the increase in maximum demand. During this work, the ratio of total system capacity against total system maximum load, 2.58, has been used in place of α. If the networks were to be left in the same level of utilisation in MVA regardless of maximum demand then an α value of 1.00 should be used.

3.3.3.2 Cost of upgrades

Once the capacity to be upgraded has been decided, the cost of those upgrades must be considered. There are two measures used within the model to calculate the allowable cost of upgrades:

- The historical cost of the network per MVA based on the Modern Equivalent Asset Value (MEAV)
- The DNOs forecast for the project specific upgrade costs

The ratio of the DNO forecast upgrade costs divided by the historical cost of their network is calculated, and is labelled β. During RIIO-ED1, Ofgem limited this value for each DNO to the median of β across the industry.

The median value of β, 0.94, has been utilised during this work.

3.3.3.3 Allowable costs

The allowable costs under the Ofgem model, for the purposes of this work, are described in equation (3.2).

$$C_{reinforcement} = G \times H \times \alpha \times \beta \qquad (3.2)$$

Where:

$C_{reinforcement}$ Allowable cost to the consumer, £m

G Growth in maximum demand, MVA

H Historic cost of the network based upon the MEAV, £m/MVA

α Allowable ratio of capacity to be upgraded relative to the growth in maximum demand

β Allowable ratio of expected upgrade costs relative to the historical network cost

The model results in a linear relationship between growth in maximum demand and the allowable cost to the consumer of network upgrades.

When there are small changes in maximum load growth and an α value of 7.69 is appropriate, the Ofgem model becomes equation (3.3).

$$C_{reinforcement} = 1.8922G \qquad (3.3)$$

However, for the EV uptake scenarios proposed and a large increase in maximum load an α value of 2.58 is more appropriate, whereby the Ofgem model becomes equation (3.4).

$$C_{reinforcement} = 0.6546G \qquad (3.4)$$

3.3.3.4 Results of the Ofgem model

The input to the Ofgem model is the maximum load growth in MVA, as estimated by the TRANSFORM model. Table 3-6 summarises the estimate of costs associated with this load growth as found using the Ofgem model for the time period up to 2030 and Table 3-7 for the time period up to 2040.

Table 3-6 Results from the Ofgem cost model, estimating total network upgrade costs up to 2030

2030	**Baseline**		**Reduced diversity**	
	BAU	Incremental	BAU	Incremental
TRANSFORM model maximum load growth (MVA)	6,268	6,268	7,755	7,755
Ofgem model cost [33 kV and above]	£4.10bn	£4.10bn	£5.08bn	£5.08bn

Table 3-7 Results from the Ofgem cost model, estimating total network upgrade costs up to 2040

2040	**Baseline**		**Reduced diversity**	
	BAU	Incremental	BAU	Incremental
TRANSFORM model maximum load growth (MVA)	27,479	27,477	33,694	33,694
Ofgem model cost [33 kV and above]	£17.99bn	£17.99bn	£22.06bn	£22.06bn

3.3.3.5 Limitations of the Ofgem model

The Ofgem model project specific upgrades includes voltages of 33 kV and higher. The MEAV includes all voltages.

The Ofgem model considers only the limited smart technologies that were proposed during the RIIO-ED1 business plans at present prices. Further expected innovation within the industry should enable new technologies to become available potentially reducing the costs, potentially involving the flexibility of the EVs being charged at the lower voltages.

Rural and urban networks have varying operating costs associated with them; based on their different nature. The Ofgem model takes this into account by comparing expected costs with historical costs. By taking the allowable costs applied across the whole country, the assumption is being made that the load increase is proportional to the size of the existing network in each area of the country. This may not be the case, and a more detailed analysis of the location of the greatest load increase may be required for more accurate upgrade cost estimation.

The model estimates the cost, at present values, to upgrade the networks by the growth in maximum demand such that the level of overcapacity remains similar to that observed within the network at the moment. It does not consider at what point in time those upgrades are undertaken and therefore the associated issues with cost of capital, change in costs for using the various upgrade technologies, or availability of labour to undertake the upgrades which may impact upon costs. Because of this, it is appropriate to compare Ofgem cost estimates with the discounted present value cost estimates of the TRANSFORM model, which is shown in Section 3.3.4.

3.3.4 Total costs

To obtain the total cost, the estimates for charger installation, service upgrades, LV & HV reinforcement (TRANSFORM model) and EHV (Ofgem model) must all be summated. In addition however, these costs do not include indirect costs such as training for technicians, design, project management and end to end procurement. Currently, technicians are not used to connecting three-phase supply to households. Necessary training needs to be provided to the technicians installing three-phase home chargers. During the implementation of network reinforcement, costs of design and project management should be considered as well. DNOs have estimated the indirect costs as a percentage of total cost. The mean value of DNOs' estimations, 27%, is used as the percentage uplift of total cost.

All costs, including the indirect costs, are shown in Table 3-8 for 2030 and Table 3-9 for 2040.

Table 3-8 All estimated costs associated with EV uptake for 2030, present value, including indirect costs

	LV+HV (<33 kV)	EHV (≥33 kV)	Services	Chargers	TOTAL
Baseline, BAU	£2.37bn	£5.21bn	£0.94bn	£11.80bn	£20.32bn
Baseline, Incremental	£1.60bn	£5.21bn	£0.94bn	£11.80bn	£19.55bn
Reduced diversity, BAU	£3.30bn	£6.45bn	£0.94bn	£11.80bn	£22.48bn
Reduced diversity, Incremental	£2.48bn	£6.45bn	£0.94bn	£11.80bn	£21.66bn

Table 3-9 All estimated costs associated with EV uptake for 2040, present value, including indirect costs

	LV+HV (<33 kV)	EHV (≥33 kV)	Services	Chargers	TOTAL
Baseline, BAU	£10.24bn	£22.84bn	£0.55bn	£26.62bn	£63.25bn
Baseline, Incremental	£7.80bn	£22.84bn	£3.55bn	£26.62bn	£60.81bn
Reduced diversity, BAU	£16.09bn	£28.01bn	£3.55bn	£26.62bn	£74.27bn
Reduced diversity, Incremental	£11.20bn	£28.01bn	£3.55bn	£26.62bn	£69.38bn

3.4 Forecasting uncontrolled electric vehicle charging load

In this Section, a methodology is developed to forecast aggregated uncontrolled EV charging load on distribution networks and quantify the UI surrounding that forecast. The methodology is developed considering standard charging in Section 3.4.1 before being applied to rapid charging in Section 3.4.2.

3.4.1 Uncontrolled standard charging

The SoC at the start of a charging event, along with the arrival and departure time has been shown to be stochastic based on time of day and the number of charging events per vehicle per day [21]. The number of charging events per vehicle per day itself is also stochastic. Therefore the electrical load on the network is also stochastic based on time of day. Using the stochastic relationships reported from real world weekday trials in [21] a MCS of 1000 simulated days has been undertaken, assuming a charge point rating of 3.6 kW, to gain a greater understanding of the uncertainty of aggregated uncontrolled EV standard charging dependent upon the time of day. The load of each individual vehicle was calculated with a minutely resolution, with the aggregated load on the network calculated as the average over each 30 minute settlement period. It was assumed that a parking bay was always available when an EV wanted to charge. The methodology used to calculate the uncertainty of aggregated uncontrolled EV standard charging dependent upon time of day is summarised in Figure 3-13.

The results of this study, displayed in Figure 3-14, shows the mean aggregated uncontrolled EV charging load for 750 EVs per day, and the associated three times diurnal standard deviation. Three standard deviations either side of the mean creates a diurnal minimum and maximum and thus an UI, shown in Figure 3-15, for which it is expected 99.7% of values will fall within. It should be noted however that the distributions used [21] are of early adopters, and could change as the market develops to a wide scale EV uptake scenario.

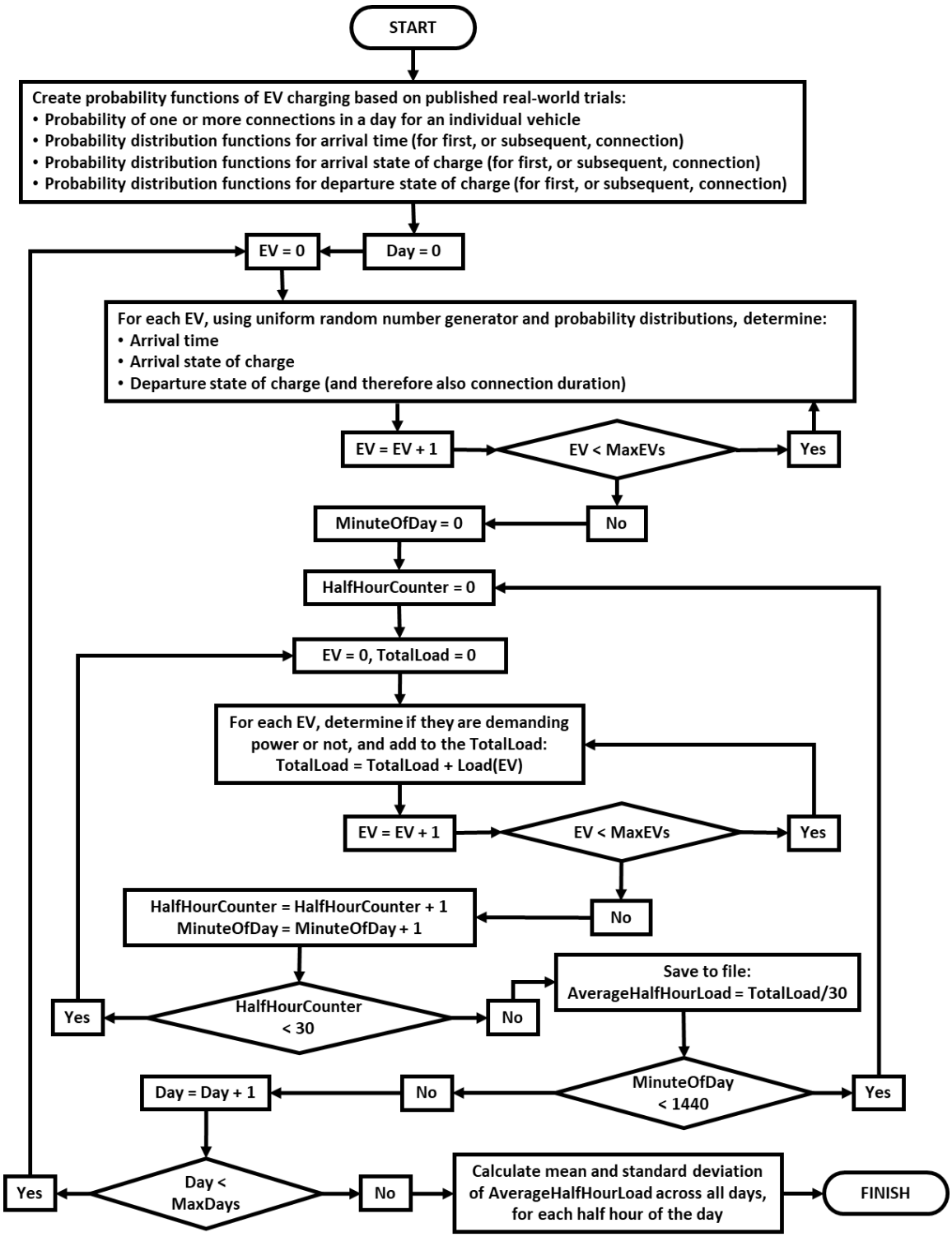

Figure 3-13 Methodology to calculate the aggregated EV standard charging load uncertainty

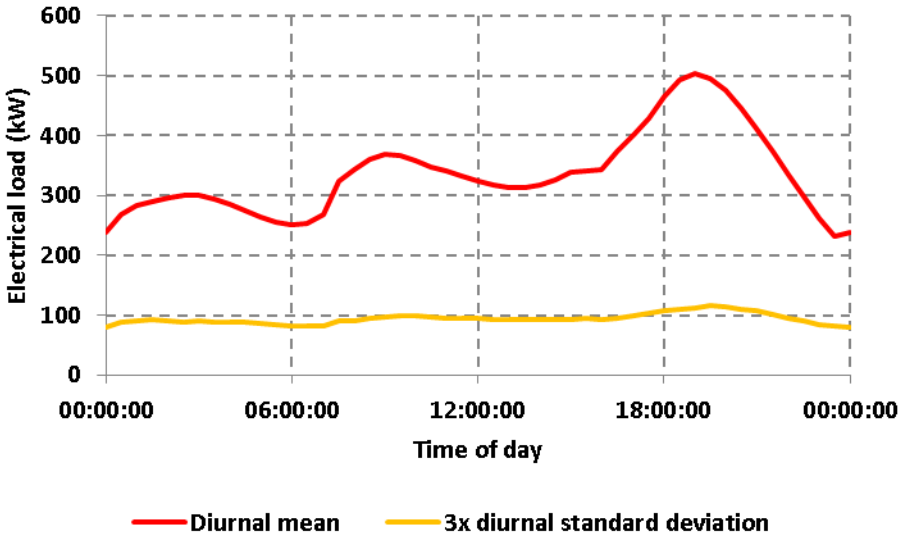

Figure 3-14 Mean load and 3x standard deviation of 750 EVs standard charging per weekday, using the arrival time and SoC statistics in [21]

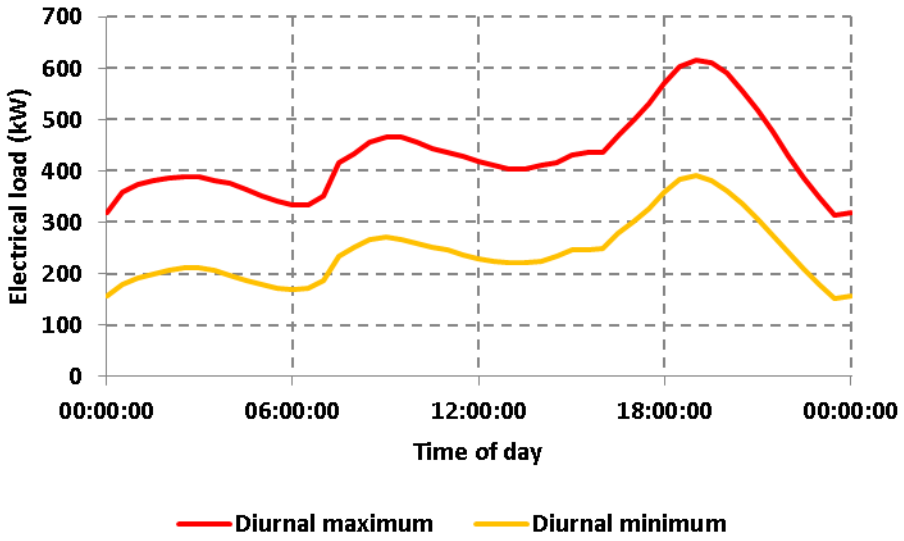

Figure 3-15 Load UI of 750 EVs standard charging per weekday, using the arrival time and SoC statistics in [21]

Figure 3-15 represents the range of aggregated diversified load for 750 EVs standard charging each day, without any prior knowledge of each individual vehicles' intentions regarding when they intend to charge. However, it is possible to imagine through smart communications that there be knowledge regarding the existing load on the network from EV charging, which could influence future load in the short term based on the stochastic time that EVs remain connected to the network for, without requiring consumers to indicate their future intentions. This is investigated below.

All load values, and the time at which they were observed within the MCS, were saved and then post-processed. The difference between a value 'here and now' and 0-48 settlement periods ahead was calculated as shown by (3.5). Over the 1000 simulated days of the MCS, 1000 different values of $\Delta L_{t,j}$ are found for each t and j, allowing for a standard deviation to be calculated. Three times the standard deviation represents the short term UI relative to the existing 'here and now' load for which 99.7% of values will fall within at j settlement periods ahead.

$$\Delta L_{t,j} = L_t - L_{t+j} \qquad (3.5)$$

Where:

$\Delta L_{t,j}$ Difference in uncontrolled EV charging load between settlement period t and settlement period t+j, kW

L_t Uncontrolled EV charging load at settlement period t, kW

L_{t+j} Uncontrolled EV charging load at j settlement periods ahead of settlement period t, kW

The short term UI was then normalised against the longer term diurnal UI (shown in Figure 3-15) for the appropriate settlement period of the day. This gives 48 normalised values, one for each 'here and now' settlement period, for each horizon looking forward. The value represents the proportion of the longer term diurnal UI which is appropriate in the shorter term relative to the existing 'here and now' load. Therefore, a value greater than 1.0 becomes meaningless since it exacerbates the UI to be greater than that observed with no knowledge of the existing load. The minimum, maximum and mean of the normalised values for each horizon looking forward is shown in Figure 3-16, and demonstrates that reduced uncertainty based on existing 'here and now' load can be estimated up to 1.5 hours ahead for standard charging.

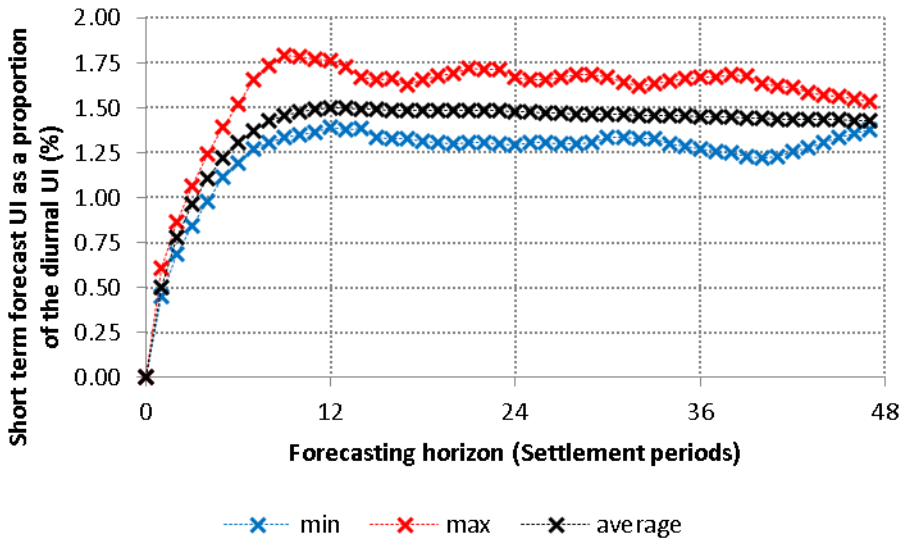

Figure 3-16 Proportion of the diurnal UI that can be reduced based on the existing 'here and now' known EV standard charging load and the forecasting horizon looking forward

Therefore the minimum and maximum bounds for which all values are expected to fall within can be estimated by (3.6).

$$P_{t,j}^{forecast} = L_t + D_{t,t+j} \pm n_j W_{t+j}^{diurnal\ standard\ charging} \qquad (3.6)$$

Where:

$P_{t,j}^{forecast}$	Expected uncontrolled EV charging aggregated load range at settlement period t, looking forward by j settlement periods, kW
L_t	'Here and now' uncontrolled EV charging load at settlement period t, kW
$D_{t,t+j}$	Difference between the longer term diurnal expected uncontrolled EV charging load at settlement period t and settlement period t+j, kW
n_j	Short term forecast UI of aggregated uncontrolled EV charging load as a proportion of the diurnal UI for a forecast horizon of j settlement periods, as shown in Figure 3-16, %
$W_{t+j}^{diurnal\ standard\ charging}$	Three times the standard deviation of the longer term expected diurnal aggregated uncontrolled EV charging load at settlement period t+j, kW

The method results in a ‘cone’ of increasing uncertainty, from zero uncertainty at the ‘here and now’, up to the full diurnal UI 1.5 hours ahead. This is shown in Figure 3-17 for a ‘here and now’ load at the mid-point of the diurnal expected range at settlement period 0.

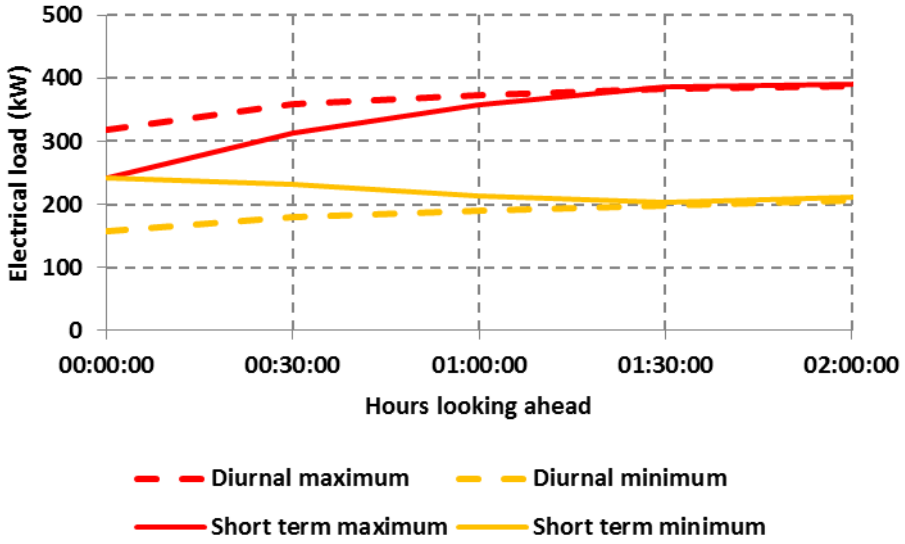

Figure 3-17 Cone of increasing uncertainty looking forward from settlement period 0, assuming the ‘here and now’ load is the mid-point of the diurnal expected range

To check the methodology and the formula given in (3.6), two forecasts have been developed using a ‘here and now’ load at the mid-point of the longer term diurnal expected range at settlement period 0 in Figure 3-18 and settlement period 30 in Figure 3-19. For each example, the maximum and minimum $\Delta L_{t,j}$ has been plotted relative to the ‘here and now’ value to demonstrate that the method works effectively when the ‘here and now’ load is at the mid-point of the diurnal expected range.

The methodology proposed means that if the ‘here and now’ load is higher than the midpoint of the diurnal range, then the forecasted minimum and maximum will be higher than the diurnal minimum and maximum respectively when looking forward more than 1.5 hours ahead. The assumption being made here is that all stochastic decisions are independent, which is a valid assumption regarding new vehicles arriving and their initial SoC. However, it is not necessarily a valid assumption regarding when vehicles leave since this is in part dependent upon arrival time and initial SoC. Therefore the methodology is appropriate when the aggregate ‘here and now’ load is close to the mid-point of the diurnal range. When the ‘here and now’ load is close to the extremes of that expected by longer term diurnal analysis, the method is expected to become less accurate of the true uncertainty bounds.

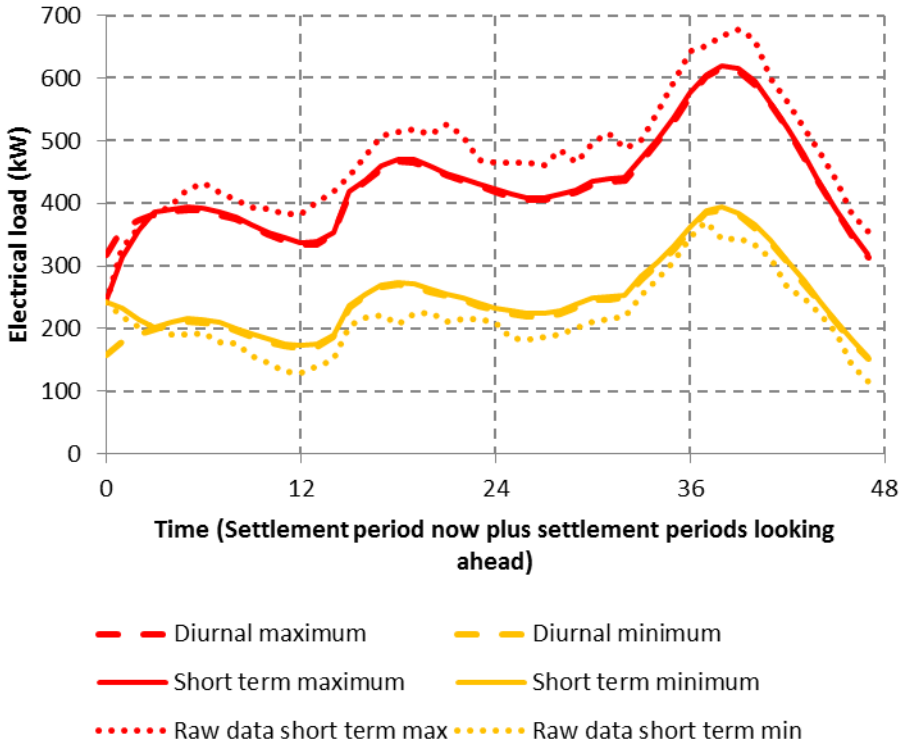

Figure 3-18 Derived short term forecast looking forward from settlement period 0 and the maximum and minimum experienced load relative to the 'here and now' load during all 1000 days of the monte-carlo simulation

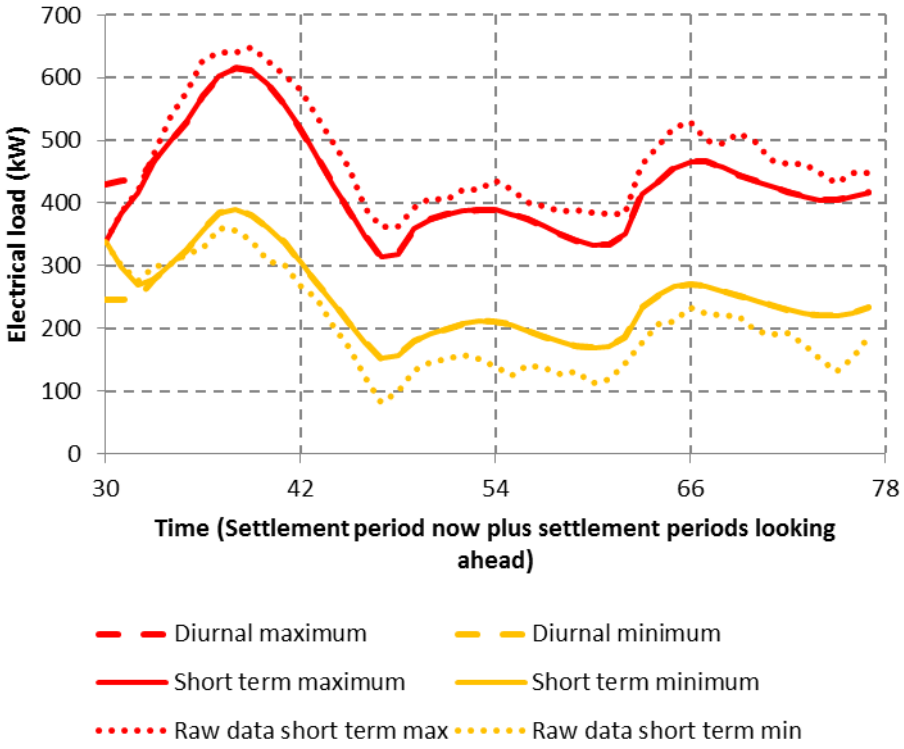

Figure 3-19 Derived short term forecast looking forward from settlement period 30 and the maximum and minimum experience load relative to the 'here and now' load during all 1000 days of the monte-carlo simulation

3.4.2 Uncontrolled rapid charging

To consider the uncertainty of forecasted rapid charging, the distribution of charge duration and the distribution of the time of arrival were taken from [128]. Similarly to Section 3.4.1 the analysis has been based on a MCS of 1000 days, however it is assumed that 100 EVs are rapid charging per day.

The UI has been calculated at each time of the day based on three times the standard deviation as was the case with standard charging. If this was an UI around the mean aggregated load however, then the expected minimum load would regularly suggest significant negative load, or V2G, which is clearly not appropriate. This is because of a higher aggregated load uncertainty caused by the larger charge point rating of the rapid charger, and a lower aggregated mean load because of only 100 EVs per day instead of the 750 EVs studied for standard charging in Section 3.4.1. The midpoint between the maximum and minimum load observed within the MCS was chosen as appropriate since it results in the diurnal minimum load being approximately zero (as opposed to negative) throughout the day. The resulting diurnal expected aggregate load range for the 100 rapid charging EVs each day is shown in Figure 3-20. As with Section 3.4.1, the load of each individual vehicle is calculated on a minutely resolution, and the diurnal expected range is shown in Figure 3-20 is calculated based on the average aggregate load over each 30 minute settlement period. Furthermore, it should be noted that the time of arrival and charge duration probability distributions used [128] are of early adopters, and could change as the market develops to a wide scale EV uptake scenario.

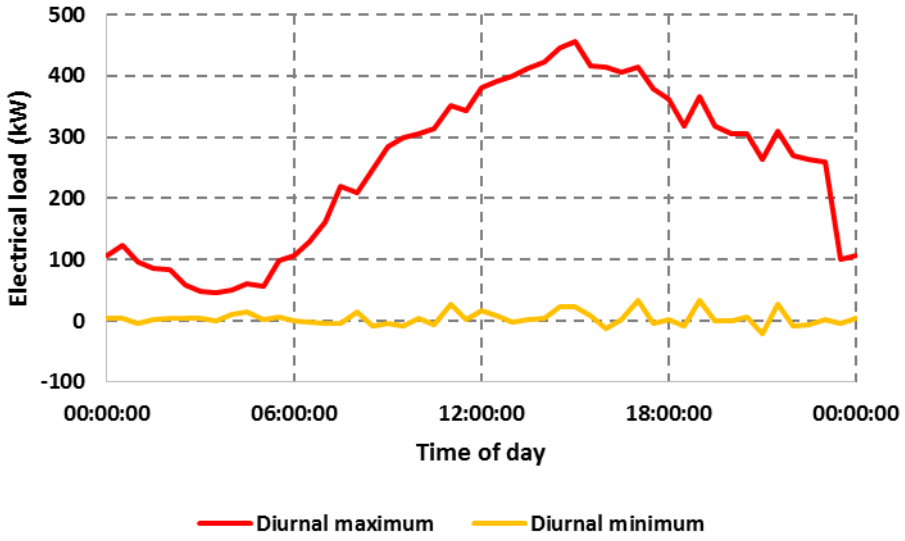

Figure 3-20 Load UI of 100 EVs rapid charging per day, using the arrival time and duration statistics in [128]

The same method used in Section 3.4.1 has been utilised to estimate the UI derating relative to the diurnal rapid charging load. This has been done on a 4 minutely resolution rather than 30 minutes, since EVs come and go much more frequently when rapid charging than standard charging. A 4 minute resolution was chosen since it was the smallest time step that could be calculated with the 4 GB RAM of computing resource available at the time of the calculation. The resulting proportion of the diurnal UI that can be reduced based on the existing 'here and now' known EV rapid charging load and the forecasting horizon looking forward is shown in Figure 3-21.

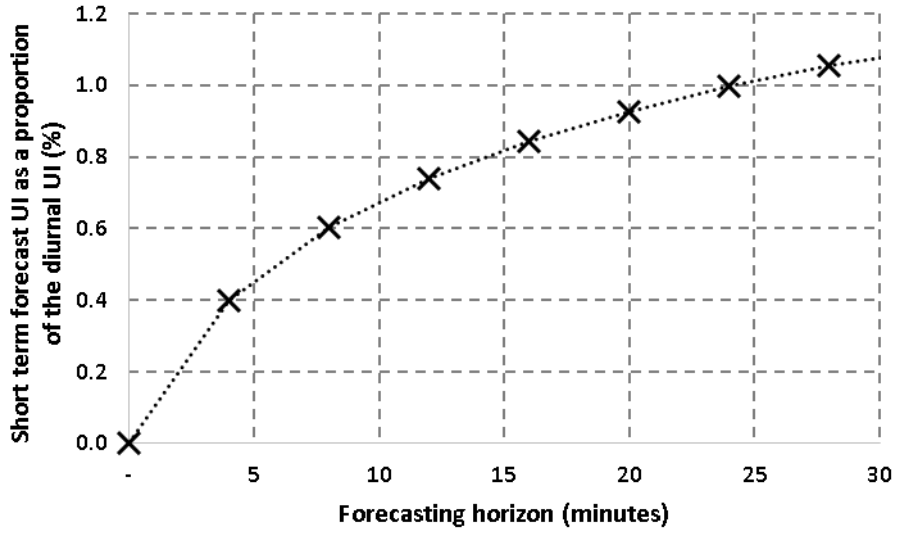

Figure 3-21 Proportion of the diurnal UI that can be reduced based on the existing 'here and now' known EV rapid charging load and the forecasting horizon looking forward

It can be seen in Figure 3-21 that the reduced uncertainty based on existing 'here and now' load can be determined up to 24 minutes ahead for rapid charging.

This analysis assumed that no queuing takes place which may not be the case in the future according to [70]. Knowledge regarding queue length may enable short term forecasting over a longer time period than 24 minutes.

3.5 Chapter conclusions and contributions to knowledge

A comprehensive study considering the complex interactions of real world measured domestic EV charging load and measured domestic household load has been investigated, for its impact on transformer thermal loading, voltage magnitude and voltage unbalance. This is the first such study that the author is aware of that has investigated these impacts using real world measured EV charging loads. It was identified that the first constraint likely to impact EV uptake is the thermal limit of the transformer, however it was also shown that the average load

at 100% EV penetration was below the transformers limit suggesting that ESS or smart charging could potentially be a solution. Furthermore, the cost of upgrading the network if smart charging was not implemented was estimated for wide-scale EV uptake in the UK. This is the first study to investigate the allowable cost to the consumer of upgrades associated with wide-scale EU uptake, taking into account the individual network characteristics of each DNO. This cost also represents the potential maximum value that is economical for DNOs to pay smart charging EV aggregators over the typical life of a reinforced network asset to compensate them for delivering services to offset the reinforcement.

A methodology has been developed to forecast uncontrolled EV charging load, and the uncertainty around that forecast dependent upon the time looking forward. After around 1.5 hours, the uncertainty is as wide as that which could be determined by long term diurnal analysis for standard charging. For rapid charging, the time at which the uncertainty is as wide as that which could be determined by long term diurnal analysis is 24 minutes. The smaller the forecast horizon, the smaller the UI was observed. For both standard and rapid charging, the analysis was undertaken for a set number of vehicles per day. If this were to change, the level of diversity would change resulting in different levels of uncertainty. It is unknown to what extent this would impact upon the reduced UI that can be determined from a short forecast horizon, and is an area for potential future research.

Chapter 4 Available flexibility of electric vehicles

4.1 Introduction

The approach adopted in this Chapter is to determine the power range flexibility, and duration over which it can be maintained, that can be reliably called upon from EVs in aggregate to form a VESS. Using the VESS as an input to wider microgrid control systems has advantages over considering the EVs individually through reduced computational challenge leading to better scalability with EV uptake, while also enabling the microgrid control algorithms to optimise the EV power demand flexibility alongside other forms of power flexibility.

The available power and energy flexibility that could be called upon from an EV fleet in aggregate is investigated in Section 4.2. An algorithm to control the energy management within the EV fleet to achieve the flexibility is developed in Section 4.3, before being tested in relation to a work based car park in a case study in Section 4.4. This work was presented at the CIRED conference in 2017 in Glasgow, with the oral presentation available to watch online on IET TV [129] and the associated paper was published in the subsequent CIRED journal [130].

An algorithm to utilise the work based car park within a VPP delivering an EFR service to the wider grid is then developed in Section 4.5. This work was published at the CIRED workshop in 2016 in Helsinki [131].

The Chapter and how it fits within the Thesis as a whole is summarised in Figure 4-1

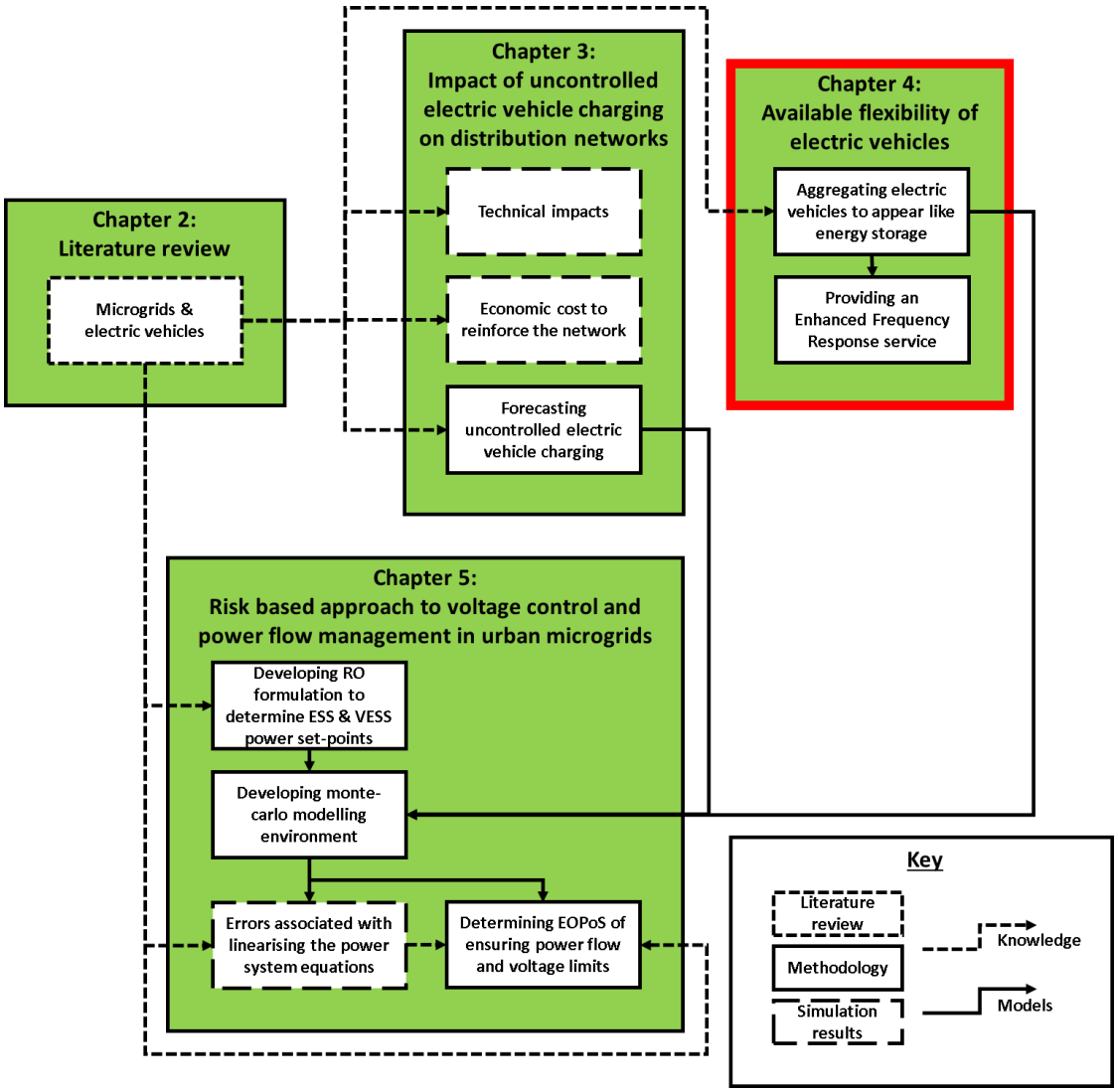

Figure 4-1 How Chapter 4 fits into the wider Thesis

4.2 Aggregated power and energy flexibility from an electric vehicle fleet

In order for EVs to be considered as a VESS, the equivalent energy capacity and power rating of the fleet in aggregate must be established. Provided the energy management within the EV fleet ensures no vehicle reaches a SoC limit before any other vehicle, the aggregate maximum and minimum power and energy demands can be defined as follows:

- The maximum potential power demand is the sum of all the charge point ratings where vehicles are plugged in.
- The minimum potential power demand (or maximum V2G supply) is the sum of all the charge point V2G ratings.
- The maximum potential energy demand is 100% minus the present SoC, multiplied by the battery capacity.
- The maximum potential energy supply is the present SoC, multiplied by the battery capacity.

Since the arrival time, arrival SoC and departure time are all stochastic [21] for which the aggregate power and energy are dependent; the aggregate power and energy flexibility is also stochastic.

4.3 Electric vehicle fleet energy management

The algorithm developed to control the internal energy management of the EV fleet to form a VESS is shown in Figure 4-2 and described next. A deterministic rule based algorithm has been developed for fast real time implementation without requiring, or potentially in the absence of, certain knowledge of future grid requests.

In any EV flexible charging algorithm, it must be ensured that all vehicles have sufficient energy at departure; otherwise consumers will not charge their EVs by plugging into a charger utilising the control strategy. How the EVs get to that minimum SoC at the time of departure is irrelevant (if neglecting battery degradation issues). Therefore, if a vehicle requires its charge point's fully rated demand to achieve the minimum SoC in the time remaining before departure, this is allocated to those vehicles. The remaining power requirement to meet that requested of the VESS must then be shared between all other vehicles.

In being sympathetic to battery degradation, the remaining power required should be shared between as many vehicles as possible. In that way both C-rates and V2G-induced additional cycles' depths of discharge are kept to a minimum. The downside to this simple concept is that those vehicles that have an initially high SoC can easily reach 100% SoC resulting in them losing the ability to demand power. To reduce the occurrence of this situation, when the remaining required aggregate power is charging power, it is averaged between only the EVs that are presently below the SoC required at departure. Those vehicles with a SoC above the minimum at departure only demand power if additional aggregated power is required to meet the grid request. When V2G power is required in aggregate, the power is shared between all vehicles that do not require fully rated demand to meet the minimum SoC at departure, regardless of their SoC.

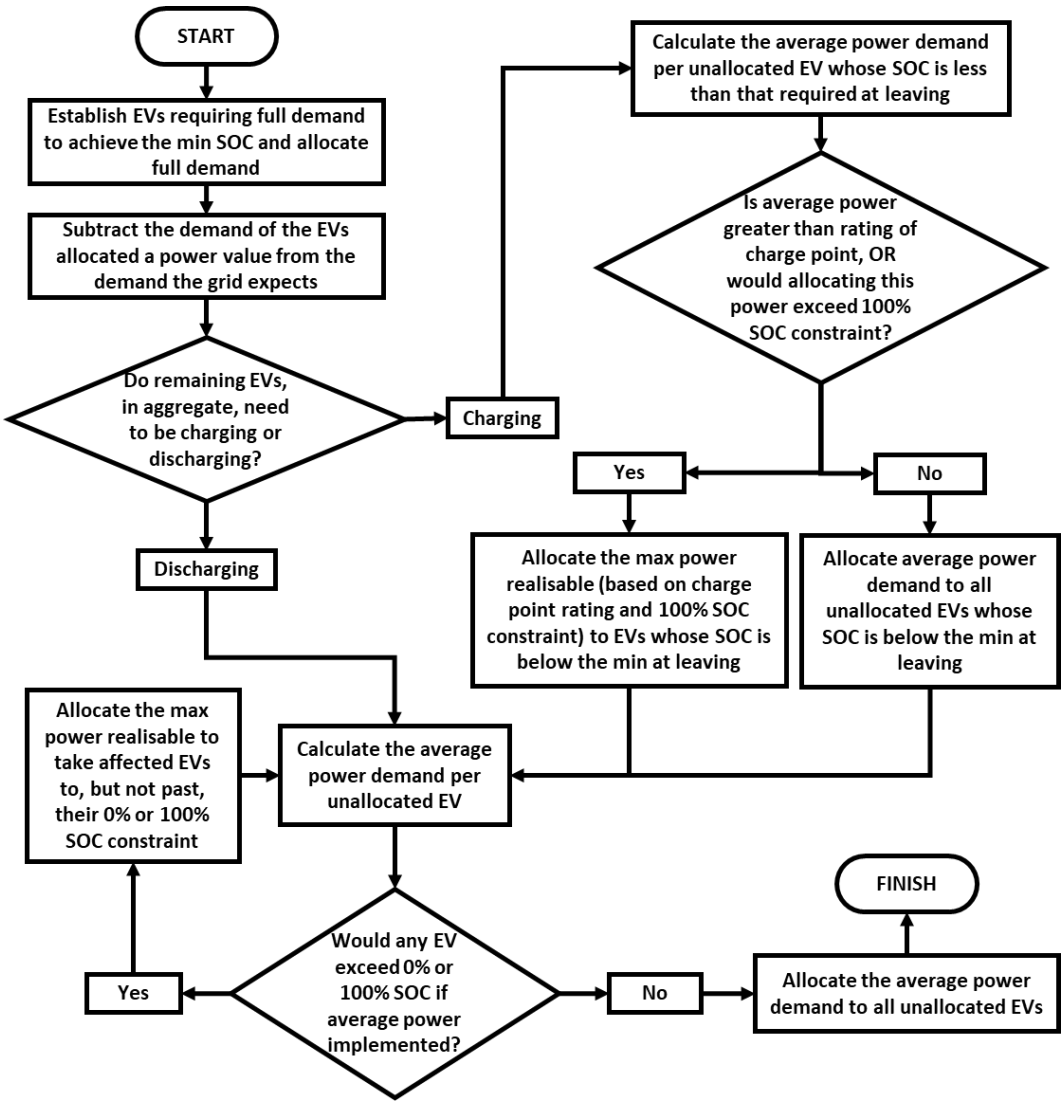

Figure 4-2 Algorithm deciding individual EV power exchange

By actively controlling the charging process, there will inevitably be an impact on the EV battery degradation and consequentially an economic impact on the EV owner. This cost is very difficult to quantify, and an active area of research in its own right. A qualitative assessment of the impact is given below, based on the battery degradation characteristics described in Section 2.3.1.

Additional cycling: With the proposed control algorithm, it is expected that an individual vehicle will rarely give up energy to charge another vehicle via the grid, and in most cases will only act as V2G when the aggregate power requirement of the grid is from the VESS and to the grid. Therefore additional charging cycles, causing additional degradation, are likely to only be created when the aggregate power required is V2G.

Charging rates: At present, vehicles charge at the rating of the charge point. In the proposed algorithm, the averaging of power across all vehicles reduces the charge rate meaning that the

battery degradation through charging could be expected to reduce, relative to present charging arrangements.

State of charge: By charging at a rate lower than the charge point rating, or using V2G, the SoC will be at a lower level relative to uncontrolled charging. This results in a reduced degradation effect on the battery.

Overall impact: It is expected that charging flexibility can be realised, using the algorithm presented, with reduced degradation in the majority of situations relative to uncontrolled charging. If the VESS is supplying power to the grid then an increase in degradation could be expected.

4.4 Case study: work based car park

In this case study, the VESS is applied to a work based car park and the response to two grid defined power set-point profiles is tested. The car park characteristics are described along with the resulting power and energy availability of the VESS in Section 4.4.1. The response to the two power set-point profiles is then tested in Section 4.4.2.

4.4.1 Characteristics of the work based car park

Consider an EV charging station with 50 spaces at a work-based site. The number of vehicles arriving in a day is assumed to follow a normal distribution, with a mean of 45 and standard deviation of 3. The arrival time for each vehicle is established using a normal distribution, with the average car arriving at 09:00 with a standard deviation of 1.2 hours. Similarly for departure time, a normal distribution is used with the average car departing at 18:00 with a standard deviation of 1.2 hours. This is consistent with the weekday modelling approach used in [107]. A more detailed statistical analysis of EV charging times was undertaken in [21]. The SoC on arrival is based on the SwitchEV project [16] and is established using a normal distribution with an average of 53% and a standard deviation of 15%. The battery capacity of all vehicles was assumed to be 24 kWh, with a requirement for 80% SoC on departure. It was assumed that the charge rating is 7 kW and V2G rating is 3 kW.

A model of the work based car park was developed in Python based on the statistical distributions described and calculated based on a time-step of 1 minute. Based on a MCS of 1000 days, the stochastic maximum and minimum aggregate power demand percentiles of the parked EV fleet is shown in Figure 4-3 and Figure 4-4 respectively.

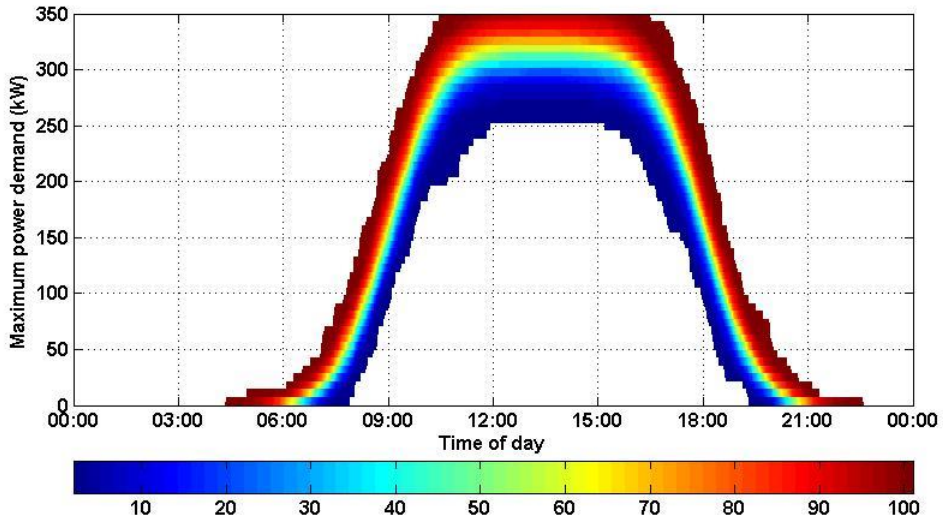

Figure 4-3 Maximum aggregate power demand percentiles of the VESS on the grid

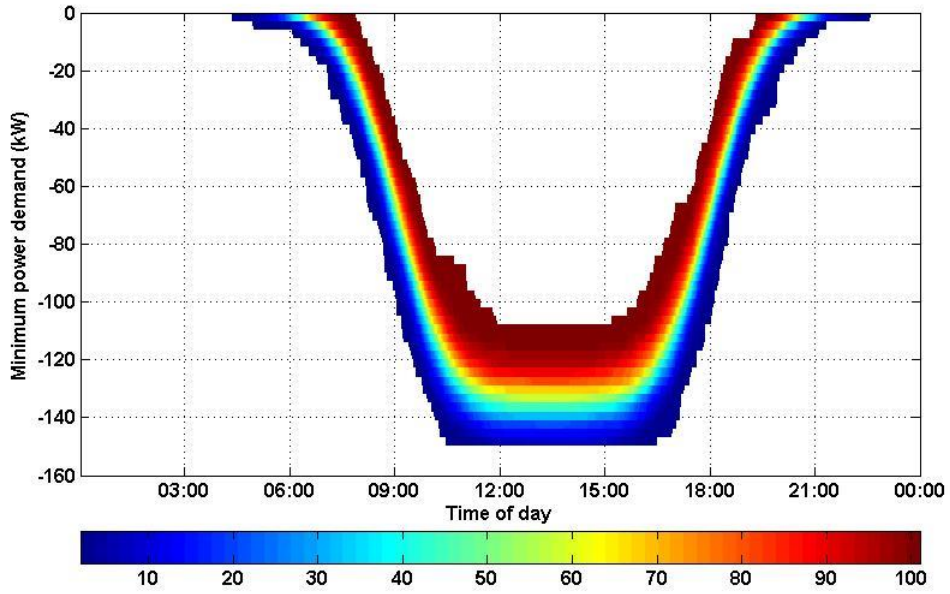

Figure 4-4 Minimum aggregate power demand (or maximum power supply) percentiles of the VESS on the grid

If the higher level controller of VESS output can handle uncertainty, such as that proposed in [54], then a greater level of flexibility can be utilised than if the VESS alone is being relied upon to ensure the robustness of the network against thermal and voltage limit violations. In such a situation where the EVs are being fully relied upon, then the VESS power should be limited to the region bounded by the minimum of Figure 4-3 and the maximum of Figure 4-4. This could be considered somewhat pessimistic and in this Chapter the 5^{th} and 95^{th} percentiles have been used as the maximum and minimum bounds, respectively, giving a 90%

confidence. A 90% confidence interval was chosen as it corresponds to the qualitative term ‘almost certain’ [132].

Figure 4-3 and Figure 4-4 assume that no vehicles have reached their SoC limits and can contribute their fully rated power. This may not be the case depending on the internal energy management of the EV fleet, and the previously called services of the VESS by the grid controller.

The percentiles of maximum and minimum aggregate energy available based on the arrival SoC as determined by the stochastic modelling and a departure SoC of exactly 80% for all vehicles is shown in Figure 4-5 and Figure 4-6, respectively. To achieve a 90% confidence of delivering to the grid what is requested, the energy exchange should remain within the region bounded by the 5th percentile in Figure 4-5 and the 95th percentile in Figure 4-6. These two lines cross shortly after 18:00, however making it impossible to achieve. This is due to the assumption that all vehicles leave with exactly 80% SoC in the figures, which may not be exactly true depending on the internal energy management of the EV fleet and the number of vehicles parked on any particular day. Instead the range should consider the potential for some vehicles to leave with more than the minimum 80% SoC and as such the 5th percentile in Figure 4-5 is taken to not reduce once it reaches its maximum value and corresponds to all the vehicles having 100% SoC or less on leaving, 95% of the time, assuming the internal energy management ensures all EVs would reach 100% SoC at the same time.

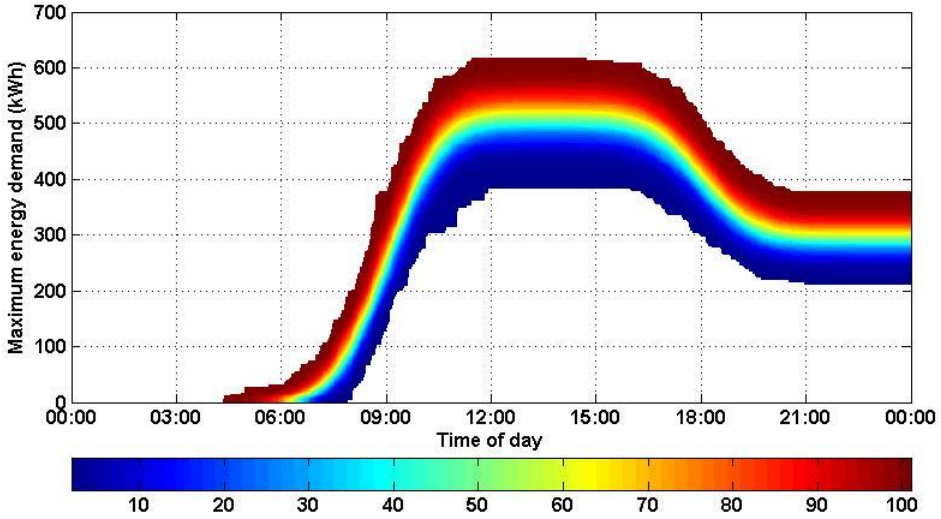

Figure 4-5 Maximum aggregate energy demand percentiles of the VESS on the grid

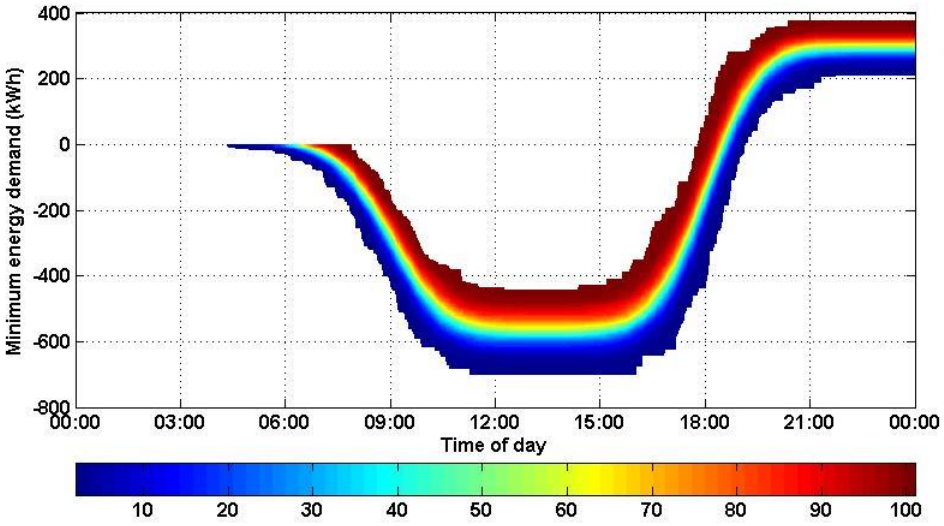

Figure 4-6 Minimum aggregate energy demand (or maximum power supply) percentiles of the VESS on the grid

4.4.2 Response of the VESS

Using the power and energy bounds defined from the probabilistic analysis in Section 4.4.1, two possible VESS service requests have been developed within MS Excel. Profile A is shown in Figure 4-7 and displays a low constant load while profile B shown in Figure 4-8 displays higher load variability while reaching the defined power and energy bounds numerous times throughout the day.

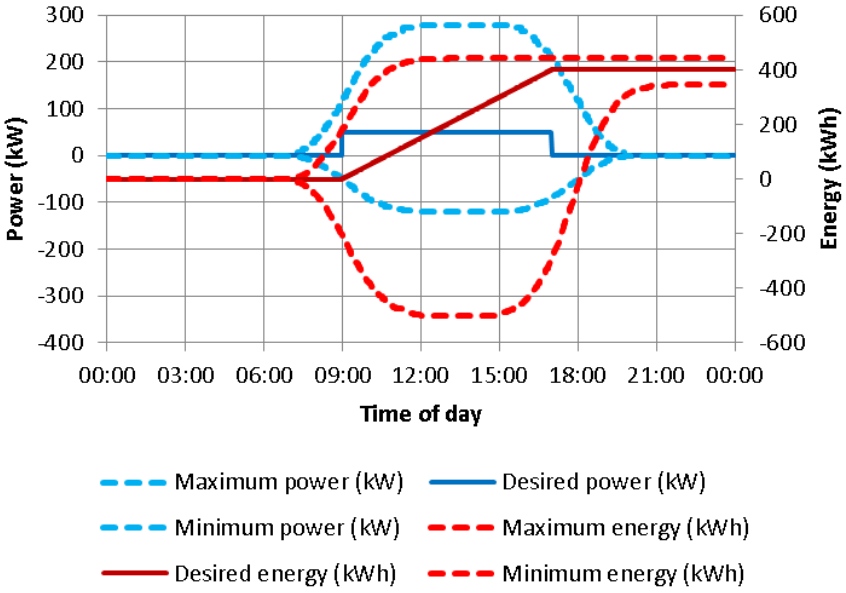

Figure 4-7 Grid power decision, Profile A: Low constant load

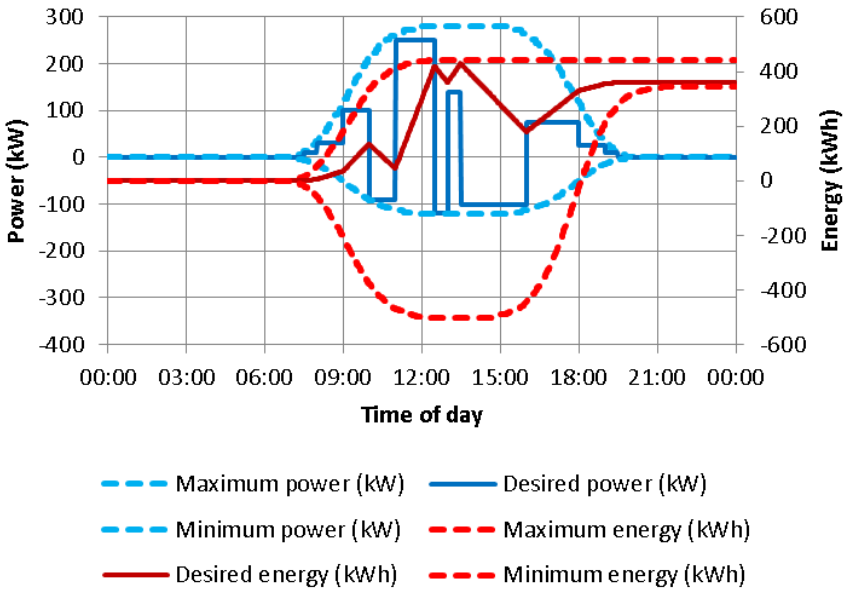

Figure 4-8 Grid power decision, Profile B: High variability load reaching both power and energy bounds

For each VESS power profile, 1000 days of MCS was undertaken using the Python model as described previously in Section 4.4.1 and the internal energy of the EV fleet is managed using the control logic of Figure 4-2. The realised percentiles of power delivered to the grid within the MCS is shown in Figure 4-9 for profile A and in Figure 4-10 for profile B. In both profiles, the grid demanded output is realised in the majority of cases, and when it is not then the value delivered is often close to that requested. Over the full day, the probability of realising profile A was 99.98% and the probability of realising profile B was 98.83%.

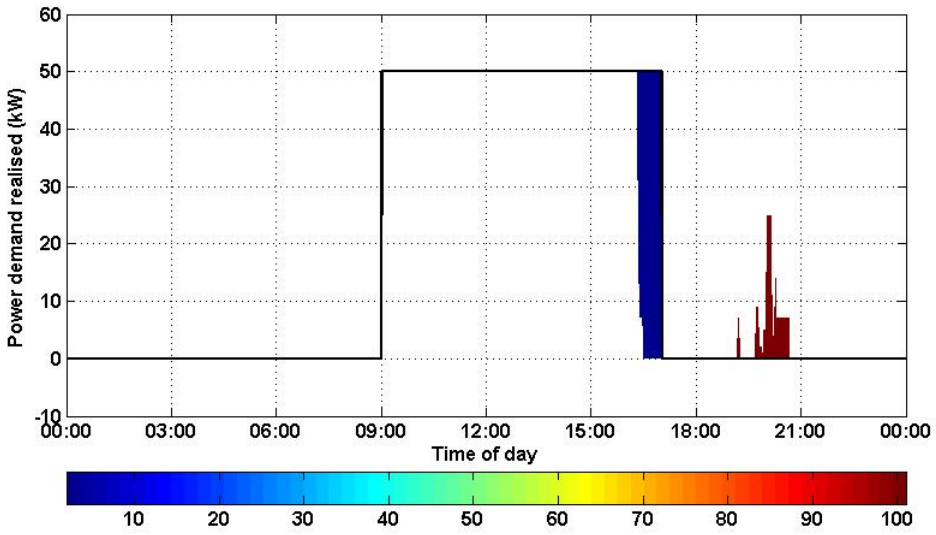

Figure 4-9 Resulting power percentiles delivered to the grid, Profile A: Low constant load

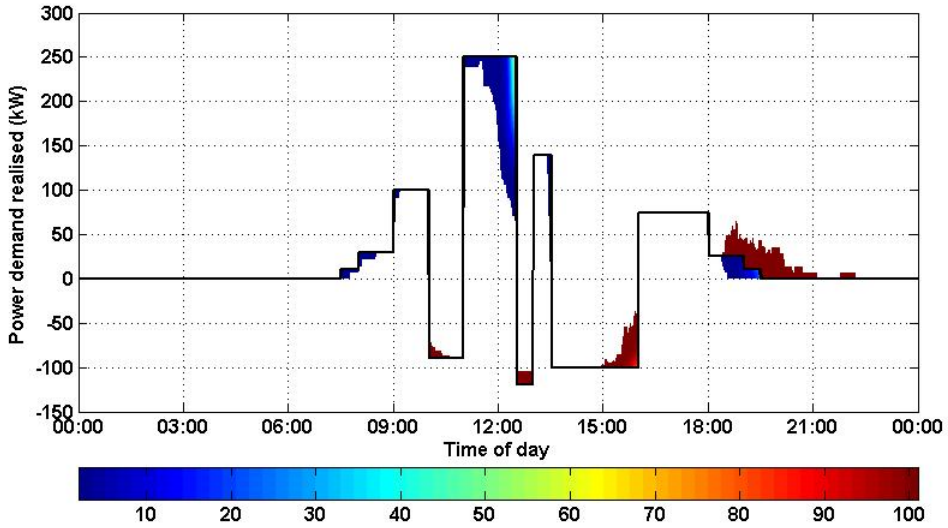

Figure 4-10 Resulting power percentiles delivered to the grid, Profile B: High variability load reaching both power and energy bounds

In Figure 4-9 at around 16:20, there are some days within the MCS that the VESS was unable to deliver the service requested by the grid. It is unlikely to be as a result of vehicles leaving earlier than normal because the power demanded is significantly below the maximum power bound in Figure 4-7. The energy delivered to the VESS is, however, relatively close to the maximum energy bound and as such the loss of control is due to some vehicles reaching 100% SoC and being unable to demand any further energy. Additional power is demanded on some days within the MCS at around 20:00. This is because the SoC of some EVs are below the minimum at departure when the desired VESS demand is zero.

In Figure 4-10, the power delivered around mid-day is less than that requested of the VESS. This is likely to be due to some days within the MCS having either too few EVs, or EVs reaching 100% SoC, or a combination of the two, since both desired power and energy are close to the bounds at this point in time in Figure 4-8. In a similar way to that described for profile A, there is a limited loss of control at around 19:30 when the EVs start to leave, where the VESS request is close to both the power and energy bounds.

From these studies, it can be concluded that there is a high degree of controllability of the VESS for the majority of the day. When vehicle numbers reduce to very low numbers, the EV fleet becomes less reliably controllable. If the car park was located where new EVs were always arriving as suggested in [21] then this limited loss of control would be reduced, however new vehicles always arriving would make it more difficult to know the available energy, or Virtual State of Charge (VSoC). In the case study shown there is always a recalibration point at the start and end of the day when there are zero vehicles in the car park.

The closer the energy delivery is to the mid-point of the upper and lower energy bounds in Figure 4-7 and Figure 4-8, the less likely and severe the reduced controllable period becomes. To consider an extreme case of the reduced controllable period of the day, one further study has been conducted whereby the VESS is requested to demand no power throughout the full day. It results in the EVs all waiting until the last moment to charge, and then do so at full charge point rating. The resulting power demand percentiles of the VESS are shown in Figure 4-11. This is similar to the load profile that could be expected from uncontrolled charging for the work based car park, but at the end of the day rather than at the start when the vehicles arrive.

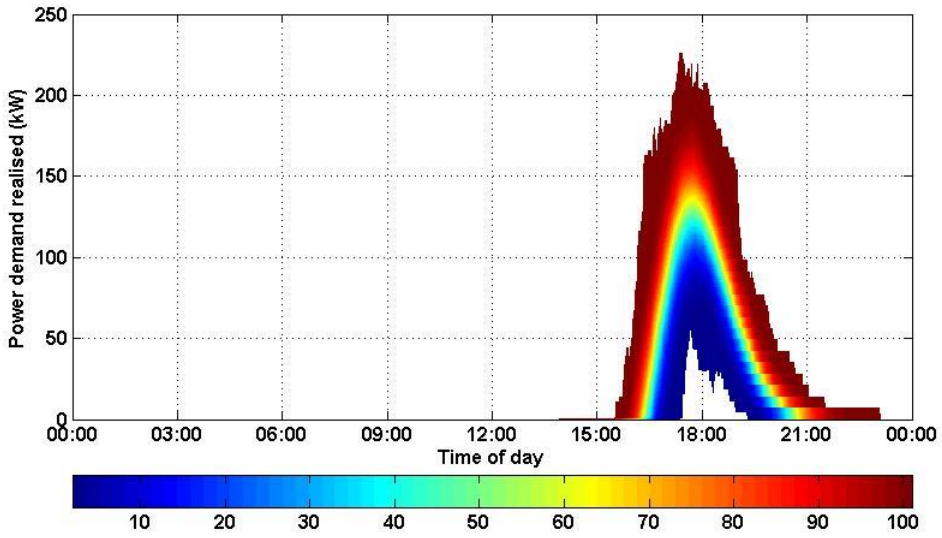

Figure 4-11 Uncontrolled charging demand percentiles at the end of the day resulting from no energy delivered throughout the day

4.5 Case study: VESS of EVs within a VPP delivering frequency response services

In this section, the ability of the VESS developed in Section 4.4 to support frequency response services is investigated within the context of a real VPP being developed in Newcastle-Upon-Tyne, UK. The required response of the VPP is described in Section 4.5.1 and the VPP is described in Section 4.5.2. A control algorithm for the VPP is developed in Section 4.5.3, before its ability to deliver the EFR service from the VPP is investigated in Section 4.5.4 using a MATLAB Simulink model replicated in Appendix C.

4.5.1 Response required of the VPP to deliver an EFR service

EFR is a new market to help maintain system frequency and started operating Winter 2017/18. The required response is dependent upon system frequency, as shown in Figure 4-12. The service allows an envelope of deviation from the set point curve, widening around

the normal operating frequency. This is designed to enable SoC management, however in 2016 when this work was undertaken the magnitude of this range was still to be determined by National Grid. The output must be delivered within 1 s of being called, and support the grid for at least 9 s until the primary FFR service can take over.

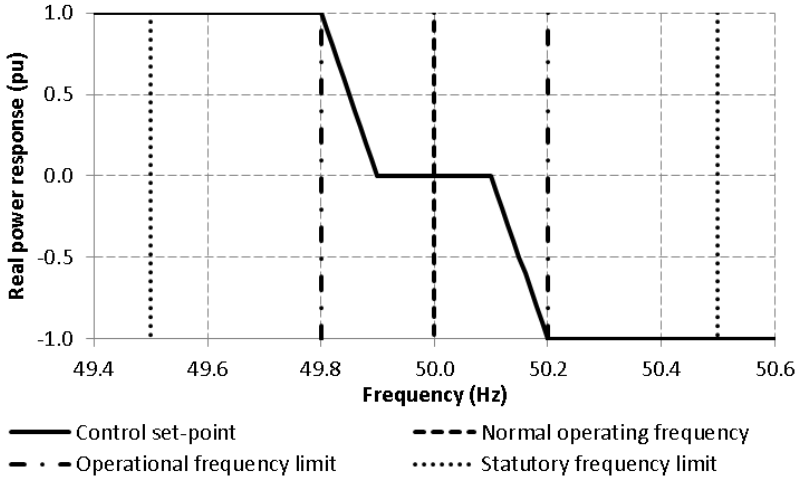

Figure 4-12 Service requirements for EFR (as of 2016) [133]

4.5.2 VPP description: Newcastle Science Central

Newcastle University and Newcastle City Council, are collaborating to redevelop a 24 acre city centre brownfield site to be an exemplar sustainable urban environment encompassing Smart Grid technologies throughout [134]. Electrically, the site will contain an ESS [135], an EV charging station, a CHP plant, solar PV generation and both residential and commercial buildings with the potential to provide DSR [134]. The proposed electrical distribution of the site is shown in Figure 4-13.

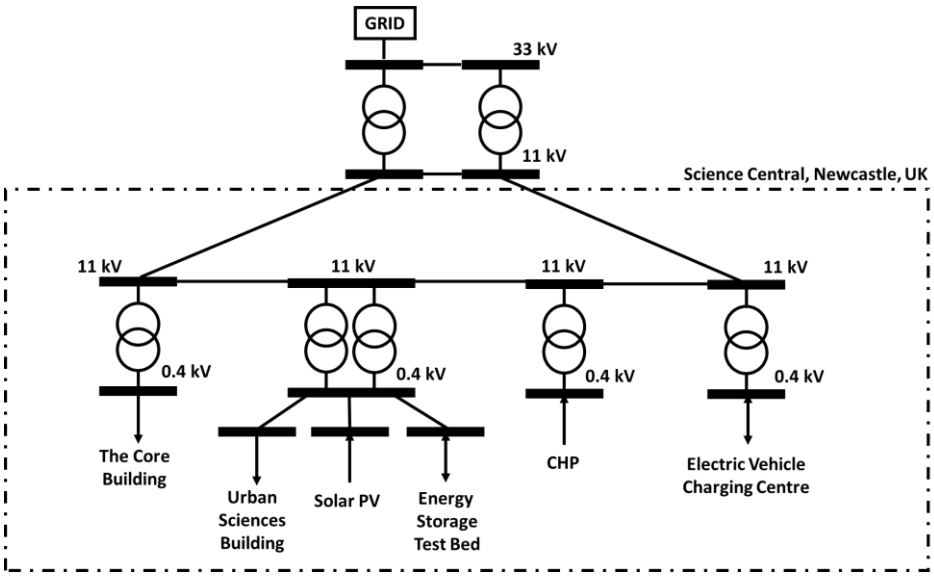

Figure 4-13 Proposed electrical distribution of phase 1 of Science Central, Newcastle, UK

There is considerable choice in how to control each of these flexible assets in order to provide services to the grid at the point of connection whilst also providing value to the various stakeholders on the site. The characteristics of the ESS is described in Section 4.5.2.1, the CHP in Section 4.5.2.2, the smart charging EVs in Section 4.5.2.3 and the DSR potential of the Core and Urban Sciences Building (USB) are described in Section 4.5.2.4. The characteristics of all flexible assets on the site are summarized in Table 4-1. These characteristics are based on the expectations of the site when this work was undertaken in 2016, and since then there has been considerable development of the site.

Table 4-1 Summary of flexible asset characteristics on Science Central

	Min power (kW)	**Power to maintain constant VSoC (kW)**	**Max power (kW)**	**Energy capacity (kWh)**	**Time to charge 0% to 100% VSoC (minutes)**
ESS	-360	0	360	100	17
CHP	0	-	2000	-	-
EV charging (at 12:00)	-120	0	280	1077	231
The Core DSR	0	31	70	9	14
USB DSR	0	240	500	69	16
Aggregation of the whole site (at 12:00)	-480	271	3210	1255	-

4.5.2.1 Energy storage

The ESS will be built to allow different cell chemistries to be evaluated in response to real grid disturbances and new control algorithms. The inverter is rated at 360 kVA, and is assumed to have a storage capacity of 100 kWh.

4.5.2.2 Combined Heat and Power

A gas turbine CHP plant will be built with an electrical rating of 2000 kW and heat rating of 6000 kW. Since the gas will be supplied via the national gas networks, it is assumed that this power can be supplied at all times. The heat generated will supply a heat network on the site which is not the subject of this Thesis.

4.5.2.3 Electric vehicle charging station

The site is to have six rapid EV chargers, and it is possible that adjacent to these will be a smart EV charging station, similar to the VESS proposed in Section 4.4. The individual vehicle modelling is not modelled in this Section, and it is assumed that the EV fleet in aggregate can deliver what is requested provided the power and energy remain within the defined aggregated power and energy bounds.

4.5.2.4 Building demand side management

As the site progresses, numerous commercial and residential buildings will be erected to include HVAC DSR capabilities. The first two building on site have now been opened; The Core, and the USB.

Both buildings are to be heated using electrical pumps and the site heat network. The heat model of Figure 4-14 was implemented in MATLAB Simulink for both buildings to control the electrical demand of the heating system while calculating the temperature response from DSR calls to be estimated. It was assumed the air condition deterioration takes place at the same rate as the heat energy dissipates to the external atmosphere.

For the purposes of this study, it was assumed that the Core needs 31 kW and the USB needs 240 kW to maintain a constant temperature and air condition, based on an engineering judgement that HVAC DSR can achieve up to 33% reduction in a buildings demand [136]. The minimum power for each building was set to 0 kW (representing an effective generating power of 31 kW and 240 kW respectively). The maximum power demand was set to 70 kW for the Core and 500 kW for the USB. For an allowable temperature variation of 4°C, the model estimated the Core and USB to have an effective storage capacity of 9 kWh and 23 kWh respectively.

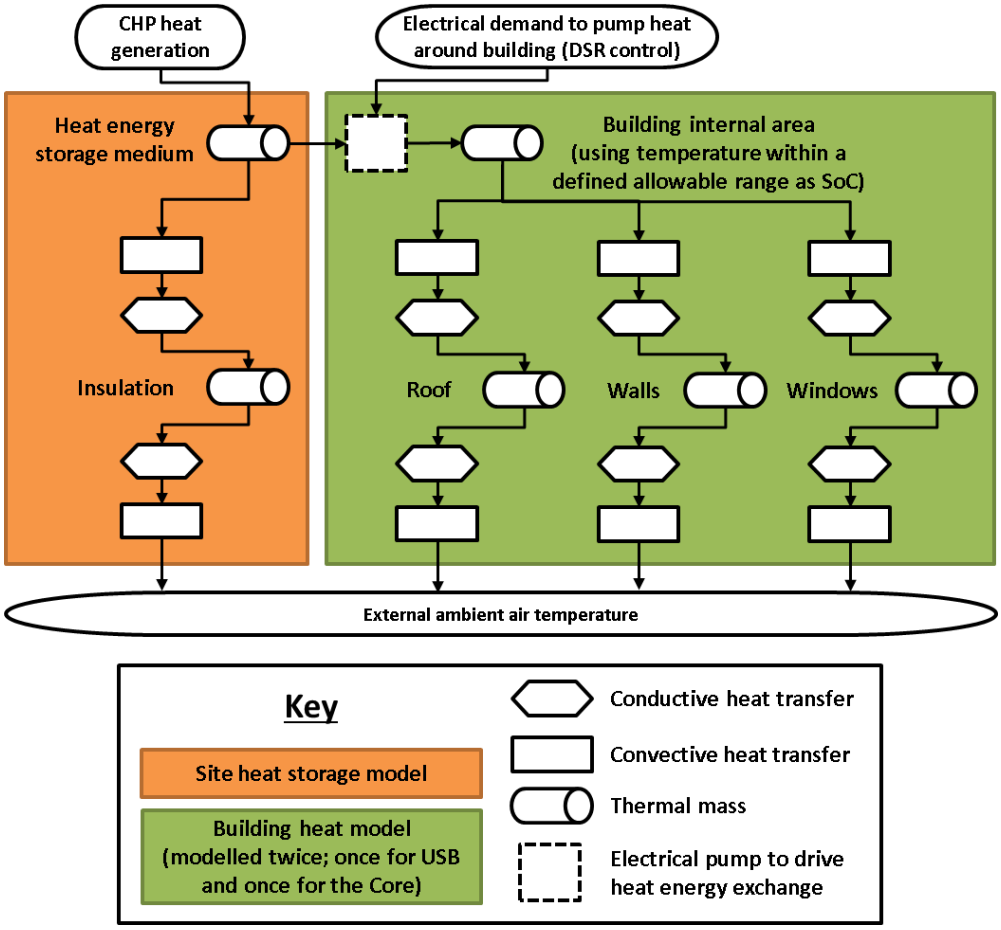

Figure 4-14 MATLAB Simulink heat model

4.5.3 VPP control to maximise aggregate power availability

The EFR service requires full requested output to be delivered for at least 9 seconds with just one second of notice. Despite this short duration, National Grid's initial analysis of frequency data indicates that the optimal battery capacity is that which corresponds to a 45 minute duration (0%-100%) [133]. It can be seen in Table 4-1 that only the EVs, which are not available at all times, have a duration above this. All the other assets have a duration significantly below 45 minutes. A control scheme has been developed to combine the high power ratings of the DSR and ESS with the high energy rating of the EVs, through intelligent energy management to ensure that the aggregate maximum power of the site is realisable, with little to no notice. The control scheme is designed to be scalable such that any flexible asset can be utilised. Each asset is considered in a form similar to ESS and the equivalent VSoC is used as a common currency across the different types of assets with varying characteristics, that could otherwise be difficult to compare like for like.

In order to realise a power request, an asset must have energy available within its storage. By targeting 50% VSoC, an asset without any prior knowledge of the service can maximise the amount of time a power request can be delivered for. During the service however, the VSoC

will deviate from 50% at varying rates for each asset dependent upon their power and energy ratings. To maximise the power availability, all assets should approach their energy capacity limits at the same time. To implement these ideas, the time each asset can deliver maximum (positive or negative) power for is considered. The asset that can deliver for the longest period of time is used primarily for its energy and no target VSoC is set. All other assets are used primarily for their power and assigned a 50% VSoC target, unless the energy asset is approaching its VSoC limits in which case the energy of these assets is needed. In this situation, the power assets are assigned a VSoC target that would result in reaching their VSoC limit at the same time as the energy asset.

A single fuzzy logic control surface is used multiple times, once for each asset as shown in the block diagram of Figure 4-15. Fuzzy logic allows multiple variables to be considered at once, similarly to human thinking, and an intelligent decision to be made [137]. In this implementation, it ensures the overall requested microgrid power is delivered whilst managing the internal energy of individual assets to be as close as possible to their respective VSoC targets. Each controller has three inputs:

- Output power – the output of the asset's fuzzy logic controller is fed back as a reference signal to be increased or decreased based on the error and SoC difference.
- Error – the power outputs of all assets are summated and compared against the total microgrid desired power output. The resulting error is fed into all fuzzy logic controllers.
- SoC difference – the difference between an assets VSoC and its target VSoC.

Fuzzy logic rules were created to prioritise the reduction of the error so the correct power output is delivered. At high power requests the error is picked up faster or slower depending on the SoC difference. When the power request and error are both low, the rules try to reduce the SoC difference. Therefore, a secondary control brings all assets towards their target VSoC if possible. The 4-dimensional control surface, with axes in per unit, is shown in the three 3-dimensional figures of Figure 4-16.

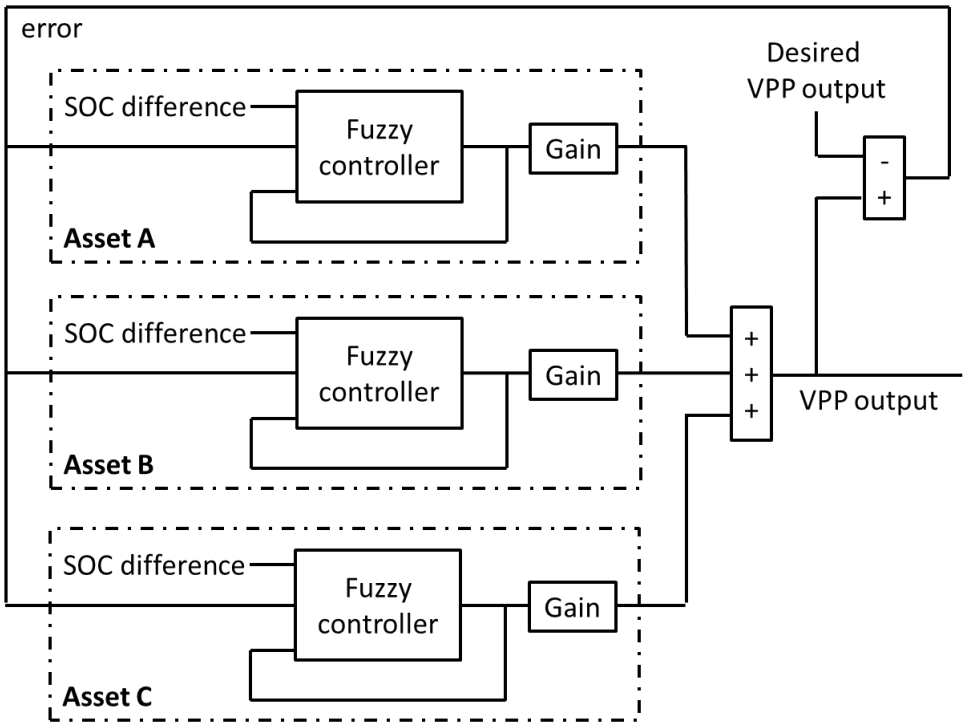

Figure 4-15 Block diagram of the scalable fuzzy logic based control

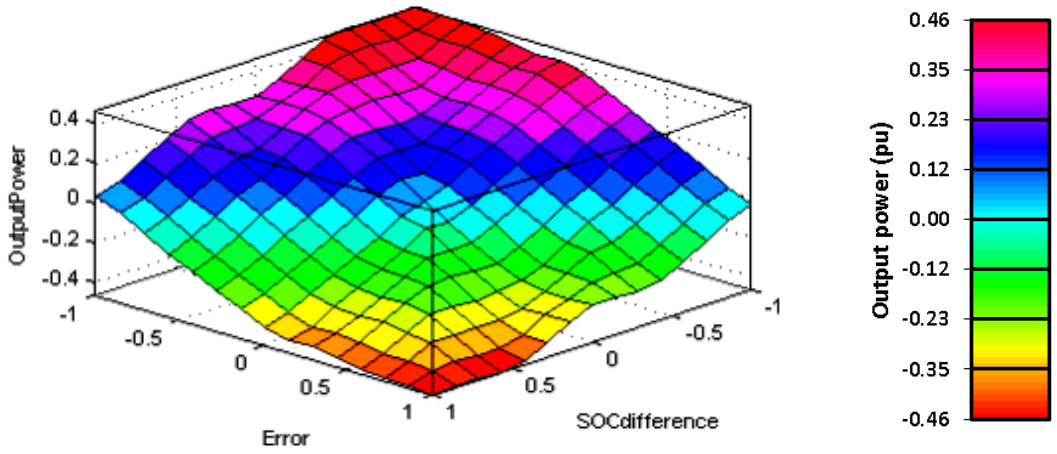

A: Output power based on error and SoC difference, when feedback output power is at 0 pu

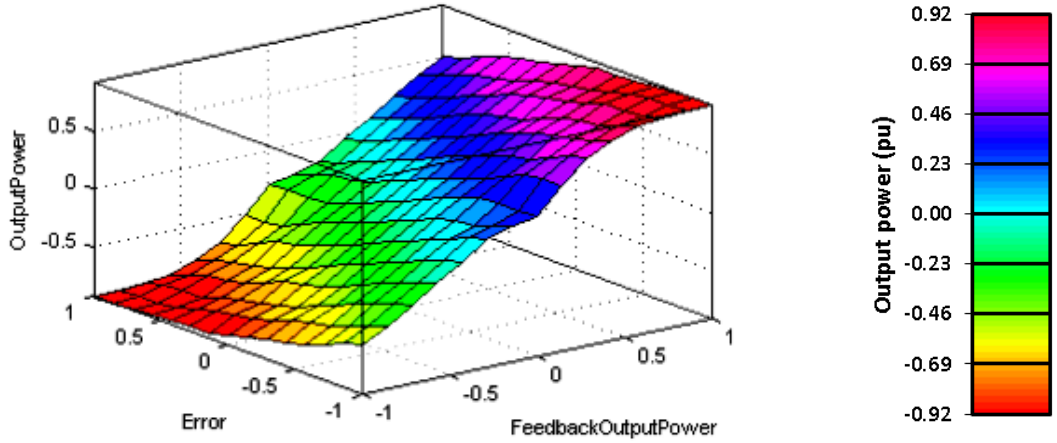

B: Output based on error and the output power feedback, when SoC difference is 0 pu

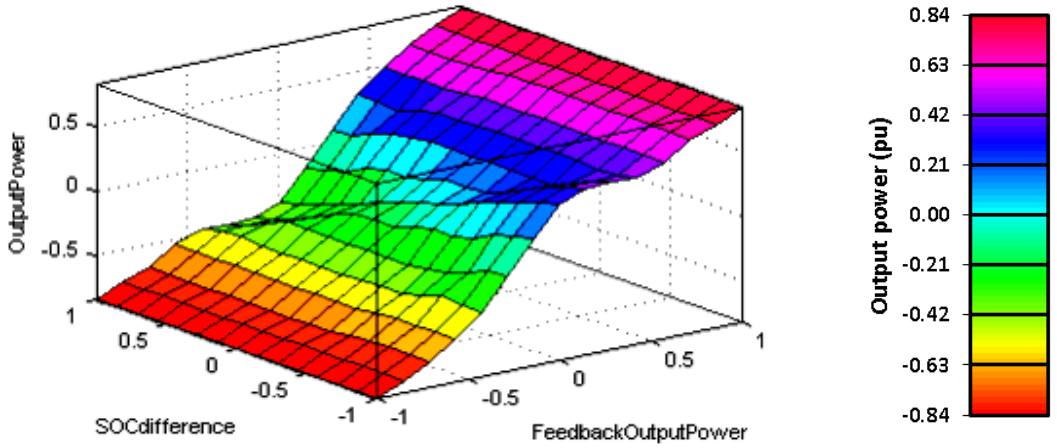

C: Output power based on SoC difference and the output power feedback, when error is 0 pu

Figure 4-16 Fuzzy logic 4-dimendisonal control surface displayed as three 3-dimensional control surfaces; A, B, C (all axes per unit)

4.5.4 Ability of the VPP to deliver the EFR service using the developed control algorithm

In order for potential EFR providers to demonstrate their offering, National Grid has published system frequency data at a one second resolution. One representative day has been simulated using this data, in conjunction with Figure 4-12 and the proposed control algorithm.

The aggregate load of the VPPs flexible assets is shown in Figure 4-17 along with each assets VSoC. The same study was undertaken without managing the VSoC of the assets, shown in Figure 4-18. During the day of simulation there were 11 minutes when a service could not be realised, during which the service was requested for 5 minutes. The deadband of Figure 4-12 could have been used to ensure VSoC when the assets are operating individually and without coordination, however with the proposed algorithm this is not required meaning the deadband could be used to layer other commercial services, thus increasing revenues. Furthermore, it can be observed in Figure 4-17 that the VSoC for the ESS, Core and USB remain close to 50% with a relatively large headroom of storage capacity unutilised. This suggests that by using the proposed control algorithm either; the storage capacities could be minimised reducing initial capital expenditure, or power ratings increased maximising potential EFR revenues.

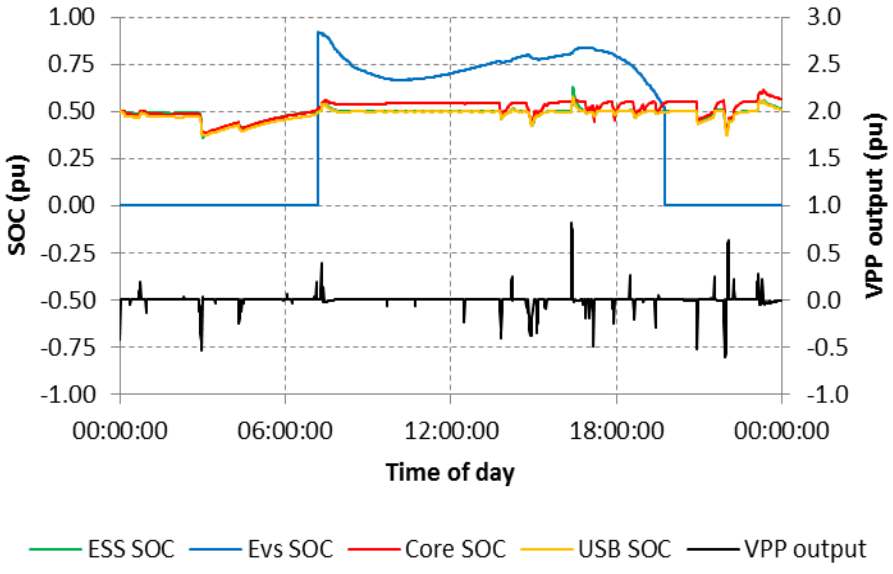

Figure 4-17 Aggregate load of the VPPs flexible assets and their VSoC

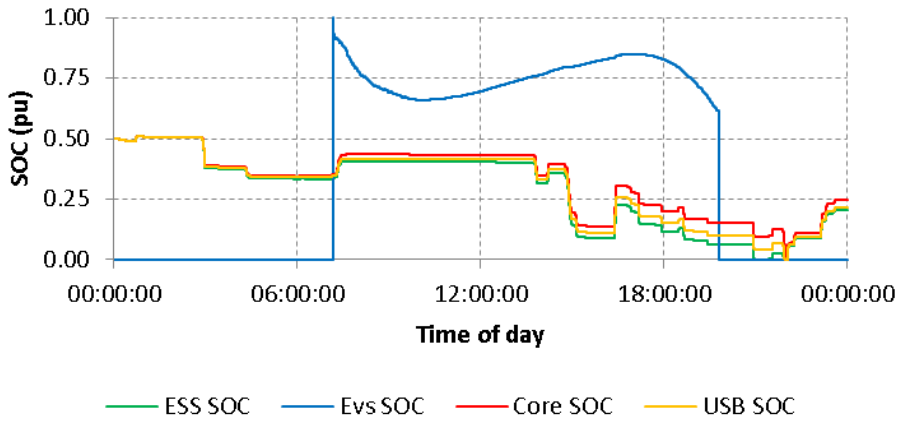

Figure 4-18 VSoC of assets delivering the service without coordination

The proposed algorithm successfully maximizes power availability, however it does this without considering the economical or environmental costs associated with the use of each of the assets.

4.6 Chapter conclusions and contributions to knowledge

The stochastic nature of EV charging requirements has been considered and the aggregate flexibility calculated for the grid. When aggregated to form a VESS, a higher level controller can consider the vehicles as a more traditional ESS but with varying power and energy limits in time. An internal energy management control scheme has been developed to realise the grid requested demand within the advertised flexibility, prioritising at the highest level the EVs SoC to be at a minimum level at the departure time. MCS has been used to show the resulting aggregate power exchange delivered by the VESS to the grid for two fictitious grid requested demand profiles. Over the full day, the probability of realising profile A was 99.98% and the probability of realising profile B was 98.83%.

An example of how the VESS could be used within a real VPP at Newcastle Science Central has also been proposed, to deliver the new EFR service. It was shown that through coordination, the various flexible assets within the VPP could appear in aggregate to have a larger energy capacity than if operating individually. This suggests that either the storage capacities could be minimised reducing initial capital expenditure, or power ratings increased maximising potential EFR revenues.

The Science Central site was considered as a VPP, rather than microgrid, because the flexible assets can operate anywhere within their controllable power range without causing power flow or voltage constraint issues within the network. The EFR service was delivered to the wider macrogrid, rather than the local electrical network. It was shown in Section 3.2 however

that power flow constraint violations are expected in domestic distribution networks when EV penetrations reach 40%, and therefore the ability of the VESS to respond to the local needs of the network should also be considered. This is investigated in Chapter 5 where a formulation is developed to determine the optimal level of conservatism of determining ESS and VESS power set-points to protect network constraints against the load and generation uncertainty caused by uncontrolled EV charging and solar generation respectively.

Chapter 5 Risk based approach to voltage control and power flow management in urban microgrids

5.1 Introduction

It was determined in Chapter 3 that largescale uptake of uncontrolled EV charging could cause distribution networks to exceed their operational limits without mitigation measures implemented. One way of mitigating voltage and power flows limit excursions within networks is to utilise ESS, where a methodology was developed in Chapter 4 to enable a VESS from controlled EV charging. Determining the economically optimal power set-point of ESS and VESS to prevent voltage and power flow limits from being exceeded when the network is under load and generation uncertainty is the subject of this Chapter. The links of model and information flow from previous chapters is summarised in Figure 5-1.

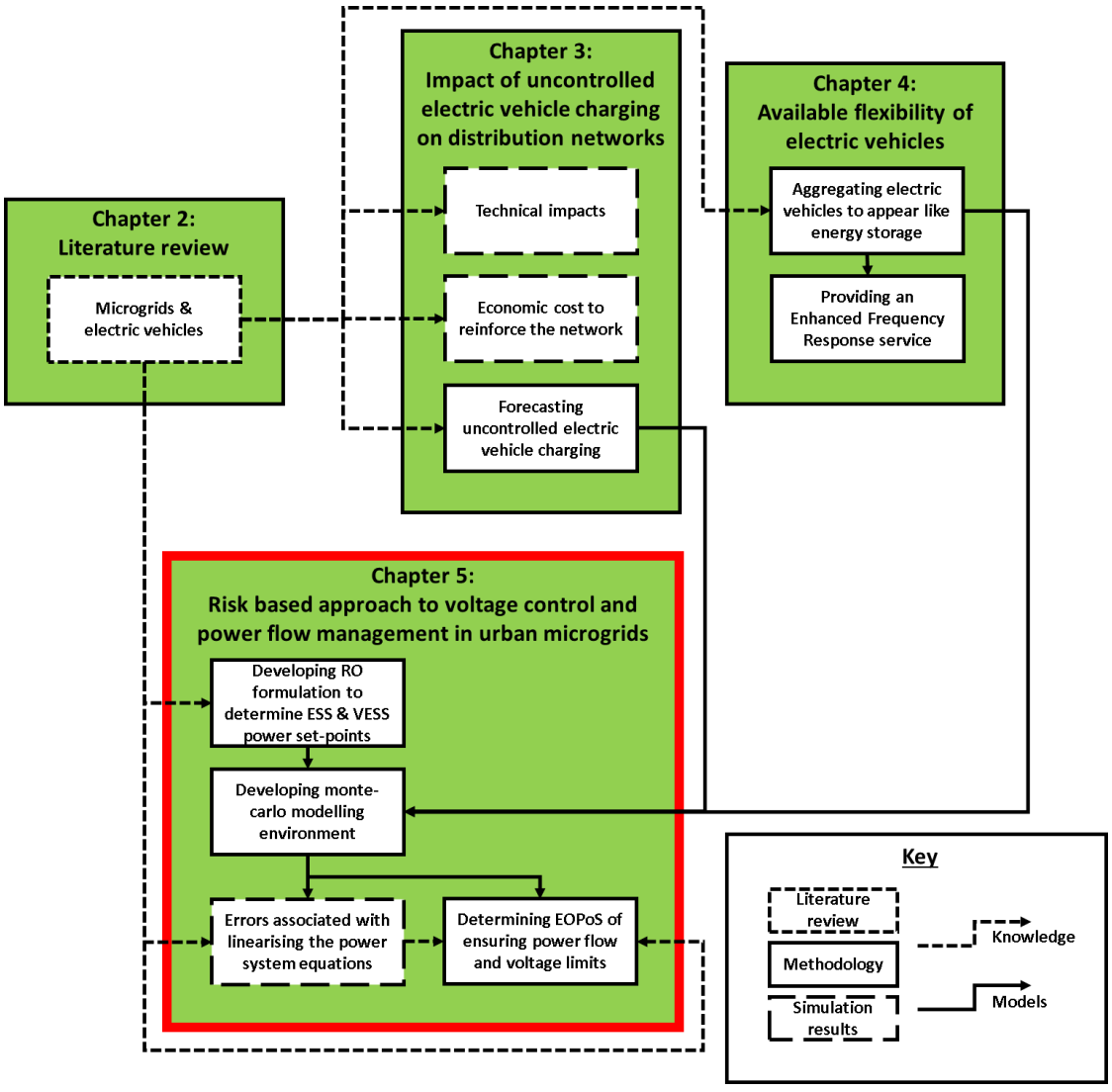

Figure 5-1 How Chapter 5 fits into the wider Thesis

When a network is operating under load and generation uncertainty, the exact power required of an ESS or VESS to mitigate voltage and power flow constraint violations is unknown. A control system could over protect thus ensuring the limits are maintained while also costing more than necessary through battery degradation. On the other hand, a control system could under protect causing a limit violation with an associated cost. This Chapter takes a risk based approach, using a RO LP formulation and the BoU that controls conservatism, to balance the costs associated with over protecting against the costs associated with under protecting the network against power flow and voltage limitations while operating under load and generation uncertainty. In this Chapter, the term 'optimal' refers to the level of conservatism displayed when determining the power output of the ESS and VESS, despite the load and generation uncertainty, to appropriately balance the costs associated with failing to protect the network from power flow and voltage limit violations with the costs of procuring services from the ESS and VESS to achieve the lowest overall network operating cost.

The modelled urban microgrid utilised during this Chapter is introduced in Section 5.2 along with the uncertainty associated with the load and generation connected to the network. The RO LP formulation to determine the power set-points of the ESS and VESS is developed in Section 5.3, with the methodology used to determine the cost of operating the network following implementation of the ESS and VESS power set-point developed in Section 5.4. The economically optimal level of conservatism, and associated probability of ensuring voltages and power flows remain within their respective limit, is determined in Section 5.5.

5.2 Urban microgrid under test

The microgrid studied during this Chapter is shown in Figure 5-2, with numerous network constraints that would be violated without smart control. It is likely that the microgrid will have been built over time to have such constraints, whereby it has been economical to utilise smart technologies rather than reinforce the network at each expansion. The progression of the microgrid from initial build to its constrained state is described below.

1. Initially only the large building is fed from the Transformers. The building peak load is within the thermal capacity of the cable supplying it from the Transformers. The Transformers are over rated with the expectation of further feeders being added with the re-development of the local area where the electrical network supplies.
2. A small solar system is installed with its exporting cable rated sufficient for the peak export.

3. An extension to the building load pushes its peak load above the capability of the supplying cable. It was economical to install a peak shaving ESS rather than reinforce the network.
4. An extension to the solar system is installed, which results in an overload of the supplying cable at peak export. A smart EV charging car park VESS is built next to the extended solar system to ensure that the power flow remains within the cable thermal limit.
5. An uncontrolled EV charging car park is built consisting of both rapid and standard charge points. This additional load means there is a risk of transformer overload and building under voltage in a transformer N-1 scenario. Due to the presence of the ESS and VESS, a smart solution was employed to protect the transformer and building under voltage in an N-1 condition.

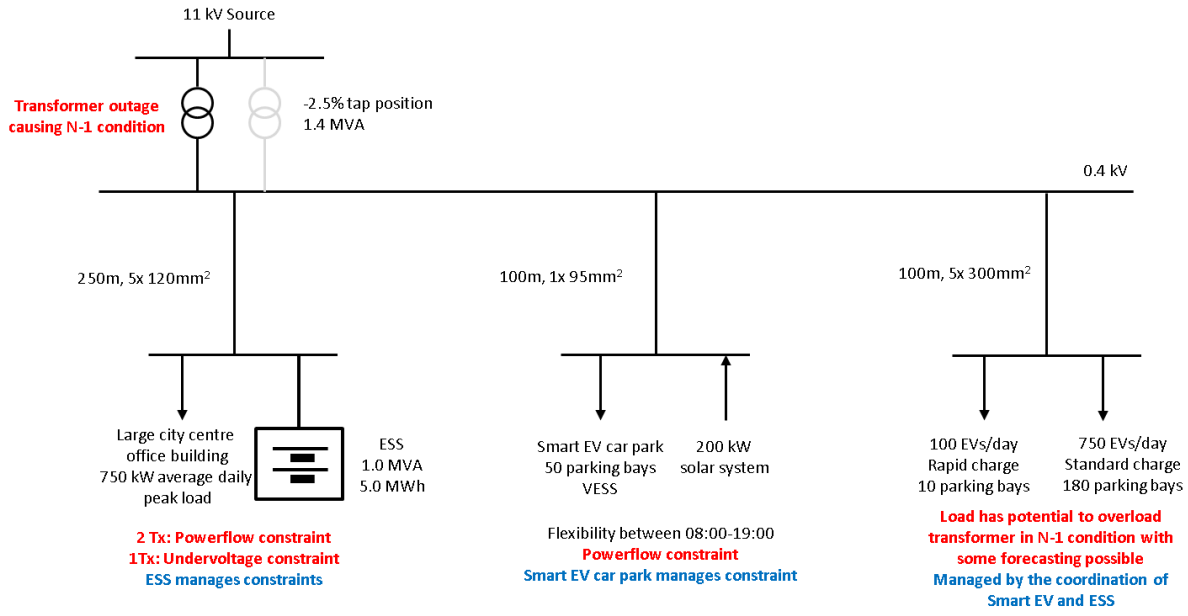

Figure 5-2 Urban microgrid under analysis

The electrical network presented in Figure 5-2 was modelled in the IPSA2 software, and the impedance parameters are described in Section 5.2.1. IPSA2 is a commercial power systems analysis software package developed initially by the University of Manchester Institute of Science and Technology (UMIST) in 1975 and is now supported by TNEI Services Ltd [138]. The IPSA2 load flow algorithm is based on the Fast Decoupled Newton–Raphson algorithm [139]. In this work, IPSA2 has been scripted using Python to apply a load profile, run a load flow, and to extract the calculated voltages, power flow and electrical losses at all locations of the network. This allows the full AC load flow calculation to be utilised during control

algorithm decision making under uncertainty as described in Section 5.3, and for determining the network state once that decision has been made as described in Section 5.4.

The modelling of the large city centre office building load is described in Section 5.2.2. The model of the ESS is described in Section 5.2.3. The modelling of the solar PV generation is described in Section 5.2.4. The model of both uncontrolled and controlled EV load is described in Section 5.2.5. The value of the energy consumed within the urban microgrid is described in Section 5.2.6.

5.2.1 Electrical network parameters

The electrical network model consists of a source supplying two transformers which in turn supplies three cable feeders and the load of the microgrid. The source is described in Section 5.2.1.1, transformers in Section 5.2.1.2 and the cables in Section 5.2.1.3.

5.2.1.1 Grid connection

The grid connection is modelled as the slack bus with a fault level of 180 MVA, based on the Corporation Street 11 kV incomer to Science Central, Newcastle-Upon-Tyne, UK [140].

5.2.1.2 Transformers

Both transformers are of the same type, as described in Table 5-1. A replacement 11/0.4 kV 1.4 MW transformer was assumed to cost £40,000 based on discussions with contacts within industry.

Table 5-1 Transformer parameters in urban microgrid model

HV (kV)	LV (kV)	Rating (MVA)	Impedance (pu)	X/R	Tap setting (%)
11.0	0.433	1.4	0.11	6.33	-2.5

5.2.1.3 Cables

The cables within the model are as described in Table 5-2. The impedance parameters are listed in Table 5-3 and based on the Universal Cable XLPE Cable Catalogue [141]. A replacement cable was assumed to cost £75/m based on [142, 143].

Table 5-2 Cable types in urban microgrid model

From	To	Cable type (mm^2)	Number of cables	Cable length (m)
Transformer	Building	120	5	250
Transformer	Solar	95	1	100
Transformer	EV charging	300	5	100

Table 5-3 Cable parameters

Cable type (mm^2)	Voltage (kV)	Ampacity (A)	Resistance (Ω/km)	Reactance (Ω/km)
95	0.4	319	0.247	0.073
120	0.4	363	0.197	0.073
300	0.4	592	0.080	0.072

5.2.2 Large city centre office building

Load data was taken from the Newcastle University Business School for a single representative day, 22 July 2013, and scaled to an average daily peak load of 750 kW. A summer day is chosen in order to be consistent across the network and is required in order to obtain a large uncertainty in solar generation. With regular repeat business operations based on time of day, it was assumed that this load profile could be forecasted with small variations, assumed to be within 5% of the load experienced on the representative day. The load for a particular settlement period is determined by sampling a normal distribution assuming 3 standard deviations between the nominal forecast value and the largest variation expected. Therefore 99.7% of all sampled values should fall within the modelled UI.

5.2.3 Energy storage

The ESS is assumed perfectly controllable with no uncertainty. It is appropriately sized such that its power and energy constraints are sufficiently large (1.0 MVA, 5.0 MWh) to not place additional constraints on the power set-points determined by the RO LP formulation developed in Section 5.3. It is assumed the ESS is based on Vanadium Redox Flow technology, where the half cycle degradation cost was assumed to be £12/MW over a 30 minute settlement period with a round trip efficiency of 80% based on [144-146].

5.2.4 Solar PV generation

Assuming clear skies and a solar collector produces it's rated power when the sun is directly overhead, and that solar collectors are on average placed facing normal to the earth's surface, the maximum available power can be calculated using the cosine of the solar zenith angle, in per unit on the system's rated power. The solar zenith angle is the angle between the ray normal to the earth's surface at the point of interest and the ray that points directly at the sun [147]. The minimum generation of a solar collector is always zero. Based on this analysis, the nominal forecast value and largest variation expected around that forecast can be set equal to one another and to half the maximum generation calculated by the solar zenith angle based on time of day and time of the year. The load for a particular settlement period is determined by sampling a normal distribution assuming 3 standard deviations between the nominal forecast value and the largest variation expected. Therefore 99.7% of all sampled values should fall within the modelled UI.

5.2.5 Electric vehicle load

The smart charging EV car park is a VESS based on the analysis presented in Chapter 4 however the maximum and minimum power and energy bounds are considered uncertain and an appropriate UI is applied in this Chapter. Similar to the ESS described in Section 5.2.3, the power and energy bounds of the VESS are such that they do not place additional constraints on the power set-points determined by the RO LP formulation developed in Section 5.3. The VESS parameters were based on li-ion technology [144-146] since this is used for the majority of EVs [64-66, 75]. The degradation cost was applied only when discharging and thus the full cycle degradation cost of £30/MW over a 30 minute settlement period was used. The degradation cost associated with charging was assumed zero since the vehicles must charge anyway. A round trip efficiency of 95% was assumed.

The uncontrolled standard charging EVs are based on the analysis presented in Section 3.4.1. When considering the uncertainties associated with a 30-minute-ahead forecast, the developed forecasting model is employed. When considering the uncertainties associated with day-ahead forecasts, the longer term diurnal analysis uncertainty is applied.

The uncontrolled rapid charging EVs are based on the analysis presented in Section 3.4.2. Since the time-step of 30 minutes used in this Chapter is longer than the 24 minutes identified in Section 3.4.2 as that where the uncertainty can be reduced from the long term diurnal analysis, the long term diurnal uncertainty is applied regardless of whether considering the uncertainties associated with 30-minute-ahead or day-ahead forecasts.

5.2.6 Value of energy

The value of energy was assumed at £45/MWh based on UK wholesale spot prices observed during 2016-2017 [148].

5.3 Linear programming formulation

The general form of LP is discussed in Section 5.3.1, before Section 5.3.2 builds upon the general form to create an uncertain LP problem. Section 5.3.3 then introduces the RO technique which turns an uncertain LP problem into a certain LP problem such that it can be solved deterministically. Turning the urban microgrid presented in Figure 5-2 into the form required for LP is the subject of Section 5.3.4. Since the power system is non-linear, it is important to use an appropriate network operating state when undertaking the linearization for LP, which is discussed in Section 5.3.5. It is possible that the LP will experience infeasibility and this is discussed in Section 5.3.6.

5.3.1 General form of linear programming

A LP problem can be generalised by (5.1) [54]. In this Thesis, the Python function "scipy.optimize.linprog()" [149] was utilised to solve the LP problem once it was transformed into a form described by (5.1).

$$\min \boldsymbol{c'x}$$

subject to:

$$\begin{aligned} \boldsymbol{Ax} &\leq \boldsymbol{b} \\ \boldsymbol{Dx} &= \boldsymbol{e} \\ \boldsymbol{l} \leq \boldsymbol{x} &\leq \boldsymbol{u} \end{aligned} \qquad (5.1)$$

Where:

$\boldsymbol{c}$	The vector of coefficients for the cost function
$\boldsymbol{c'}$	The inverse of $\boldsymbol{c}$
$\boldsymbol{x}$	The array of decision variables or control variables
$\boldsymbol{A}$	The matrix of constants for constraints
$\boldsymbol{b}$	The right hand side vector of constraints
$\boldsymbol{D}$	The matrix of coefficients for equality constraints

$\boldsymbol{e}$	The right hand side vector of equality constraints
$\boldsymbol{l}$	The lower limit of decision variables
$\boldsymbol{u}$	The upper limit of decision variables

5.3.2 Uncertainty in the linear programming formulation

Uncertainty could exist in any part of the generalised LP form of (5.1), however the uncertain LP problem can be simplified by transferring all the uncertain elements to be described within the $\boldsymbol{A}$ matrix as shown below [54].

Through introducing an additional control variable, $d = 1$, the inequality constraints can be reformulated as (5.2).

$$\min \boldsymbol{c'x}$$

subject to:

$$\begin{matrix} \boldsymbol{Ax - bd \leq 0} \\ \boldsymbol{x - ud \leq 0} \\ \boldsymbol{-x + ld \leq 0} \end{matrix} \qquad (5.2)$$

Therefore all inequality constraints can be represented by a new constraints coefficient matrix described by (5.3).

$$\boldsymbol{A'} = \begin{bmatrix} \boldsymbol{A} & \boldsymbol{-b} \\ \boldsymbol{D_n} & \boldsymbol{-u} \\ \boldsymbol{-D_n} & \boldsymbol{l} \end{bmatrix} \qquad (5.3)$$

Where $\boldsymbol{D}_n$ is a diagonal matrix and for $i = 1,2, \dots, n, D_{ii} = 1, D_{ij,i \neq j} = 0$ as shown in (5.4).

$$\boldsymbol{D}_n = \begin{bmatrix} 1 & & & \\ & 1 & & \\ & & \ddots & \\ & & & 1 \end{bmatrix} \qquad (5.4)$$

The equality constraints of (5.1) can be reformulated as two inequality constraints as shown in (5.5), allowing the equality constraints to also be included within the $\boldsymbol{A'}$ matrix.

$$\boldsymbol{-e \leq Dx \leq e} \qquad (5.5)$$

Uncertainty in control variables, $\boldsymbol{x}$, can be transferred so the uncertainty is applied on the appropriate coefficients within the $\boldsymbol{A'}$ (described fully in Section 5.3.4.2) which allows the control variable to be modelled certain within the formulation.

Therefore the generalised uncertain LP problem can described by (5.6) where the accent character (~) stands for uncertainty.

$$\begin{aligned} &\min \boldsymbol{c'x} \\ \text{subject to:} \quad & \\ &\widetilde{\boldsymbol{A}}\boldsymbol{x} \leq 0 \end{aligned} \qquad (5.6)$$

In order to utilise RO, the uncertainty is described by a range within which the true value will fall. This can easily be determined from historical data. Utilising a range of uncertainty is beneficial in contrast to other uncertainty methods which would require a PDF and is difficult to derive in reality. The uncertainty of each entry $a_{ij} \in \boldsymbol{A}$ can be described by (5.7).

$$a_{ij} - \hat{a}_{ij} \leq \tilde{a}_{ij} \leq a_{ij} + \hat{a}_{ij} \qquad (5.7)$$

Where:

a_{ij}	The nominal value of one element within matrix $\boldsymbol{A}$
$\tilde{a}_{ij}$	The real value of a_{ij}
$\hat{a}_{ij}$	The maximum variation of a_{ij}

5.3.3 Transformation into robust optimisation

RO is a process that transforms an uncertain LP problem into a certain LP problem such that it can be solved deterministically, and the formulation used in this Thesis was proposed by Bertsimas and Sims in 2004 [150]. The method introduces three additional control variables $\boldsymbol{z}$, $\boldsymbol{p}$ and $\boldsymbol{y}$, and the BoU, Γ. The value of BoU represents the number of uncertain coefficients that the constraints are protected against, although its value does not need to be an integer. The RO formulation is described by (5.8).

$$\min \boldsymbol{c}'\boldsymbol{x}$$

subject to

$$\begin{gathered}
\sum_j a_{ij}x_j + z_i\Gamma + \sum_{j\in J_i} p_{ij} \le b_i \\
z_i + p_{ij} \ge \hat{a}_{ij}y_i \\
-y_i \le x_j \le y_j \\
l_j \le x_j \le u_j \\
p_{ij} \ge 0 \\
y_j \ge 0 \\
z_j \ge 0
\end{gathered} \qquad (5.8)$$

For the remainder of this Thesis, the BoU will be normalised against the number of uncertain coefficients and quoted in per unit terms, which is more intuitive.

When the BoU is at a value of 1.0, the RO formulation protects against the worst case of all uncertainties which is very pessimistic. It is likely that there will be some diversity as to the value of $\tilde{a}_{ij}$ relative to its maximum or minimum value, and thus a lower BoU than 1.0 can achieve a high Probability of Success (PoS) in terms of maintaining the system within the set constraints. The BoU can therefore allow the level of conservatism (and resulting cost of failure to protect against the constraints) to be balanced against the cost of the formulation objective function.

5.3.4 Modelling the urban microgrid as an uncertain linear programming problem

In order to utilise LP; the decision variables, constraints and optimisation objective function must be defined for the urban microgrid. The decision variables are defined in Section 5.3.4.1. The powerflow constraints and voltage constraints are defined in Section 5.3.4.2 and Section 5.3.4.3 respectively. The SoC management of the ESS and VESS are discussed in Section 5.3.4.4. The optimisation objective function is defined in Section 5.3.4.5.

5.3.4.1 Decision variables

In this formulation, all load and generation elements are considered a decision variable, within an upper and lower bound set as a constraint. For the microgrid controllable elements, such as ESS and the VESS, the upper and lower bound are set based upon the inverter power limits. For non-controllable loads and generation, such as the large office building, solar PV and uncontrolled EV charging, the upper and lower bounds are set at the nominal forecast value expected.

An additional decision variable fixed with a value of 1.0 is also introduced, to enable network calibration when considering the power flow, voltage and electrical loss sensitivity factors, which are described in full in the following sections.

5.3.4.2 Power flow constraints

The power flow through each transformer and cable is dependent upon the network state of load and generation. With the load and generation considered decision variables within a LP optimisation, their impact upon the power flow through each component must be calculated and included as a constraint.

Using scripted IPSA2, the nominal forecast value for all load and generation is applied to the network and a load flow undertaken, providing the nominal forecast network state. The influence of each decision variable against each cable and transformer is calculated through undertaking two load flows for each decision variable; one with the load increased slightly and one with the load decreased slightly. This results in the calculation of a power flow sensitivity factor, as shown in (5.9).

$$\varphi_{db} = \frac{\partial S_b}{\partial P_d} \qquad (5.9)$$

Where:

φ_{db}	Power flow sensitivity factor between decision variable, d, and branch (cable or transformer), b, kVA/kW
S_b	Apparent power through the branch (cable or transformer), kVA
P_d	Real power of the decision variable, kW

The sensitivity factors allow the change in power flow through a transformer or cable to be calculated based on a change in a decision variable however in order to compare to a

transformer or cable power flow limit, it must be calibrated against the existing power flow through the transformer or cable. The calibration values are calculated by (5.10).

$$\boldsymbol{R} = \boldsymbol{S} - \boldsymbol{\varphi}'\boldsymbol{x} \qquad (5.10)$$

Where:

$\boldsymbol{R}$	Array of calibration values, kVA
$\boldsymbol{S}$	Array of apparent power flow through each branch (cable or transformer) for the nominal forecast network state, kVA
$\boldsymbol{\varphi}'$	The inverse of the matrix of power flow sensitivity factors, kVA/kW
$\boldsymbol{x}$	The array of decision variables, kW

The full AC load flow calculated by IPSA2 is a non-linear system, while the power flow sensitivity factors are a linear approximation to the non-linear system. As a result the nominal forecast network state and choices made regarding the controllable decision variables influences the sensitivity factors, and thus the load and generation uncertainty causes uncertainty in the sensitivity factors. The sensitivity factor uncertainty is assumed small relative to the impact of the load uncertainty itself on causing a limit violation. To account for this and rounding errors, a per unit derating is applied to each constraint.

By utilising the additional decision variable of 1.0 introduced in Section 5.3.4.1 in combination with the calibration value, and the constraint derating factor to account for errors during linearisation, the resulting power flow constraints for use in the LP optimisation are shown in (5.11).

$$\gamma\boldsymbol{S}^{-}_{\boldsymbol{limit}} \leq [\boldsymbol{\varphi}' \quad \boldsymbol{R}] \begin{bmatrix} \boldsymbol{x} \\ 1.0 \end{bmatrix} \leq \gamma\boldsymbol{S}^{+}_{\boldsymbol{limit}} \qquad (5.11)$$

Where:

γ	Constraint derating value, per unit
$\boldsymbol{S}_{\boldsymbol{limit}}$	Array of power flow limits, kVA

$\boldsymbol{\varphi'}$	The inverse of the matrix of power flow sensitivity factors, kVA/kW
$\boldsymbol{R}$	Array of calibration values, kVA
$\boldsymbol{x}$	Array of decision variables, kW

As discussed in Section 5.3.2, to ensure that the decision variables remain certain within the optimisation, the load uncertainty with regard to causing a limit violation is transferred to the sensitivity matrices. This is achieved through (5.12).

$$\hat{\varphi}_{db} = \frac{\varphi_{db}\hat{x}_d}{x_d} \qquad (5.12)$$

Where:

φ_{db}	Calculated power flow sensitivity factor between decision variable, d, and branch, b.
$\hat{\varphi}_{db}$	Maximum variation of $\varphi_{db}$to model the maximum variation of $\hat{x}_d$within the constraints matrix
$\hat{x}_d$	Maximum variation of x_d
x_d	The nominal forecast value of the decision variable

5.3.4.3 Voltage constraints

The voltage constraints are modelled through voltage sensitivity factors, calculated and implemented as constraints in the same way as described for the power flow constraints in Section 5.3.4.2.

5.3.4.4 State of charge of energy storage and smart charging electric vehicles

The power set-point of both the ESS and VESS are controllable decision variables that are time limited based on SoC. The subject of the study however is the level of conservatism to use when determining how much power is required to appropriately protect against the load and generation uncertainty. With this in mind and to reduce simulation time, only one time step is considered in the LP formulation and therefore the optimisation does not take the SoC into account when determining the power set-point. To ensure SoC feasibility, the energy capacity of the ESS and VESS have been appropriately sized for their role within the urban microgrid under test, and the ESS re-charges to 100% SoC during a period of the day when the re-charging would not cause any power flow or voltage constraint violations.

5.3.4.5 Optimisation objective function

The objective function is the minimisation of network operating costs, based on the cost associated with each controllable decision variable as defined in (5.13). In order to achieve an increase in the cost of ESS degradation regardless of whether the storage is charging or discharging, a different cost function is required dependent upon charging or discharging. The cost associated with uncontrollable decision variables is zero.

Charging:

$$c_d = D_d + \sum_{t=0}^{T} (K_t \vartheta_{dt} + K_e \epsilon_{dt}) + \sum_{f=0}^{F} \left(K_f \theta_{df} + K_e \epsilon_{df}\right) \quad (5.13)$$

Discharging:

$$c_d = -D_d + \sum_{t=0}^{T} (K_t \vartheta_{dt} + K_e \epsilon_{dt}) + \sum_{f=0}^{F} \left(K_f \theta_{df} + K_e \epsilon_{df}\right)$$

Where:

c_d	Network operating cost associated with the controllable decision variable, d
D_d	Degradation cost associated with using the controllable decision variable, d
K_t	Cost associated with replacing transformer, t
K_f	Cost associated with replacing cable, f
K_e	Value of energy
T	Number of transformers in the network
F	Number of cables in the network
ϑ_{dt}	Loss of life sensitivity factor between transformer, t, and controllable decision variable, d, % life/kW
θ_{df}	Loss of life sensitivity factor between cable, f, and controllable decision variable, d, % life/kW
ϵ_{dt}	Electrical losses sensitivity factor between transformer, t, and controllable decision variable, d, kWh/kW

ϵ_{df} Electrical losses sensitivity factor between cable, f, and controllable decision variable, d, kWh/kW

The storage degradation cost is assumed linear with real power exchange, however due to the change in sign between charging and discharging, the degradation cost applied within the cost function becomes non-linear. This is shown diagrammatically in Figure 5-3. For example if the fully linear dotted line of Figure 5-3 were implemented in a linear programming formulation targeting minimum cost, then the maximum possible ESS supply would be returned; thus not minimising ESS usage and its associated degradation.

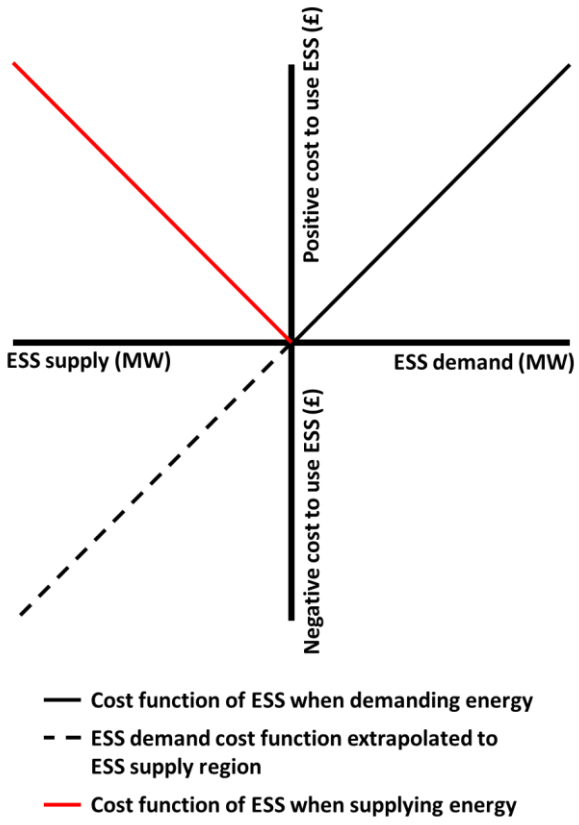

Figure 5-3 Non-linearity of ESS cost function

In the case of the VESS of smart charging EVs, charging is assumed to have no cost since the vehicles need to charge anyway. If discharging, then a linear cost with real power exchange is assumed to compensate for the additional charge-discharge cycles experienced.

Similar to the power flow sensitivity factors calculated by (5.9) the influence of each decision variable against the electrical loss and loss of life of each cable and transformer is calculated through undertaking two load flows for each decision variable; one with the load increased slightly and one with the load decreased slightly. The electrical loss sensitivity factor between each network component and each decision variable can be calculated directly

from the results of the load flow. The loss of life for the cables and transformers however must be estimated based on their loading as reported from the load flow.

The transformer loss of life is estimated based on the model proposed in IEEE standard C57.91-1995 Guide for Loading Mineral-Oil-Immersed Transformers and Step-Voltage Regulators [15]. The cable loss of life has been estimated based on [151] and plotting a linear fit through the four values for estimated life and operating temperature. It is assumed that at rated current the cable operates at 70°C and that the operating temperature is proportional to per unit loading squared. The resulting relationship between cable loading and expected cable life is shown in (5.14).

$$L_f = \zeta_0 p_f^2 + \zeta_1 p_f + \zeta_2 \qquad (5.14)$$

Where:

L_f	Life cable expectancy, years
p_f	Loading of the cable, f, per unit
ζ_0	Coefficient constant, -32.854
ζ_1	Coefficient constant, 2.2737×10^{-13}
ζ_2	Coefficient constant, 50.028

5.3.5 Appropriate network state for linearisation

In Section 5.3.4, sensitivity factors were introduced to linearize the problem, however due to the non-linear system the sensitivity factors are dependent upon the operating point of the network. It was identified in the literature that two methods exist to ensure that the sensitivity factors used are appropriate for the network operating state; a piecewise approach [61], and an iterative approach [62].

Using a piecewise approach requires a MILP solver, and a large number of constraints to bound the piecewise steps. In contrast, an iterative method uses a simpler LP solver and updates the linearised sensitivity factors based on the LP determined decision variables and re-runs the optimisation, continuing until a pre-defined convergence criteria. It is the iterative method that has been implemented within this Thesis.

On the first iteration, it is not known if the degradation cost should be applied positive or negative, because it is not known if the decision variable will be determined to be positive or negative. Therefore on the first iteration no cost is applied within the cost function and a viable starting network operating state within the constraints set is found. The cost function is then populated with the appropriate sign for the degradation cost, and the decision variable bounded as necessary, to minimise the network operating cost. It is possible however that from one iteration to the next, the decision variable may need to cross the bound and the sign of the degradation cost be swapped based on the new sensitivity factors. This happens for the next iteration if the decision variable reaches the bound. The iterative process continues until the sum of the absolute error between each decision variable on one iteration to the next is below a pre-defined value, or until a maximum number of iterations. This pre-defined stopping criteria was set as 0.001 MW multiplied by the number of controllable decision variables. Similarly, the accuracy of the linear programming function was set at 0.001 MW, and as such all decision variable results were rounded to this same accuracy. The iterative process is summarised in Figure 5-4.

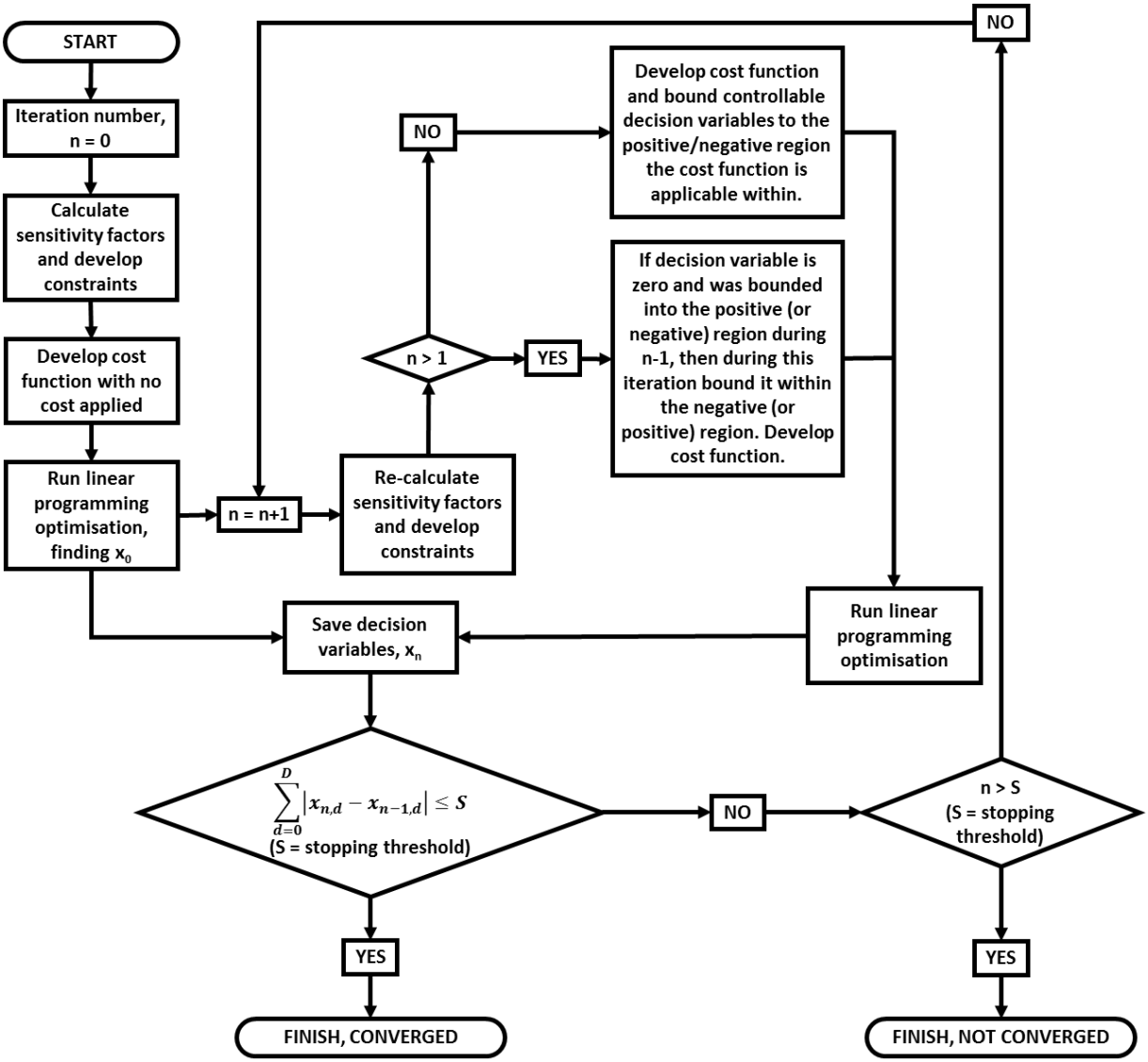

Figure 5-4 Iterative method used to determine network operating state

The method used allows the formulation to determine for itself whether storage should charge or discharge and to determine suitable sensitivity factors. This is a key improvement over and above that proposed in [54] where the charge or discharge decision and the network operating state for the calculation of sensitivity factors for each point in time was determined by intelligent human interaction in advance of executing the RO algorithm.

A counter was used in the iterative method of Figure 5-4 to prevent the potential scenario of non-convergence and entering an infinite loop. This was observed in two scenarios; including reactive power as a controllable decision variable, and when the degradation element of the controllable decision variable cost function was small relative to the cost of losses and equipment replacement.

When reactive power is included in the formulation as a controllable decision variable, its apparent power flow sensitivity factor is lower than that of its real power controllable decision variable. Assuming negligible cost to utilise reactive power since it does not impact battery degradation, the apparent power flow cost sensitivity factor is negligible for utilising reactive power while a cost is applied for utilising real power. This results in the LP formulation trying to solve apparent power flow constraint violations using the reactive power decision variable. When the feeder gets close to zero reactive power, without the apparent power close to its constraint limit, the reactive power overshoots and changes its sign resulting in a change of sign for the apparent power flow sensitivity factor. This causes the iterative method to oscillate around zero reactive power through the feeder while never achieving the required reduction in apparent power flow to meet the network constraint. The need to control reactive power in LV distribution networks, such as the test network used in this Thesis and presented in Section 5.2, is low due to the X/R ratios in such networks. Having said this, the algorithm presented is general to voltage level where the need to control reactive power might be more prevalent. Furthermore, LV microgrids could control reactive power flows at the point of common coupling to provide ancillary services to their supplying distribution networks.

If the degradation cost of a controllable decision variable is negligible, for example when the VESS demands real power, then the cost of electrical losses and equipment replacement in relation to the decision variable dominates. The optimal operating point for a single feeder in such a situation is on zero load. It is possible that progressive iterations result in the decision variable overshooting the desired zero load operating state of the feeder, thus changing the sign of the power flow sensitivity factor for the next iteration leading to non-convergence and an infinite-loop.

5.3.6 Potential for problem infeasibility

It was found in testing that the LP solver could fail to calculate and return a flag indicating an infeasible problem, even in networks that were provably feasible. Bland's anti-cycling algorithm [149] was tested due to the large number of zeros within the formulation after conversion to RO, however the probability of calculation success and time taken did not provide superior results over simply running the standard LP solver multiple times. To achieve an appropriate balance between calculation time and high probability of returning a feasible solution to a feasible problem, the solver was run multiple times as defined in Figure 5-5.

Infeasibility was a particular problem when the nominal forecast network state had a feeder on, or close to, no-load (observed in the test microgrid on the solar PV and VESS feeder). In this situation the charging current of the cable means a significantly larger reactive power than real power while calculating the apparent power flow sensitivity factors. The resulting apparent power flow sensitivity factors suggest that a much larger real power is needed than in reality to protect against the power flow constraints, which could be larger than the power capability of the VESS at that point in the day and thus the problem appears infeasible.

If the problem was concluded to be infeasible during the studies then the ESS and VESS power set-point was set to zero.

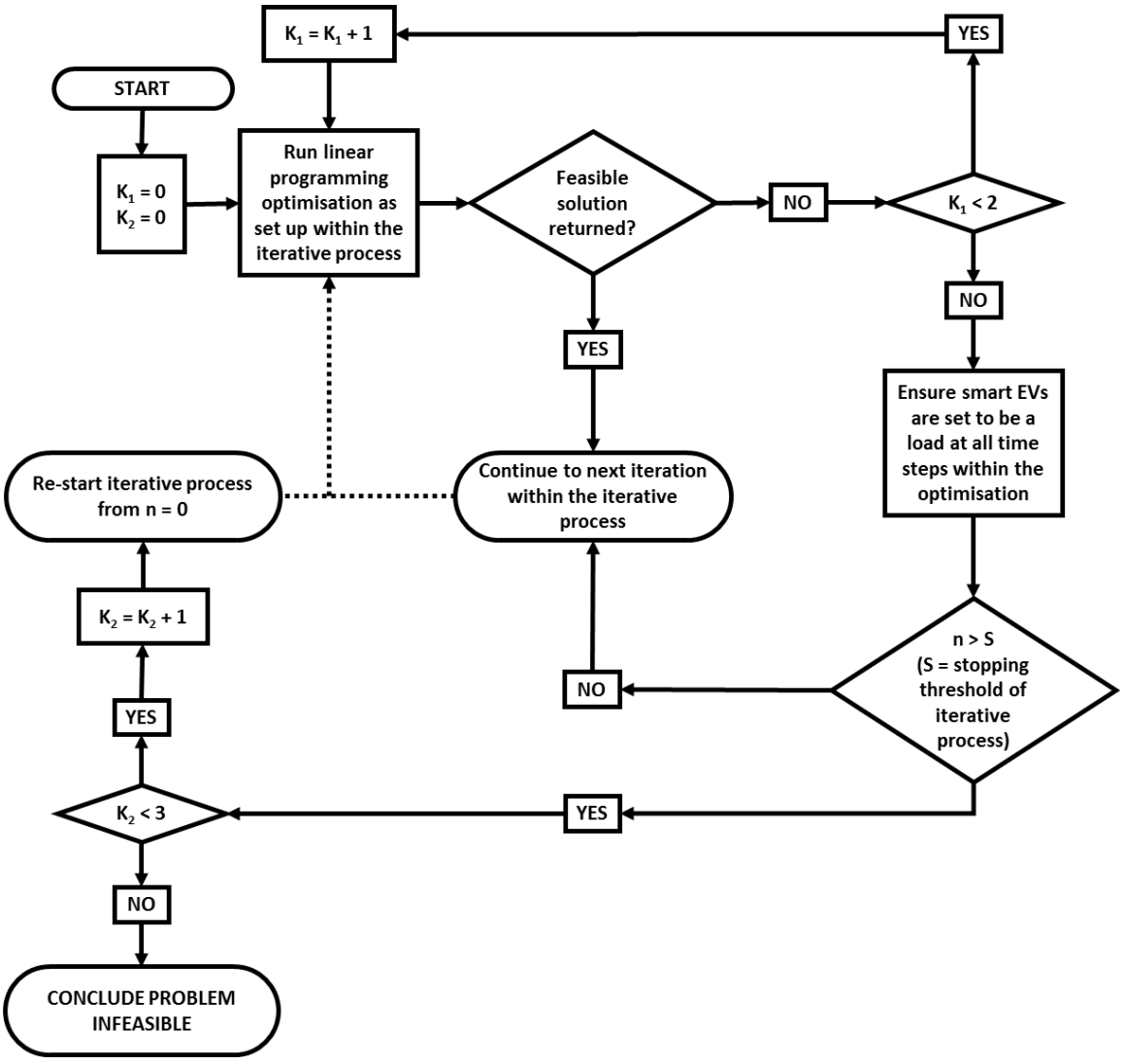

Figure 5-5 Ensuring a high probability of the solver returning a feasible solution to a feasible problem

5.4 Determining the long term average cost of network operation

It was defined in Section 5.3 how the formulation determines the ESS and VESS power set-point, where it was noted that the BoU controls the conservatism. Section 5.4.1 defines how the cost of network operation has been modelled following the implementation of the power set-points on the network for any particular point in time. Section 5.4.2 then defines the probabilistic methods used to estimate the network operating cost over the longer term.

5.4.1 Cost model

The cost function presented in 5.3.4.5 is used, however it is calculated directly from a load flow of the load and generation experienced rather than via a linear approximation of costs around the nominal forecasted network state. In addition, cost is borne if the system fails to protect the network from its power flow and voltage operational constraints.

If a network constraint is violated, it is recognised that customers downstream of that point could have a service interruption during the period of the violation. In the case of the large office building feeder and the uncontrolled EV charging feeders, this is quantified in this Thesis from the viewpoint of the DNO in (5.15) as twice the value of the energy not delivered; thus compensating both the upstream generator unable to sell their energy and the downstream customer unable to purchase energy. In the case of the VESS and solar PV feeder, this is quantified in (5.16) as the value of energy being consumed by the EVs plus the value of the energy being exported by the solar PV system; thus compensating both customers of that feeder.

$$c_{load\ only\ feeder} = 2K_e\tau P_{load\ only\ feeder} \qquad (5.15)$$

Where:

$c_{load\ only\ feeder}$	Cost of constraint violation on a load only feeder, £
K_e	Value of energy, £/kWh
τ	Time duration the constraint violation is experienced, hours
$P_{load\ only\ feeder}$	Real power load of the feeder, kW

$$c_{load\ \&\ generation\ feeder} = K_e\tau\left(|P_{load}| + \left|P_{generation}\right|\right) \qquad (5.16)$$

Where:

$c_{load\ \&\ generation\ feeder}$	Cost of constraint violation on a feeder containing both load and generation, £
K_e	Value of energy, £/kWh
τ	Time duration the constraint violation is experienced, hours
P_{load}	Real power load on the feeder, kW
$P_{generation}$	Real power generation on the feeder, kW

Each time step is based on a settlement period with a duration of 30 minutes. For each modelled day, the following is calculated:

- The PoS of protecting against the network constraints
- The cost to utilise the ESS due to degradation
- The cost to utilise the VESS due to additional degradation over uncontrolled charging
- The cost associated with loss of life of transformers and cables
- The cost of electrical losses
- The cost of not delivering energy due to excursion of limits
- The total cost of operating the microgrid (the sum of all other costs).

5.4.2 Monte-carlo modelling

A sequential MCS has been used with the probabilistic load and generation distributions as described in Section 5.2 to model the microgrid and the response given by the developed RO formulation over a period of time. Although computationally expensive, MCS modelling captures the complex interactions between the various PDFs and the non-linear response of the electrical power system.

To ensure SoC feasibility, the ESS re-charges to 100% SoC between the hours of 00:00 and 06:00. During this time period charging the ESS is not expected to cause any power flow or voltage constraint violations. At the start of the simulation, it is not known what the previous day's usage would have been and consequently the appropriate cost associated with re-charging. Therefore, the simulation starts with 100% SoC and the first day, with an unrepresentative low degradation cost, is discarded.

The accuracy of the MCS increases with the number of days being modelled, as does the computational time. Therefore there is a trade-off between accuracy and calculation time. A

study has been undertaken to quantify the accuracy and to determine the shortest acceptable period of time to use for the studies in this Thesis.

Assuming the daily cost is normally distributed, Student's T distribution was used to determine the maximum error of the mean cost per day with a defined confidence interval. A 90% confidence interval was chosen as it corresponds to the qualitative term 'almost certain' [132]. The resulting relationship between results accuracy and time taken is shown in Figure 5-6.

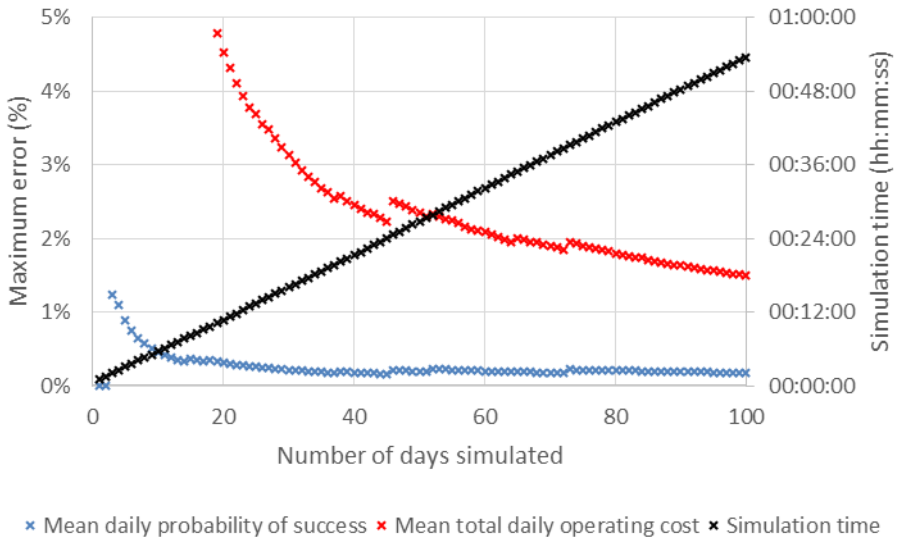

Figure 5-6 Maximum error and simulation time as the number of days simulated increases, for a confidence interval of 90%

Based on Figure 5-6 an appropriate balance between simulation time and accuracy of result was chosen as 30 simulated days. This suggests that the true mean value for PoS and total daily cost over the long term are almost certain to be within 0.22% and 3.24% of the values quoted in this Thesis respectively.

Following the decision regarding number of days to simulate, the load and generation determined from the respective PDFs modelling them for 30 simulated days was saved, and used for all other studies in this Thesis. This means that comparative studies can be compared like for like against the same load and generation scenarios making it easier to draw conclusions regarding the RO formulation performance.

5.5 Performance of robust optimisation under load and generation uncertainty

It was recognised in Section 5.3.4.2 that there are errors introduced through the linearization methods used and a constraint derating value was implemented in the formulation to take account of this and ensure 100% PoS is achievable. An investigation into the derating value

required is presented in Section 5.5.1. It was also recognised in Section 5.3.3 and Section 5.4.1 that there is a balance between the cost of protecting the network against the adverse impacts of uncertainty and the cost having failed to adequately protect the network, leading to the idea of an Economically Optimal Probability of Success (EOPoS) achieved through implementing an associated Economically Optimal Budget of Uncertainty (EOBoU). This is investigated in Section 5.5.2.

Two different levels of uncertainty are considered; that associated with 30-minute-ahead forecasts and that associated with day-ahead forecasts. When considering the uncertainty associated with 30-minute-ahead, the UI of uncontrolled EV charging is that determined using the forecasting methodology developed in Section 3.4. When considering the uncertainty associated with day-ahead forecasting, the UI of uncontrolled EV charging is based on the long term diurnal analysis within Section 3.4.

The network under test, shown in Figure 5-2, has four different constraints that could be violated. Each of these constraints have been studied independently as well as all together, and the isolation was achieved through changing network parameters as summarised in Table 5-4.

Table 5-4: Network parameters used to isolate each constraint

		Transformer	Large office building feeder cable	VESS and Solar PV feeder cable
Description	Source voltage (pu)	Number in parallel	Number of 250m 120mm^2 cables in parallel	Number of 100m 95mm^2 cables in parallel
Power flow on the large office building feeder	1.00	2	5	2
Under voltage on the large office building feeder	0.97	2	7	2
Power flow on the VESS and solar PV feeder	1.00	2	7	1
Power flow through the 11/0.4 kV transformer	1.03	1	7	2
All constraints	1.00	1	5	1

5.5.1 Investigating the accuracy of AC power system linearization with sensitivity factors

The constraints de-rating value has been investigated in two scenarios:

- When there is uncertainty over future load and generation, assuming 30-minute-ahead forecasts

- When there is perfect knowledge of future load and generation, and thus no uncertainty

When there is no uncertainty, the derating value is used to mitigate against rounding errors within the LP solver and the accuracy of the iterative method's stopping criteria. When the load and generation uncertainty is modelled, the de-rating value is used to mitigate against the uncertainty in sensitivity factors as well as rounding errors and the iterative method's stopping criteria. In this uncertain situation there is a choice of BoU. If the BoU is too low then the derating value would be the parameter determining the robustness of the network rather than the BoU while constraining the solution space of the optimisation potentially resulting in a sub-optimal solution. If the BoU is too high then the over protection provided might over compensate for an inadequate derating. During this study, a BoU of 0.5 was used.

The relationship between PoS and constraint derating value for both the uncertain and certain cases is shown in Figure 5-7 for the power flow on the large office building feeder, Figure 5-8 for under voltage on the large office building feeder, Figure 5-9 for power flow on the VESS and solar PV feeder, Figure 5-10 for power flow through the 11/0.4 kV transformer and Figure 5-11 for when all constraints are included. The derating value required to achieve 100% PoS in all situations is summarised in Table 5-5.

For certain loads in Figure 5-7 to Figure 5-11, the PoS is lowest at a constraint derating of 1.00. This is caused by rounding errors within the LP solver and the accuracy of the iterative method's stopping criteria. As the constraint derating reduces, the probability of the algorithm accuracy resulting in a constraint violation reduces and thus the PoS increases. In the case of uncertain loads however, it is not known what the BoU needs to be. The BoU was set intentionally high to ensure that 100% PoS is possible, however this could also result in the BoU over compensating for an inadequate constraint derating. This can be seen in Figure 5-7 to Figure 5-11 where at a constraint derating of 1.00 the PoS is higher for uncertain loads than certain loads in all cases. It was particularly visible in Figure 5-9 where the uncertain loads have a 100% PoS regardless of constraint derating.

Table 5-5 Summary of derating required to achieve 100% PoS

	Required derating	
Description	Certain loads	Uncertain loads
Power flow on the large office building feeder	0.992	0.960
Under voltage on the large office building feeder	0.994	0.980
Power flow on the VESS and solar PV feeder	0.990	1.000
Power flow through the 11/0.4 kV transformer	0.996	0.980
All constraints	0.984	0.990

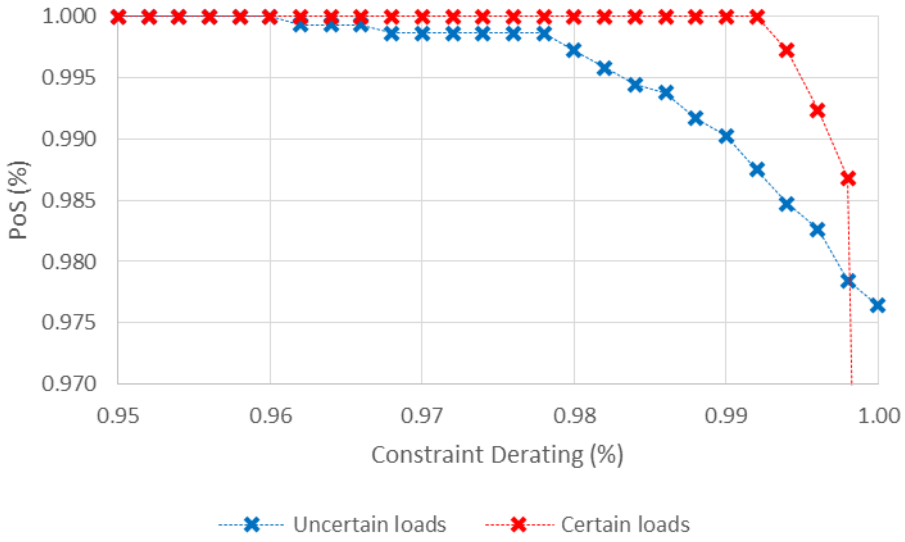

Figure 5-7 Relationship between probability of success and derating value for the power flow constraint of the large office building feeder

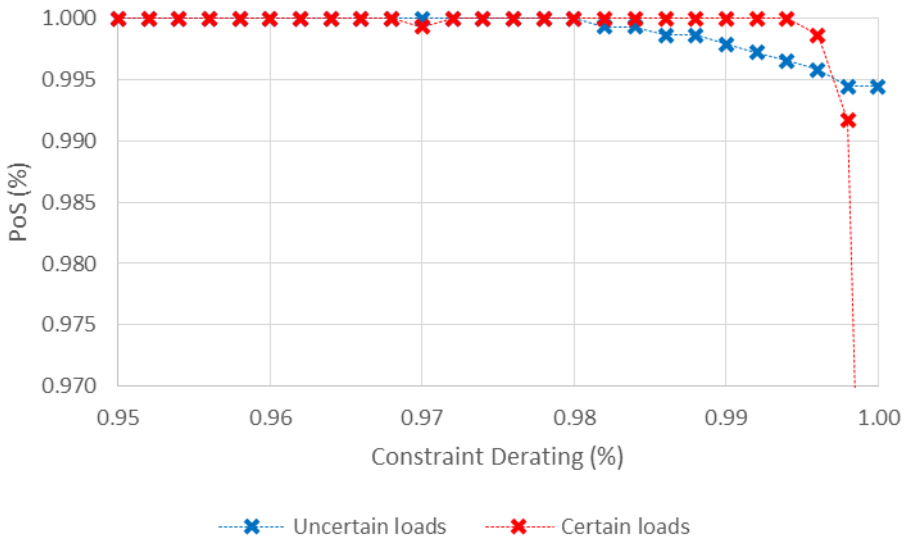

Figure 5-8 Relationship between PoS and derating value for the voltage constraint of the large office building

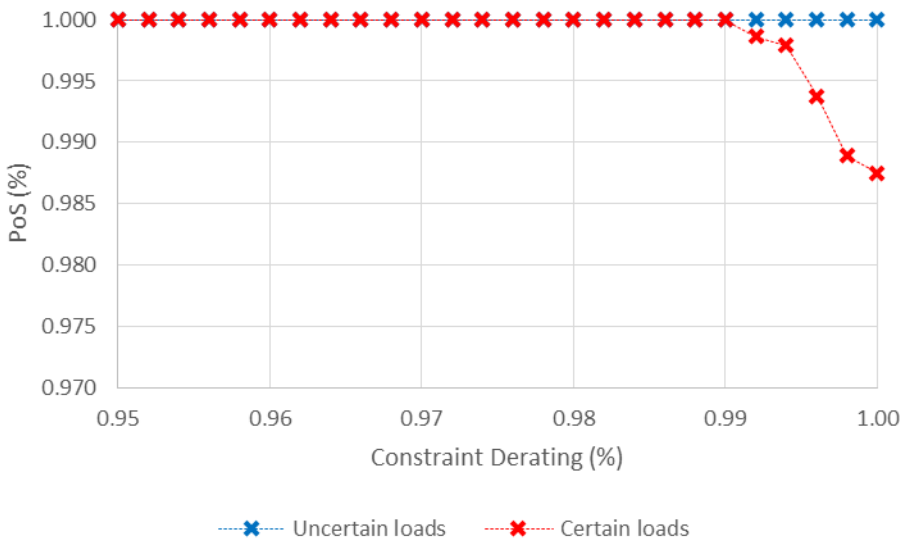

Figure 5-9 Relationship between PoS and derating value for the power flow constraint of the VESS and solar PV feeder

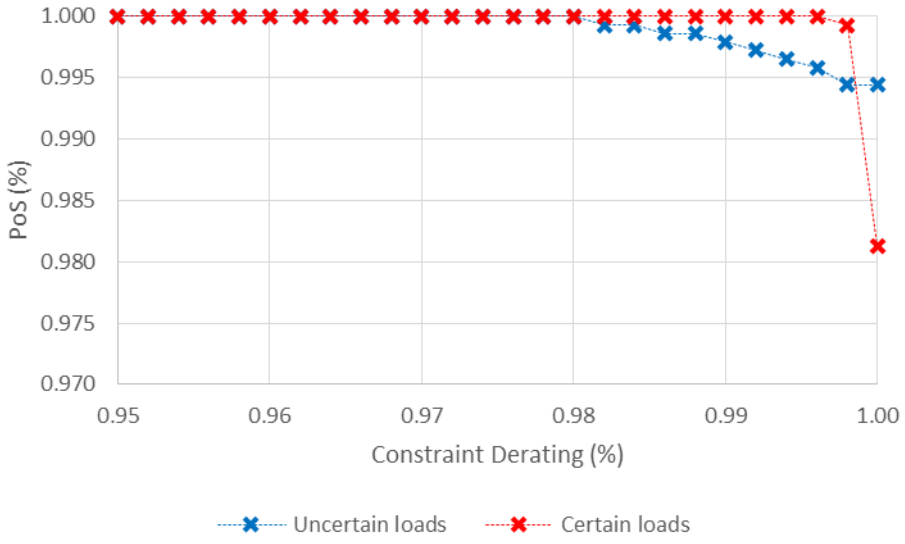

Figure 5-10 Relationship between PoS and derating value for the power flow constraint of the 11/0.4 kV transformer

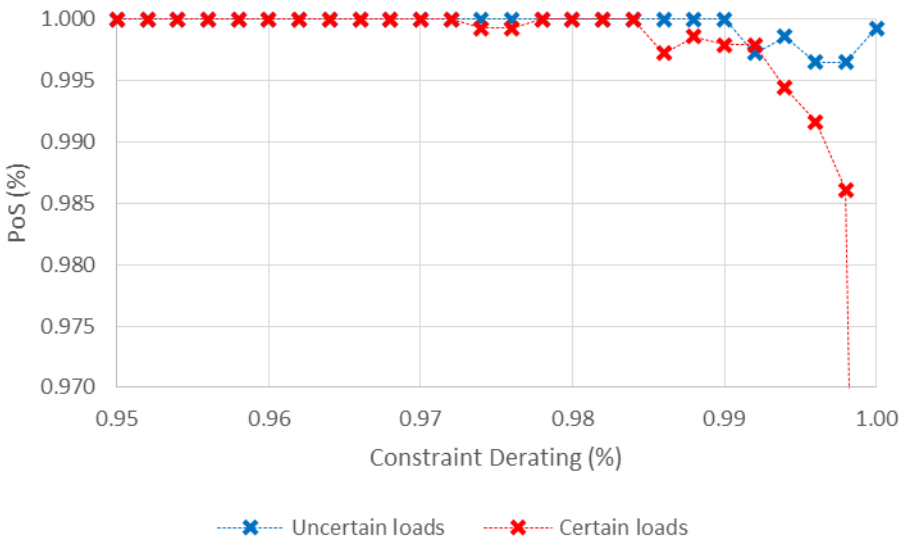

Figure 5-11 Relationship between PoS and derating value for all the constraints

Based on Table 5-5 and Figure 5-7 to Figure 5-11, it is concluded that for the network under test a derating value of 0.99 is required when there is no load uncertainty, and 0.98 when there is load uncertainty. In both the certain and uncertain load cases only one study needed a derating value lower than this to achieve 100% PoS, by a very small margin.

For the remainder of this Thesis, a derating value of 0.98 has been applied to all studies.

5.5.2 Determining the economically optimal probability of success of remaining within power flow and voltage limits when deciding ESS and VESS power set points under load and generation uncertainty

In this Section the trade-off between over utilising the ESS and VESS to mitigate the uncertainty, and the cost of failing to protect the network adequately, is investigated. This has been achieved by progressively changing the BoU and seeing the impact on network operation and the associated costs.

When all network constraints are included in the formulation and the uncertainty is that associated with 30-minute-ahead forecasts, the relationship between BoU and PoS is shown in Figure 5-12, and the relationship between BoU and average daily total operational cost is shown in Figure 5-13. As the BoU increases, the PoS increases also. Initially the increase in BoU reduces overall cost since the cost in utilising the ESS and VESS is smaller than the saving that is delivered through reduced violation of the network constraints. At a larger BoU however, the increased over protection results in greater ESS and VESS procurement cost that is not outweighed by the benefit in network reliability and thus overall costs increase.

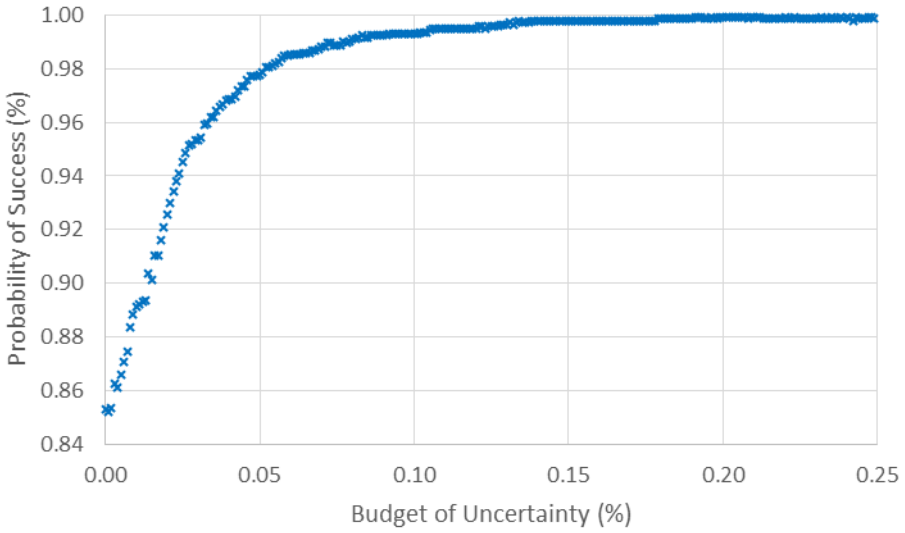

Figure 5-12 Relationship between BoU and PoS for all the constraints when using 30-minute-ahead forecasts

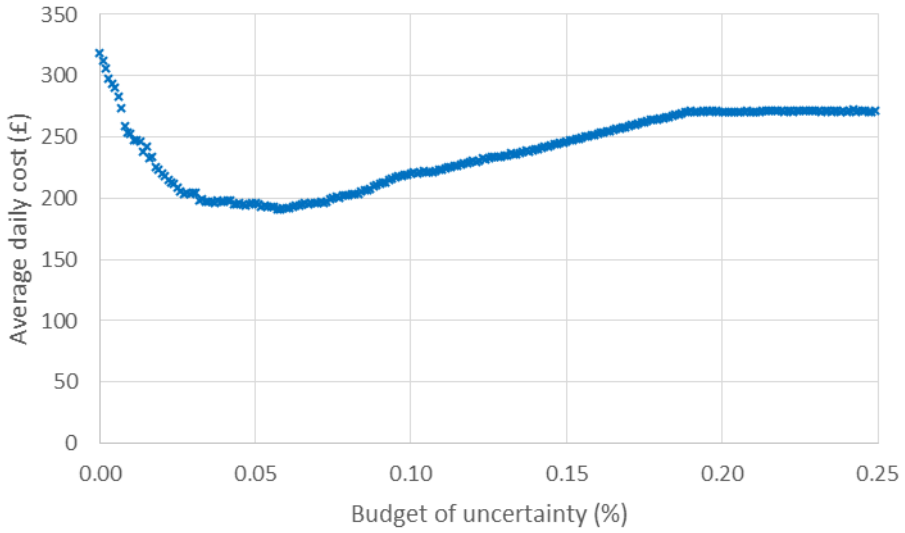

Figure 5-13 Relationship between BoU and total operational cost all the constraints when using 30-minute-ahead forecasts

The resulting relationship between PoS and average daily total operational cost is shown in Figure 5-14, alongside the relationship that would result from the formulation when modelling the uncertainty associated with day-ahead forecasting. It can be seen that the PoS with the lowest operational cost, the EOPoS, for the test network with all constraints included is 0.985 when using 30-minute-ahead forecasts and 0.976 when using day-ahead forecasts. The associated average daily network operating cost is £191/day when using 30-minute-ahead forecasts and £185/day when using day-ahead forecasts. These values can be compared

against the average daily network operating cost when the BoU is very large[1], representing the cost associated with taking a traditional worst case approach to mitigating uncertainty rather than a risk based approach, of £272/day when using 30-minute-ahead forecasts and £456/day when using day-ahead forecasts. Therefore the risk based approach has a cost 70.2%, and 40.6%, of the traditional worst case approach when using 30-minute-ahead, and day-ahead forecasts, respectively. To achieve this cost reduction, a small increase in risk has been accepted.

Similar studies for the isolated constraints are shown in Figure 5-15 for the power flow through the large office building feeder, Figure 5-16 for the voltage at the large office building, Figure 5-17 for the power flow through the VESS and solar PV feeder, and Figure 5-18 for the power flow through the 11/0.4 kV transformer. The EOPoS and average daily network operating cost for both a risk based approach and traditional worst case approach are summarised for 30-minute-ahead forecasts in Table 5-6 and for day-ahead forecasts in Table 5-7.

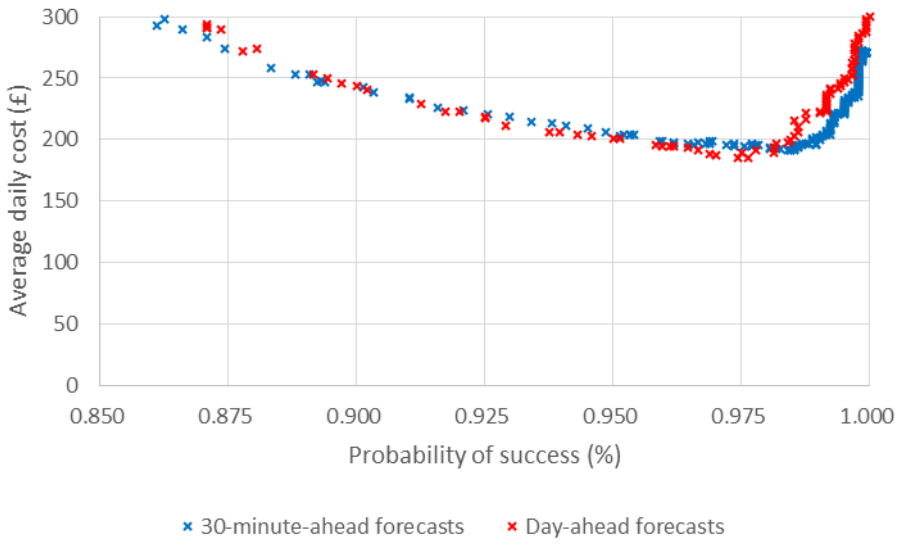

Figure 5-14 Relationship between PoS and total operational cost for all the constraints when using 30-minute-ahead and day-ahead forecasts

[1] When all the constraints were included in the formulation, very large BoU values resulted in the formulation displaying infeasibility issues which in turn resulted in an unacceptably low PoS to represent the traditional worst case approach. A BoU value of 0.249 was used to estimate the cost associated with the traditional worst case approach when all constraints were included in the formulation. For the scenarios where the constraints were isolated, a BoU value of 0.990 was used to estimate the cost associated with the traditional worst case approach.

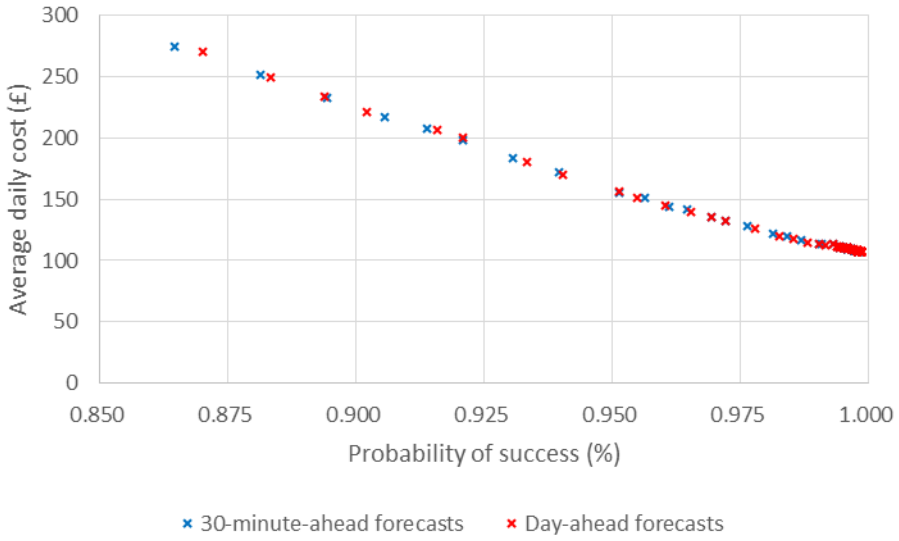

Figure 5-15 Relationship between PoS and total operational cost for the power flow constraint of the large office building feeder when using 30-minute-ahead and day-ahead forecasts

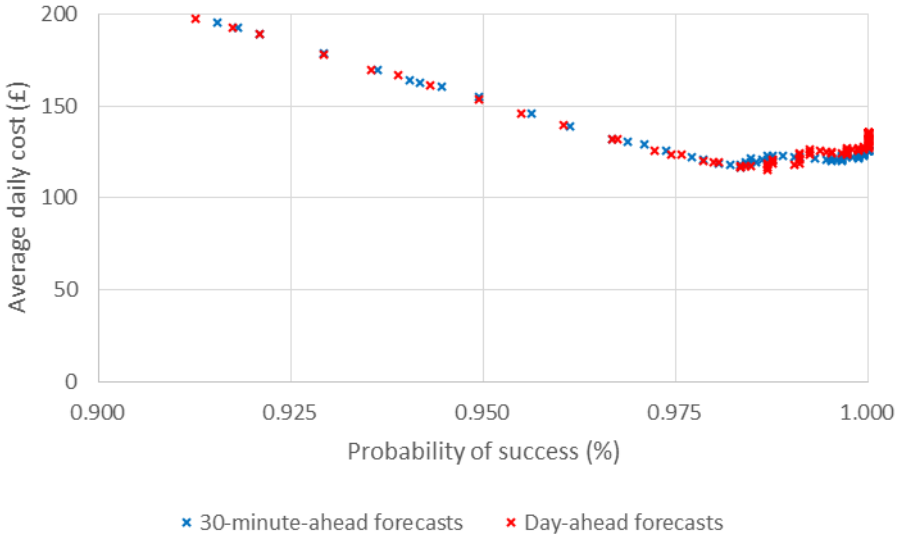

Figure 5-16 Relationship between PoS and total operational cost for the voltage constraint of the large office building when using 30-minute-ahead and day-ahead forecasts

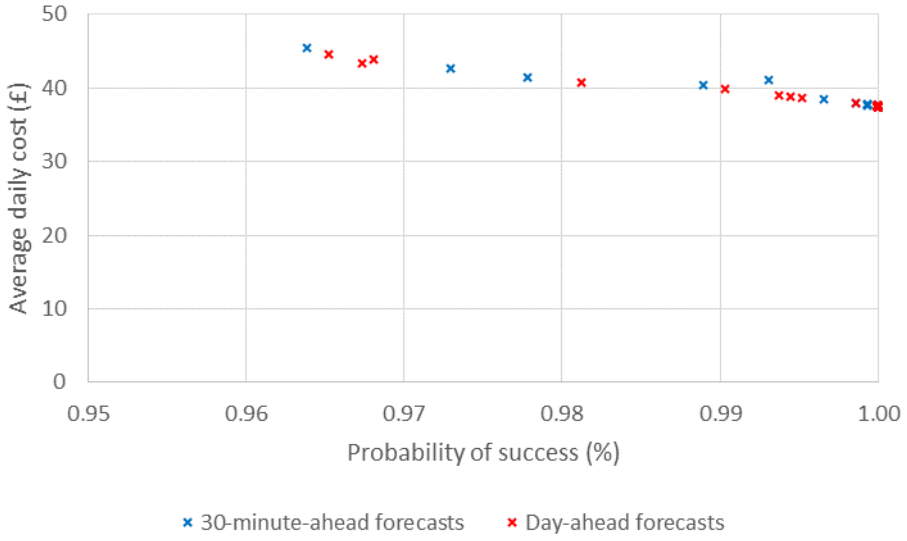

Figure 5-17 Relationship between PoS and total operational cost for the power flow constraint of the VESS and solar PV feeder when using 30-minute-ahead and day-ahead forecasts

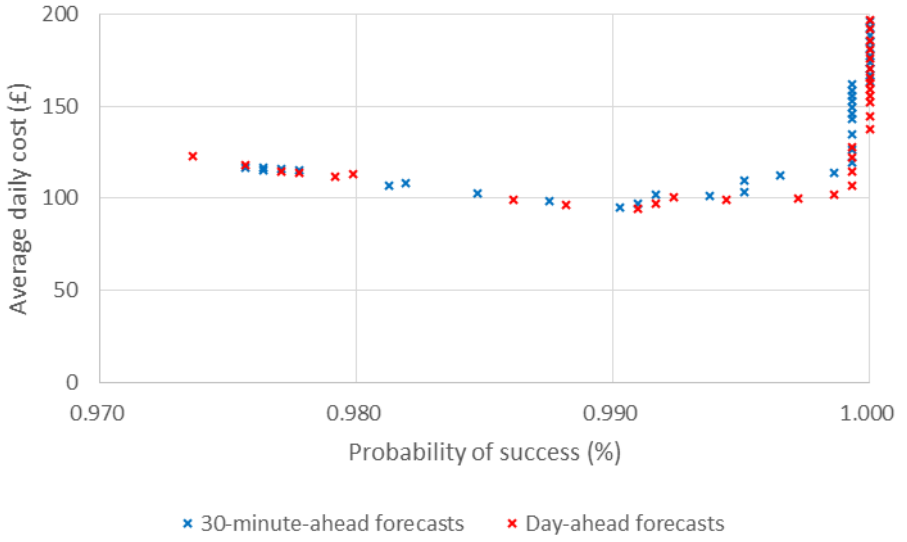

Figure 5-18 Relationship between PoS and total operational cost for the power flow constraint of the 11/0.4 kV transformer when using 30-minute-ahead and day-ahead forecasts

Table 5-6 Summary of average daily network operating cost and EOPoS for using a risk based approach and a traditional worst case approach, using 30-min-ahead forecasts

	EOPoS (%)	**Average daily network operating cost (£/day)**		**Risk based approach / traditional worst case approach (%)**
		Risk based approach	Traditional worst case approach[1]	
Power flow on the large office building feeder	99.7	107.46	107.68	99.8
Under voltage on the large office building feeder	98.3	116.84	125.71	92.9
Power flow on the VESS and solar PV feeder	100.0	37.45	37.50	99.9
Power flow through the 11/0.4 kV transformer	99.0	95.27	306.36	31.1
All constraints	98.5	191.10	271.89	70.3

Table 5-7 Summary of average daily network operating cost and EOPoS for using a risk based approach and a traditional worst case approach, using day-ahead forecasts

	EOPoS (%)	**Average daily network operating cost (£/day)**		**Risk based approach / traditional worst case approach (%)**
		Risk based approach	Traditional worst case approach[1]	
Power flow on the large office building feeder	99.9	107.06	108.41	98.8
Under voltage on the large office building feeder	98.7	115.39	135.54	85.1
Power flow on the VESS and solar PV feeder	100.0	37.45	37.50	99.9
Power flow through the 11/0.4 kV transformer	99.1	94.63	386.84	24.5
All constraints	97.6	184.92	455.56	40.6

It can be seen in Table 5-6 and Table 5-7 that in all scenarios tested the risk based approach provides superior results with a lower network operating cost than using a traditional worst case approach. It can be observed however that to achieve this lowest cost operating point within the risk based approach, each constraint has its own EOPoS. When all the constraints are included in a single optimisation, there is no differentiation between the PoS of one constraint against another when deciding the EOPoS of the whole network and thus it may result in a sub-optimal solution relative to splitting the network into multiple microgrids of singular constraints all targeting their own EOPoS. Delivering an algorithm to optimise the PoS of each individual constraint could be difficult since the flexible element could be protecting against multiple constraints each with their own EOPoS, or each constraint could be protected by multiple flexible elements. This is the subject of potential future research.

When considering the EOPoS of each constraint independently; the constraints can be split into two distinct groups:

1. Constraints that the studies suggest should target 100% PoS
    - The power flow of the large city centre office building feeder
    - The power flow of the solar PV feeder
2. Constraints that the studies suggest should target a PoS less than 100%
    - The voltage at the large city centre office building
    - The power flow through the transformer

The uncertainty in power flow through the large office building feeder is almost entirely influenced by the uncertainty in the load of the building and the uncertainty in power flow through the solar PV feed is almost entirely influenced by the uncertainty in solar generation. In comparison, the uncertainty in voltage at the large office building is dominated by the uncertainty of the building load, but is influenced by all load and generation uncertainties within the network. The uncertainty in power flow through the transformer is influenced by the uncertainty in all load and generation within the test network. These results suggest that when there is only one source of uncertainty there is little benefit in using the RO risk based approach relative to traditional worst case methods. When there is a greater number of uncertain load and generation sources then the studies suggest an EOPoS lower than 100% results, with the risk based approach providing value.

The UI associated with day-ahead forecasts is larger than the UI associated with 30-minute-ahead forecasts. This results in the network operating cost for traditional worst case being larger for day-ahead forecasts than 30-minute-ahead forecasts. Despite this, the cost at the

EOPoS within the risk based approach is very similar (within the confidence bounds specified in Section 5.4.2) regardless of the forecast type, albeit at a different EOPoS. The studies indicate that by using a risk based approach, at some PoS values the uncertainty associated with day-ahead forecasts can result in lower network operating cost than when using the uncertainty associated with 30-minute-ahead forecasts. Previous studies in the literature suggested that rolling re-calculation with updated more accurate forecasts result in lower cost [50]. The claim in the literature is supported in Figure 5-14 however, when all constraints are modelled and operating at a high PoS; there is a clear benefit to using 30-minute-ahead forecasts over day-ahead forecasts. When considering these insights, it should be remembered that the ESS and VESS are time limited resources based on SoC. The ESS and VESS were appropriately sized in the studies such that they always had sufficient SoC to deliver the power set-point determined by the formulation. If this were not the case, then some forecasting over a horizon longer than 30 minutes would likely be required to ensure the SoC is at an acceptable level.

At present, DNOs achieve a very high PoS because they are mandated to do so as a requirement of their licence to operate [152], regardless of the cost that would apply for a loss of load. When domestic customers are left without power during normal weather conditions for more than 12 continuous hours, the customer can apply for compensation from the DNO of £100 [153], equating to £19,770/MWh lost load assuming the average UK domestic load [154]. No information has been found to quantify how many customers know they are entitled to this compensation, and what percentage actually claim the compensation when they are entitled to it. This makes it difficult to ascertain with confidence the true cost of lost load to the DNO in the present regulatory environment.

The Value of Lost Load (VoLL) to the customer and wider economy has been estimated for different load types as summarised in Table 5-8 [155]. There is significant uncertainty over VoLL and UK government and regulatory decisions have used a figure of £16,940/MWh in the past [155].

Table 5-8 Range of VoLL to the customer and wider economy [155]

Customer type	Low VoLL (£/MWh)	High Voll (£/MWh)
Domestic customers	700	59,000
SME customers	9,700	225,000
Larger commercial and industrial customers	423	12,336

In this Section, the EOPoS was proposed based on a cost applied to the DNO when the power flow or voltage exceeded their respective limits. The cost each time this happened was £90/MWh based on twice the wholesale value of energy; thus compensating both the generator and load customers. This value is substantially lower than both the estimates for VoLL in Table 5-8 and the present cost to the DNO through compensation.

The EOPoS is determined through the BoU associated with the lowest total operational cost; a combination of flexibility procurement cost, electrical losses, degradation of network assets and the cost of lost load. The formulation developed achieves this lowest operational cost as an alternative to traditional reinforcement which has a high capital cost. The developed formulation should not be viewed as replacing traditional reinforcement altogether however. Determining whether a smart solution or traditional reinforcement is the most economical will depend on the reinforcement cost, the smart solution operational cost, the internal cost of capital of the DNO and their required payback period for investment capital.

5.6 Chapter conclusions and contribution to knowledge

A RO formulation has been developed to determine ESS and VESS power set-points that can effectively mitigate against load uncertainty, appropriately balancing the replacement costs of network components (storage, transformers, cables) that can be degraded based on how they are utilised.

The modelling environment employed has enabled an assessment of the errors introduced through linearization of the problem via sensitivity factors calculated based on load flows of the full AC power system equations. The errors have been quantified as up to 1.6% when there is no load and generation uncertainty, and up to 4.0% when there is load and generation uncertainty. To mitigate against the errors introduced and to allow the simpler linear optimisation methods to be utilised on the non-linear power system, a constraint derating factor has been proposed.

A methodology to determine the EOPoS has been proposed using the BoU variable within RO. It has been shown that by using a risk based approach, a lower network operating cost can be realised relative to using a traditional worst case approach; as low as 24.5% of the cost associated with the traditional worst case approach. The benefit was seen as negligible when there was only one source of uncertainty affecting a constraint, and significant benefit was achieved when there are multiple sources of uncertainty affecting a constraint. It has also been shown that different parts of a network can have a different EOPoS. At high PoS when

multiple network constraints are considered, using the uncertainty associated with 30-minute-ahead forecasts out performed using the uncertainty associated with day-ahead forecasts.

Chapter 6 Discussion

6.1 Introduction

This Thesis has investigated ESS and EVs as a means of mitigating uncertainty in urban microgrids in order to maintain safe operation within the distribution system voltage and power flow constraints without needing to reinforce the network. Chapter 2 reviewed the literature to find the state-of-the-art within the field and to inform the research direction. This led to researching the impacts of uncontrolled EV charging and proposing a methodology to forecast demand in Chapter 3, which is discussed further in Section 6.2 in relation to the research presented in later chapters. The available flexibility of EV charging demand was aggregated to form a VESS in Chapter 4 and is discussed further in Section 6.3. Chapter 4 also considered a VPP delivering frequency response services, and is discussed further in Section 6.4 in relation to when a microgrid has power flow and voltage constraints limiting the contribution each individual flexible asset can provide to the frequency response services, similar to that studied in Chapter 5. Section 6.5 discusses further the benefits and drawbacks of the various power system linearization techniques relative to the insights presented in Chapter 5.

6.2 Uncontrolled electric vehicle charging

The technical impacts of uncontrolled EV charging presented in Section 3.2 and the associated reinforcement cost presented in Section 3.3 were based upon domestic uncontrolled charging. In the case of the technical impacts this was because the existing industrial and commercial load is very business specific making it difficult to draw generalizable conclusions. The reinforcement cost was based on domestic uncontrolled charging to understand the cost that Ofgem would allow DNOs to recover from consumers through the socialised Distribution Use of System (DUoS) charging mechanism. It is expected however that significant charging will take place in public and work locations that were not considered within the scope of the Chapter 3 methodology. There is little concern among DNOs regarding the costs associated with non-domestic uncontrolled charging induced network reinforcement, because such connection offers are made on a commercial basis and thus the costs are recoverable. On this basis, the non-domestic charging business models are expected to pass on the cost of network reinforcement, or reduced cost through smart charging, to the consumer where appropriate. Therefore the consumer is expected to ultimately determine the appropriate charge point rating and associated levels of network

reinforcement and charging duration in the non-domestic setting through natural economic market forces regarding which business models emerge as successful.

It was found in the literature surveyed in Chapter 2 that although a significant number of consumers would be willing to partake in smart charging, not all would be willing [71]. Previous studies in the literature also found that forecasting uncontrolled charging is critical to utilising the flexibility of smart EV charging [97], and thus Section 3.4 proposed a methodology to forecast the uncertainty of uncontrolled EV charging load. The methodology proposed is most accurate when the existing uncontrolled charging load is central to that expected from long term diurnal analysis. When the existing uncontrolled charging load is on the extremes of that expected from long term diurnal analysis, the methodology is significantly less accurate and therefore there is scope for further research. The forecasting methodology was utilised for standard charging in Chapter 5 when modelling the uncertainty surrounding 30-minute-ahead forecasts, where it was shown that a higher network PoS could be achieved for the same network operating cost relative to the uncertainty surrounding day-ahead forecasts when all constraints are considered. Despite this, the day ahead uncertainty for rapid uncontrolled EV charging was used because it was shown in Chapter 3 that when the forecast horizon is greater than 24 minutes then the uncertainty surrounding uncontrolled rapid EV charging cannot be improved relative to that calculated using long term diurnal analysis. The higher the charge point rating, the shorter forecast horizon needs to be to gain value from short-term forecasting uncontrolled EV charging relative to using the long term diurnal analysis.

6.3 Flexibility of electric vehicle charging

In Chapter 4, a methodology was developed to utilise the flexibility of EV charging to develop what appears to the grid as a VESS, allowing the EV flexibility to be optimised relative to other power system flexibility such as ESS. It was shown that EVs can reliably be called upon (~99%), in aggregate, to supply services to the electrical distribution network while also ensuring that the vehicles have sufficient energy within them for their primary purpose of transport by the time the energy is needed. There is a period of the day when there is a limited loss of controllability when the numbers of vehicles becomes low, due to the prioritisation of the vehicles need for energy over the grid request. This could be accepted as part of the price to pay to leverage the high level of controllability during the majority of the day, since without the guarantee of prioritising the EVs need for energy the number of consumers willing to use the smart charging system would be reduced.

The ability of the VESS to deliver a power request is dependent upon the SoC of each individual vehicle and thus based upon the control algorithm and previous grid requests of the algorithm. Therefore there is scope to improve upon the reliability of the VESS to deliver grid power requests through forecasting future power requests and optimising the internal energy management of the fleet. Having said this, optimising the VESS to improve reliability of delivering power requests may increase the additional charge-discharge cycles imposed on some vehicles causing an impact on battery degradation. Minimising degradation is not in itself single vector. The objective could be to minimise the maximum degradation within any one vehicle thus sharing the cost. Alternatively, the objective could be to minimise the total degradation to minimise operational cost for the VESS operator. Investigation into these multiple objectives and identification of the pareto front may inform the optimal business model for a VESS, and is the subject of potential future research.

6.4 Delivering frequency response services

A methodology was developed in Chapter 4 to successfully deliver an EFR service through utilising numerous flexible assets that individually would not have been able to deliver the service. The methodology centred around maximising power availability through maintaining a SoC as close to 50% as possible during normal operation, and when all assets are close to their SoC limits then aiming for all assets to reach their limit at the same time. Through this SoC management it was shown that only a small proportion of the available energy capacity was utilised meaning that the power rating could be increased to maximise revenue, or energy capacity reduced to minimise costs; both increasing profitability of the system. Having said this, the methodology did not consider the relative cost of utilising the flexibility of one asset relative to another when controlling the internal energy management and could be the subject for potential future research. Including the cost to utilise a flexible asset within the control could impact on the energy capacity required. A methodology could also be developed in future research to optimise the extent to which the VPP system delivering an EFR service tries to maximise power availability relative to minimising operational cost.

During Chapter 4, the EFR service was delivered from a VPP where there were no network constraints limiting the available power flexibility that could be delivered from any one flexible asset. In the future however, the flexibility could be embedded within a distribution network with power flow and voltage constraints similar to that studied in Chapter 5. It was observed in Chapter 5 that each constraint could be considered independently resulting in an understanding that the EFR service could be split between multiple flexible assets; some able to demand additional power but not supply, while others are able to supply additional power

but not demand. Through intelligent coordination, a full frequency response service could be provided to the wider network from within a constrained microgrid and is the subject of potential future research. This would increase the number of flexible assets able to partake in frequency response services increasing competition and reducing costs for the TSO while concurrently adding an additional layer of potential revenues for the flexible asset operator helping their business case as an alternative to network reinforcement.

These ideas can be discussed further by taking the microgrid under test in Chapter 5 as an example. At the times when there are no constraint limitations both the ESS and VESS of smart charging EVs could deliver the full EFR service. When the feeder supplying the large city centre office building is constrained by power flow or voltage limitations the ESS is required to supply a minimum amount of real power generation to the network, and thus could supply a greater amount of real power generation for frequency response. In contrast, when the feeder supplying the solar PV system is constrained by power flow, the VESS is required to demand a minimum amount of real power load, and thus could demand a greater amount of real power load for frequency response. Together, despite these limitations, the ESS and VESS could work together to provide a full EFR service. The microgrid under test in Chapter 5 however has one further limitation of the power flow through the transformer when in N-1 condition; in this situation the microgrid would have times when the full EFR service could not be provided to the wider macrogrid, and another microgrid elsewhere within the network would need to work collaboratively in a similar manner. Such a system of constrained frequency response would rely on the diversity of flexibility availability.

6.5 Linearisation of the power system

The linearization of the power system allows the use of deterministic optimisation algorithms such as LP and can be transformed through RO to operate effectively under uncertainty. It was noted in the literature that through utilising a DC load flow within the linear optimisation could result in power flow and voltage constraint violations when modelled on the AC system [60], with errors up to 4.46% [93]. It has been shown in this Thesis however that linearization through calculating power flow and voltage sensitivity factors based on the full AC power system equations can display reduced linearization errors. Without load and generation uncertainty the maximum error observed was 1.6% and with load and generation uncertainty the maximum error observed was 4.0%. Furthermore, by basing the linearization on the full AC power system equations instead of a DC load flow enables the sensitivity factors to be calculated for both real and reactive power relative to the voltage and apparent power flow through each part of the network. In theory, this should mean that reactive power could be

implemented as a decision variable within the uncertain deterministic optimisation methodology as well as real power. Since reactive power does not impact upon the degradation of an ESS battery, its use to solve a network constraint violation could be more cost effective than utilising real power. It was found during development of the formulation used in this Thesis that reactive power as a decision variable within an iterative method, to ensure representative sensitivity factors are used, could become unstable and result in non-convergence. This issue could be mitigated by using a more complex MILP solver and a piecewise approach similar to that proposed in [61] where load and generation certainty was assumed. The transformation to RO to account for load and generation uncertainty vastly increases the number of decision variables and constraints and implementing this within a MILP solver is the subject for potential future research.

The non-convergence when using reactive power as a decision variable was caused because the cost function assumed zero cost to utilising the reactive power. Regardless of the magnitude of the real power decision variable to apparent power flow sensitivity factor relative to the reactive power decision variable to apparent power flow sensitivity factor, the cost function meant the LP always utilised the reactive power. This was unable to achieve the required reduction in apparent power flow resulting in the non-convergence. There are two potential modifications that could prevent this situation while still using a LP solver. One option is to implement a cost to utilise the reactive power; small enough to be representative to ensure an optimal solution is achievable, yet large enough that a real power decision variable is used when it is more appropriate. Another option is to consider the results of Chapter 5 in that each network constraint could be considered independently to achieve its own EOPoS. In this situation, it would be an easier task to intelligently select the appropriate decision variable for a particular network constraint; generally a real power decision variable for an apparent power flow constraint, and a reactive power decision variable for a voltage constraint. Exploring these ideas is the subject of potential future research.

Chapter 7 Conclusions and future work

7.1 Overview

A literature review was undertaken in Chapter 2 to find the state-of-the-art within the field of urban microgirds and EV charging. From this, Chapter 3 considered the technical and economic impacts of uncontrolled EV charging, and developed a methodology to forecast uncontrolled EV charging load. Chapter 4 developed a methodology to aggregate a number of smart charging EVs into a VESS, which was then utilised with other flexible loads within a VPP to deliver an EFR service to the wider grid. In Chapter 5, an algorithm was developed to utilise flexible loads to mitigate uncertainty within the power system and prevent, with economically optimal probability, power flow and voltage limits from being exceeded. Finally, all chapters were compared, contrasted and discussed in Chapter 6.

The specific conclusions and contributions to knowledge from the research are listed in Section 7.2, and the areas of potential future research are listed in Section 7.3.

7.2 Conclusions and contributions to knowledge

- A study has been undertaken to quantify the EV penetrations that would result in domestic distribution networks exceeding statutory power flow, under voltage and voltage unbalance limits. It was found that:
    - Transformer power flow limits in a heavily loaded generic network are expected to be exceeded when EV penetration reaches 40%
    - Average load is within the power flow limits of the transformer within a heavily loaded generic network even at 100% penetration, suggesting ESS or smart charging could be an alternative solution to transformer reinforcement
    - Under voltage limits are not expected to be exceeded even when EV penetration reaches 100% in a heavily loaded generic network
    - Voltage unbalance limits are expected to be exceeded when EV penetration reaches 60% in a heavily loaded generic network
- A study has been undertaken to estimate the expected network reinforcement cost that Ofgem would allow DNOs to recover from consumers under a largescale uptake scenario. Total present value costs are expected to be within the range:
    - £19.55bn - £22.48bn to 2030, assuming 8.2m EVs by 2030
    - £60.81bn - £74.27bn to 2040, assuming 31.1m EVs by 2040

- A methodology has been developed to forecast future uncontrolled EV charging load and the uncertainty surrounding that forecast, based on the 'here and now' uncontrolled EV charging load experienced on the network. Using the methodology and historical charging probability distribution functions of early adopters, it was found that the UI could be reduced relative to that developed from long term diurnal analysis by looking ahead no more than:
    - 1.5 hours for standard charging of 750 EVs per day
    - 24 minutes for rapid charging of 100 EVs per day
- A methodology has been developed to aggregate a number of smart charging EVs to form a VESS able to deliver services to the distribution network with a high degree of controllability (~99% for the two power request profiles under test), while also guaranteeing the EVs with the energy they need by the time it is needed for their primary objective of transportation.
- A methodology has been developed to combine any number of flexible loads and through effective energy management coordination maximise their individual power availability to deliver an EFR service to the macrogrid. Through utilising the algorithm and an example based on Newcastle Science Central, it was shown that storage capacities could be reduced minimising initial capital cost or power ratings increased maximising potential EFR revenues, relative to the flexible loads operating in isolation from one another.
- A RO formulation has been developed to calculate the power set-point that an ESS and VESS should operate at in order to protect a microgrid from power flow and voltage limit violations caused through load and generation uncertainty. Using this formulation, a specific LV test network and associated load and generation profiles:
    - The errors introduced through linearization of the power system via sensitivity factors calculated based on load flows of the full AC power system equations were calculated as:
        - Up to 1.6% when there is no load and generation uncertainty
        - Up to 4.0% when there is load and generation uncertainty
    - A lower network operating cost can be realised by taking a risk based approach relative to using a traditional worst case approach. The benefit was larger when there were multiple sources of uncertainty impacting upon a constraint. The greatest benefit found was:
        - The risk based approach costing 31.1% of the traditional worst case approach cost, when using 30-minute-ahead forecasts

        - The risk based approach costing 24.5% of the traditional worst case approach cost, when using day-ahead forecasts
    - A methodology was developed to determine the EOPoS, where it was shown through the studies that different parts of a network can have different EOPoS.
    - At high PoS when multiple network constraints are considered, using the uncertainty associated with 30-minute-ahead forecasts out performed using the uncertainty associated with day-ahead forecasts.

7.3 Areas of potential future research

- Improve the ability to forecast uncontrolled EV charging:
    - When the existing charging load is not close to the centre of the long term diurnal UI.
    - When the numbers of EVs charging per day changes and consequently there are different levels of diversity to that studied in this Thesis
- Investigate the multiple objectives that the internal energy management of a VESS of smart charging EVs could be optimised for, and investigate the viability of potential business models for each point on the pareto front.
- Develop new control algorithms to improve the coordination of flexible loads to deliver EFR services to the macrogrid:
    - Include the individual flexible load procurement cost within the formulation, and investigate the impact this has on reduced power availability and resulting revenue generation.
    - Develop algorithms that allow multiple sources of flexibility, all constrained through power flow and voltage limits within a microgrid, to deliver an EFR service through intelligent coordination.
- Investigate RO formulations to calculate ESS and VESS power set-points further:
    - Investigate how a RO formulation could be implemented within a MILP solver to improve reliability of solution convergence and to enable the use of reactive power decision variables
    - Investigate the potential to split the problem into numerous sub-problems, despite the potential for multiple sources of flexibility that could apply to each constraint, and for multiple constraints that could apply to each source of flexibility:
        - To allow appropriate decision variables to be intelligently selected for a particular constraint

- To allow each constraint to target its own EOPoS

Appendix A Images of PSCAD model used in Chapter 3

Screen shots of the PSCAD model used in Chapter 3 are shown in Appendix Figure A-1, Appendix Figure A-2, Appendix Figure A-3 and Appendix Figure A-4.

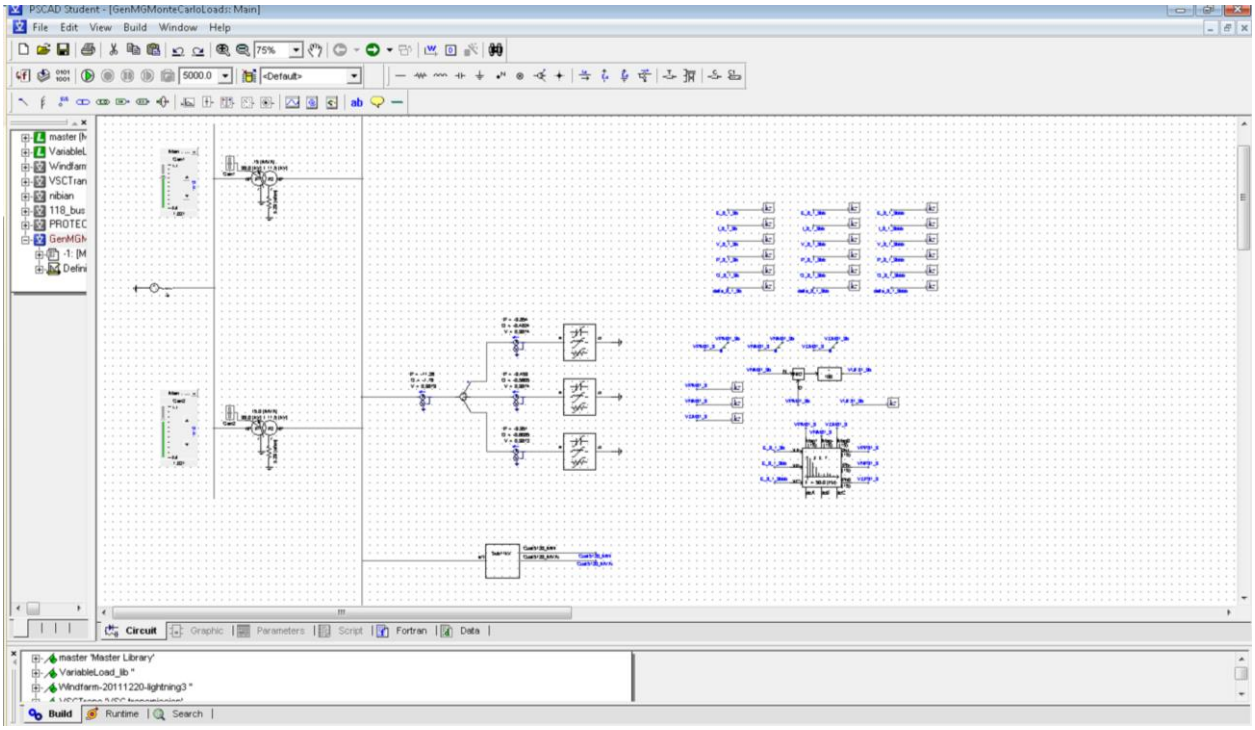

Appendix Figure A-1 PSCAD model 33/11 kV transformers, 11 kV lumped loads and link to the model shown in Appendix Figure A-2

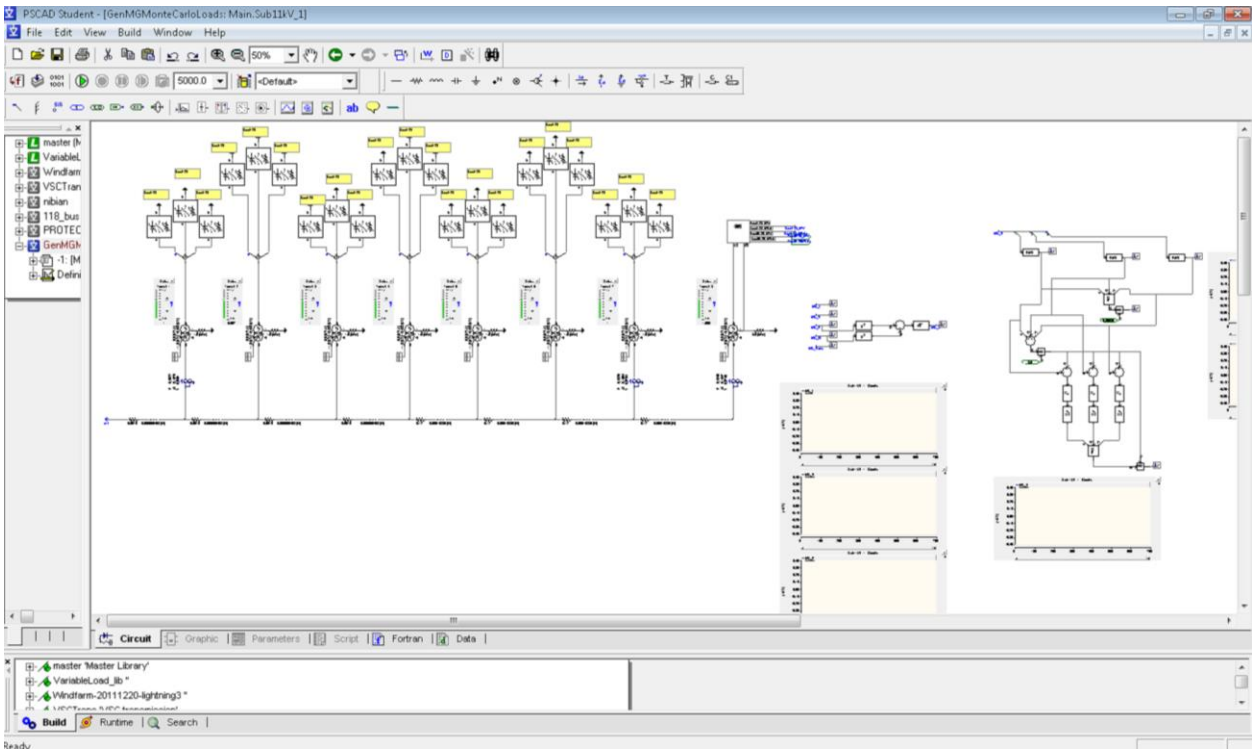

Appendix Figure A-2 PSCAD model 11/0.4 kV transformers and link to the LV model shown in Appendix Figure A-3 and Appendix Figure A-4

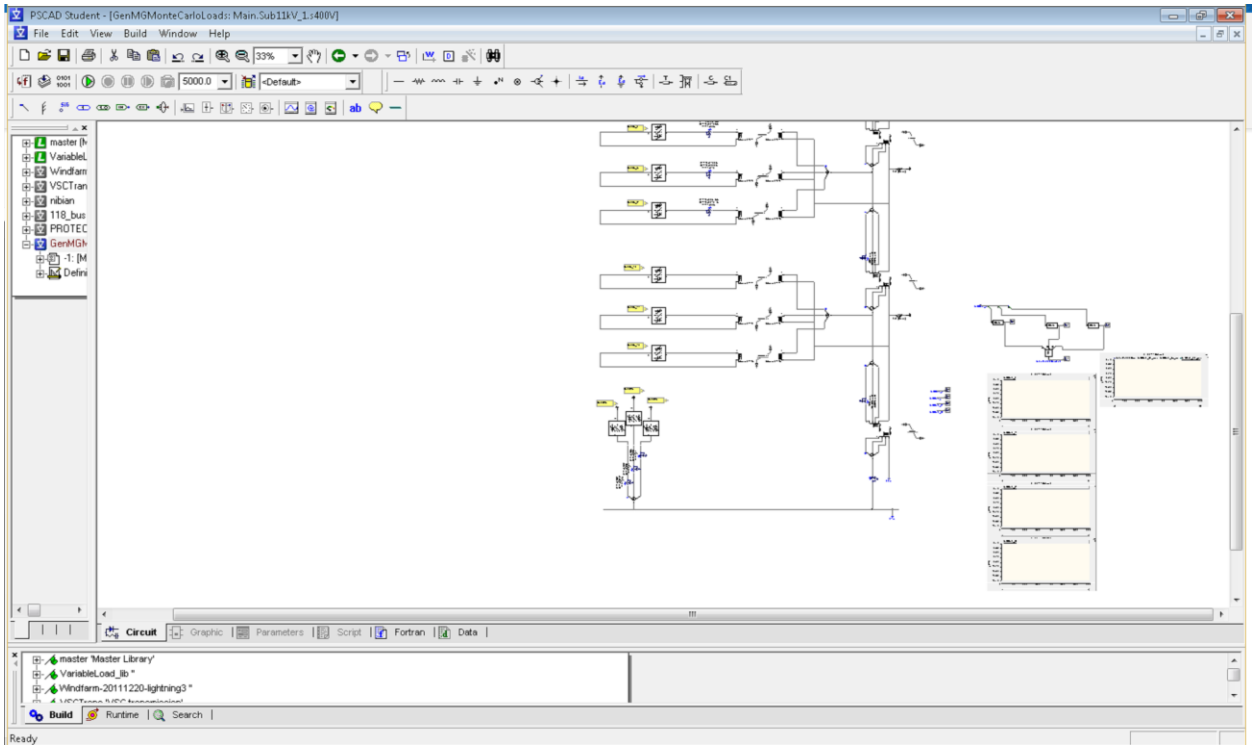

Appendix Figure A-3 PSCAD model LV lumped load and start of LV cable feeder

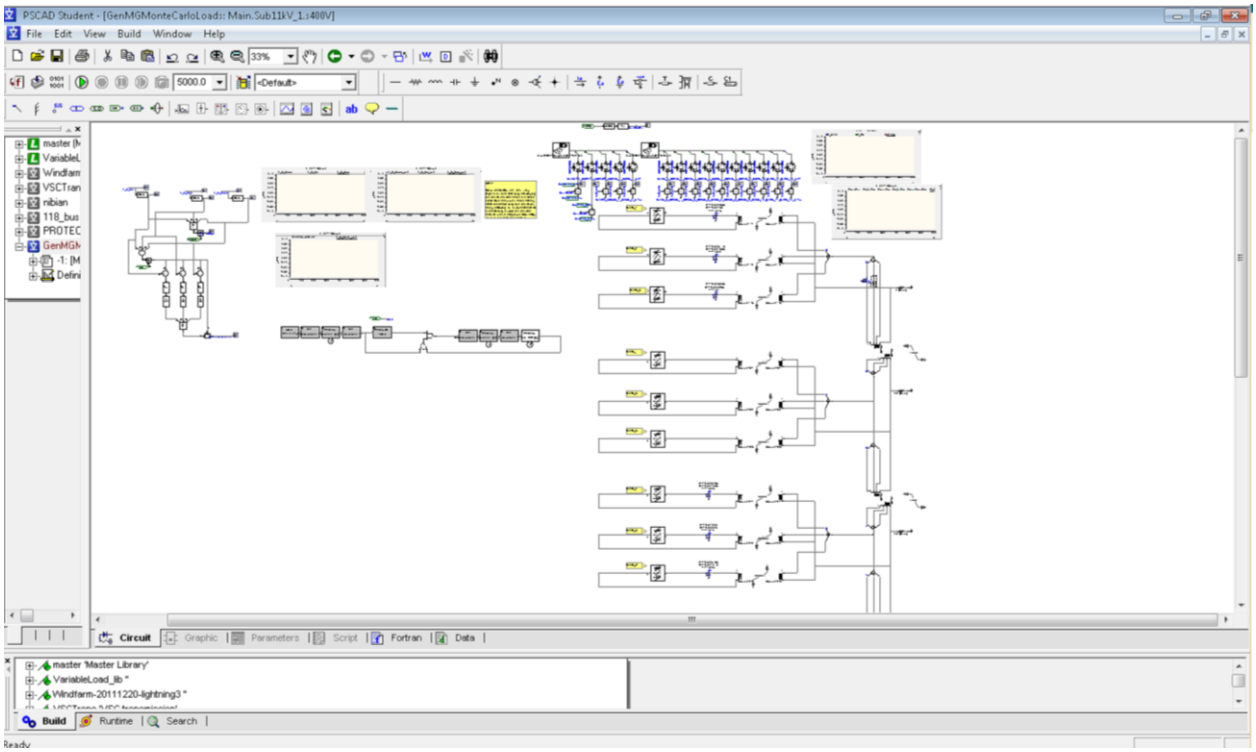

Appendix Figure A-4 PSCAD model LV feeder remote end

Appendix B Frequency domain IPSA2 results associated with the PSCAD analysis presented in Chapter 3

This appendix reproduces the frequency domain IPSA2 results that were referred to in the PSCAD analysis of the impact of uncontrolled EV charging on distribution networks presented in Chapter 3. These figures were produced by others in the development of the journal paper co-authored by the author of this Thesis [16].

Appendix Figure B-1 displays the convergence of the MCS simulation, giving justification of the 1000 simulated days used in Chapter 3, using the urban test network with an EV penetration of 60%.

Appendix Figure B-2 displays the demand on the 11/0.4 kV transformer, as calculated in IPSA2, for a number of EV penetrations. This result gives justification for focusing on the worst case period 17:00-05:00 in the PSCAD analysis of Chapter 3.

Appendix Table B-1 displays the voltage drops calculated by IPSA2 for the generic network for a number of EV penetrations.

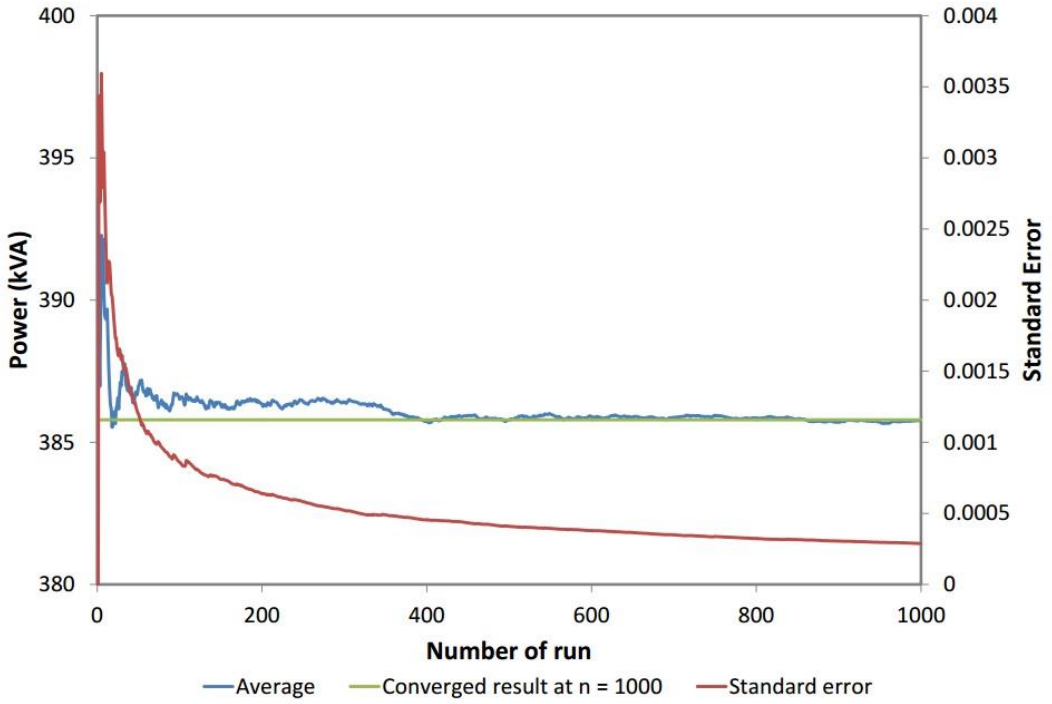

Appendix Figure B-1 Convergence of the MCS with number of simulated days, for 60% EV penetration on the urban test network. The average values (blue curve) and standard error (red curve) of the apparent power on the transformer under study.

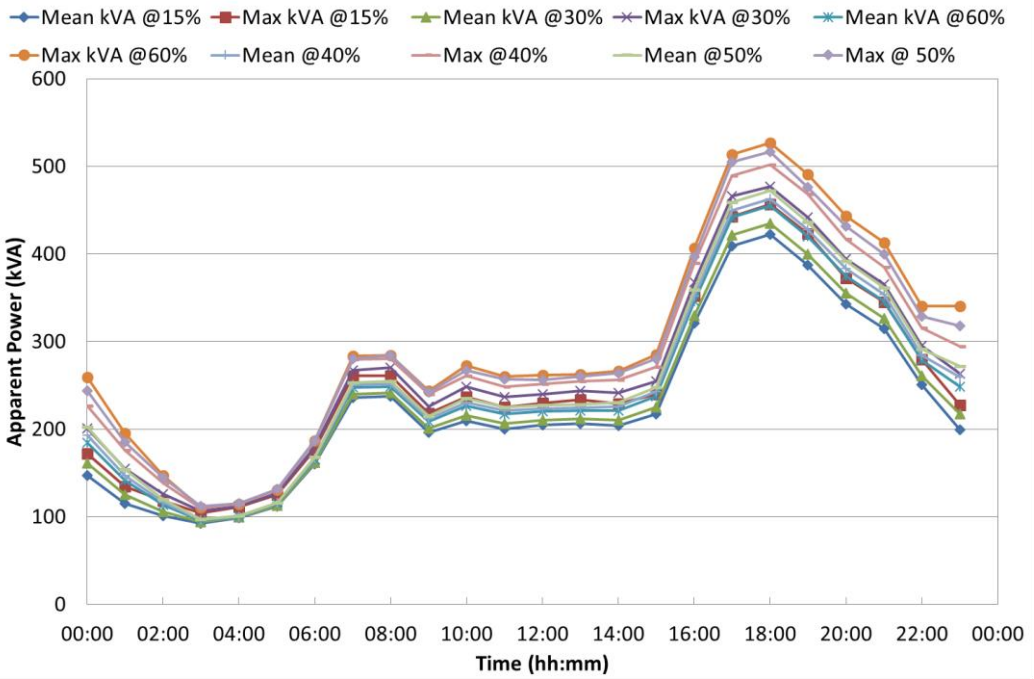

Appendix Figure B-2 Test day critical demand for the generic network, using IPSA2 calculation

Appendix Table B-1 Maximum voltage changes in the generic LV network (negative is a voltage drop), using IPSA2 calculation

Lowest voltage	15% EVs	30% EVs	60% EVs
ΔV –Mean	-1.58%	-1.64%	-1.73%
ΔV –Max	-2.67%	-2.79%	-3.02%

Appendix C MATLAB Simulink model of Newcastle Science Central and associated control for Section 4.5

Screen shots of the MATLAB Simulink model used in Section 4.5 are shown in Appendix Figure C-1, Appendix Figure C-2, Appendix Figure C-3, Appendix Figure C-4, Appendix Figure C-5 and Appendix Figure C-6.

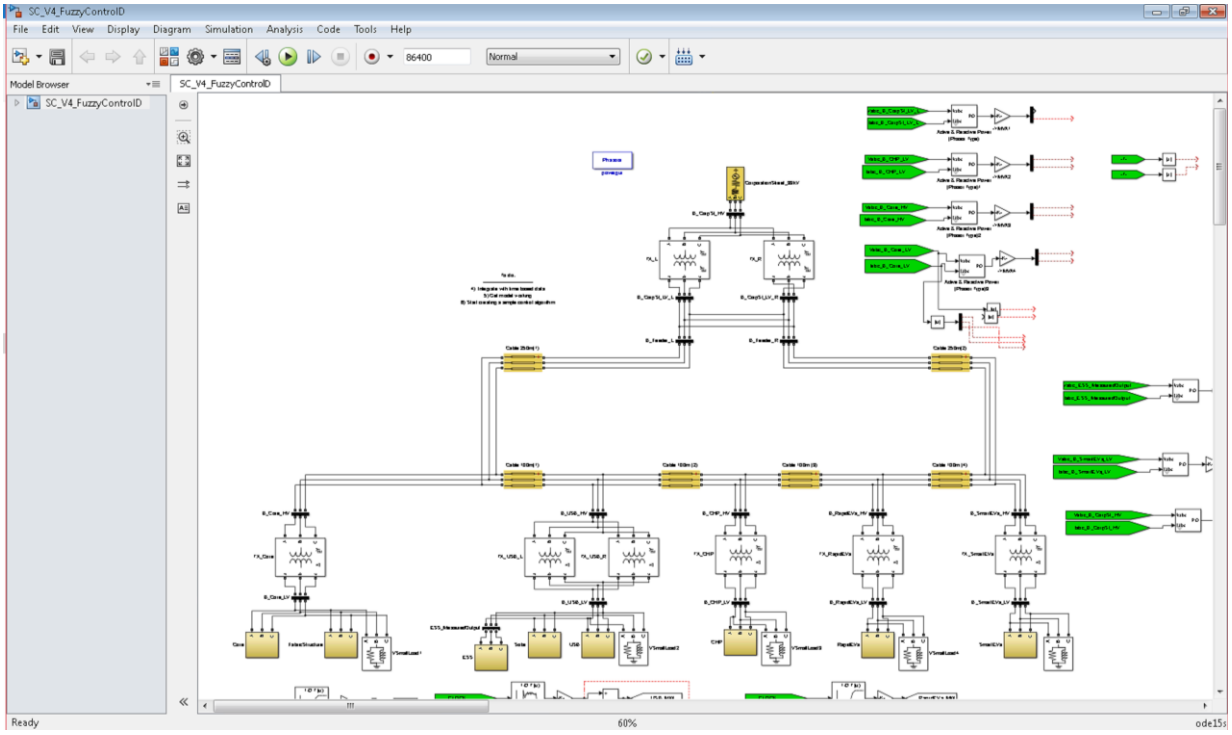

Appendix Figure C-1 MATLAB Simulink model of the Newcastle Science Central electrical distribution system

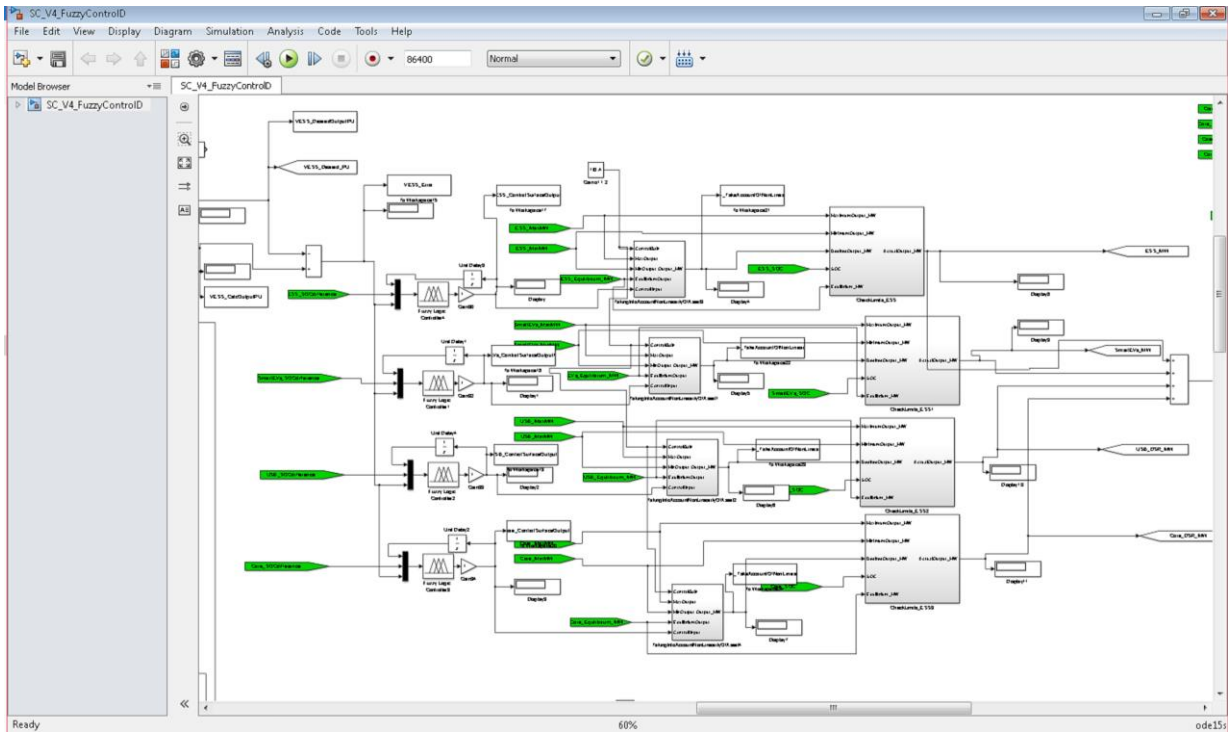

Appendix Figure C-2 MATLAB Simulink fuzzy logic control system

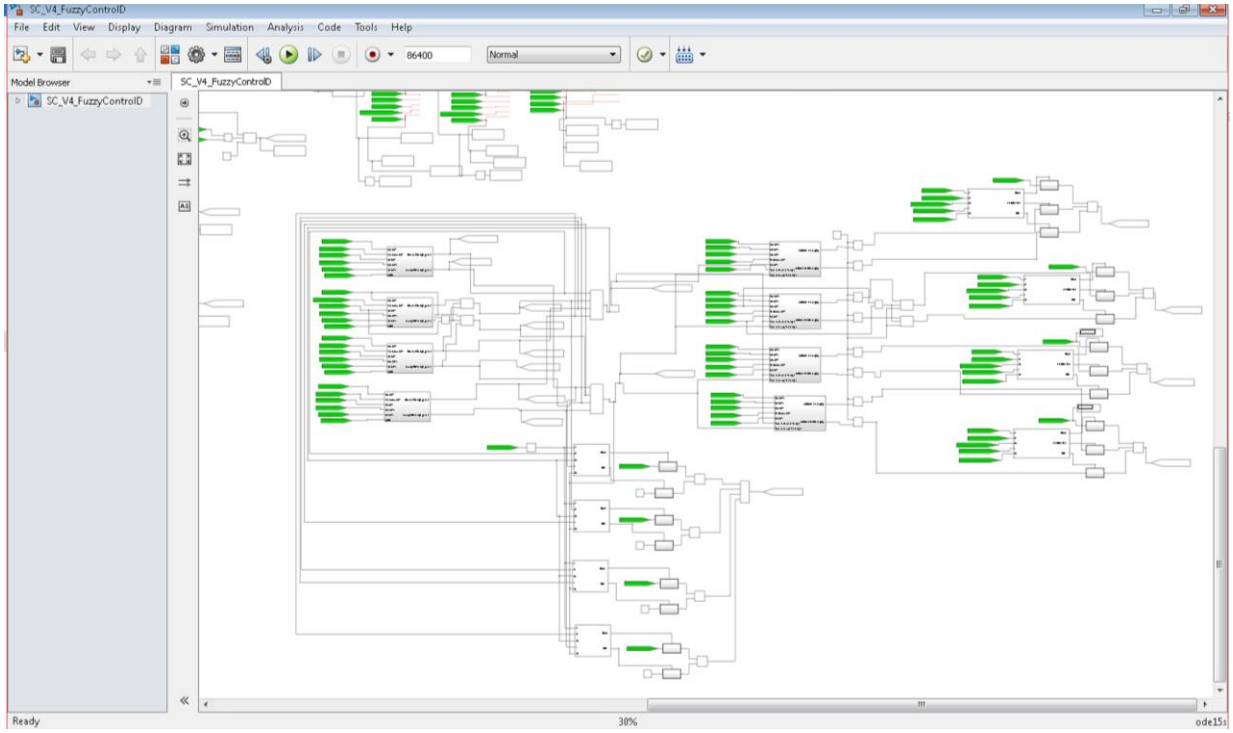

Appendix Figure C-3 MATLAB Simulink target SoC calculation

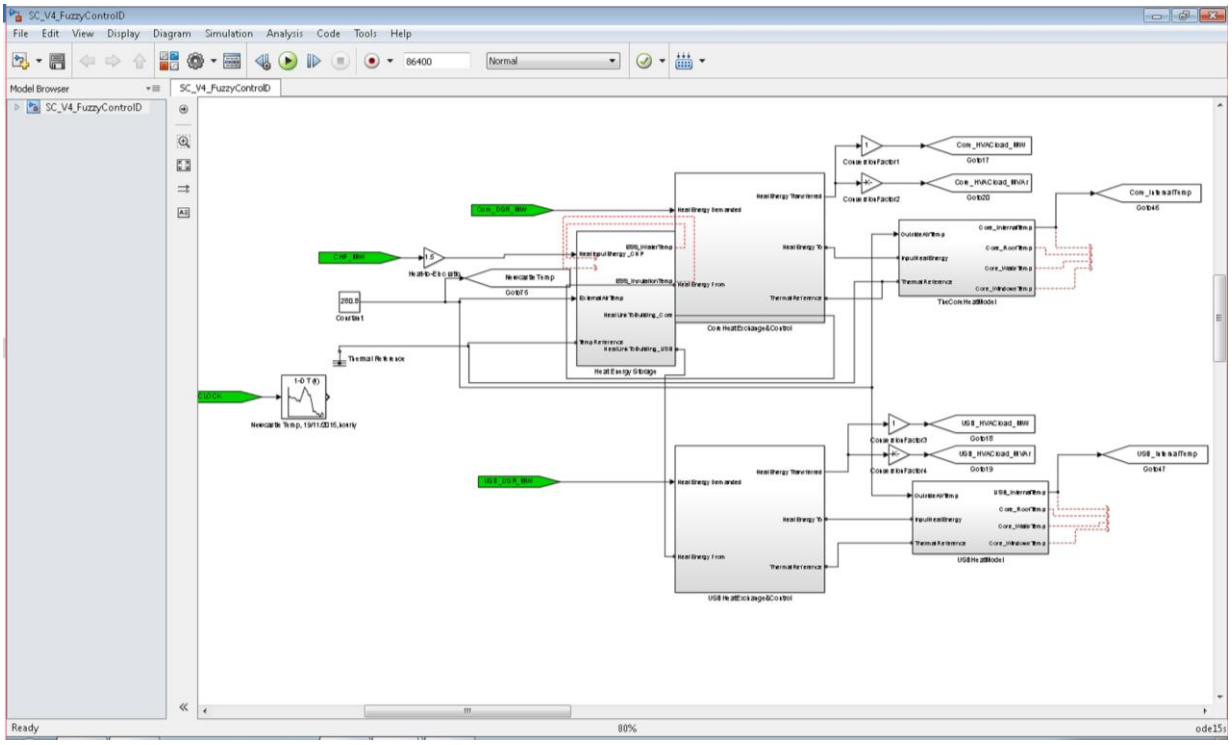

Appendix Figure C-4 MATLAB Simulink heat model overview for building DSR

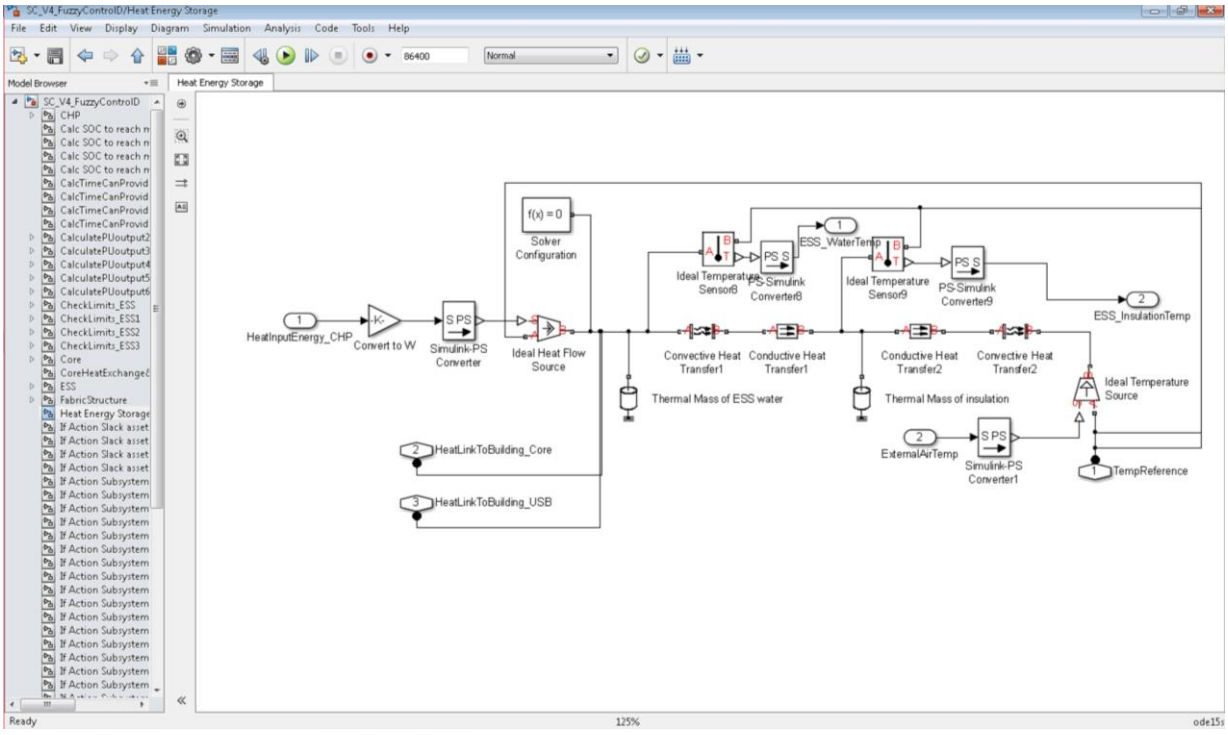

Appendix Figure C-5 MATLAB Simulink heat energy storage model

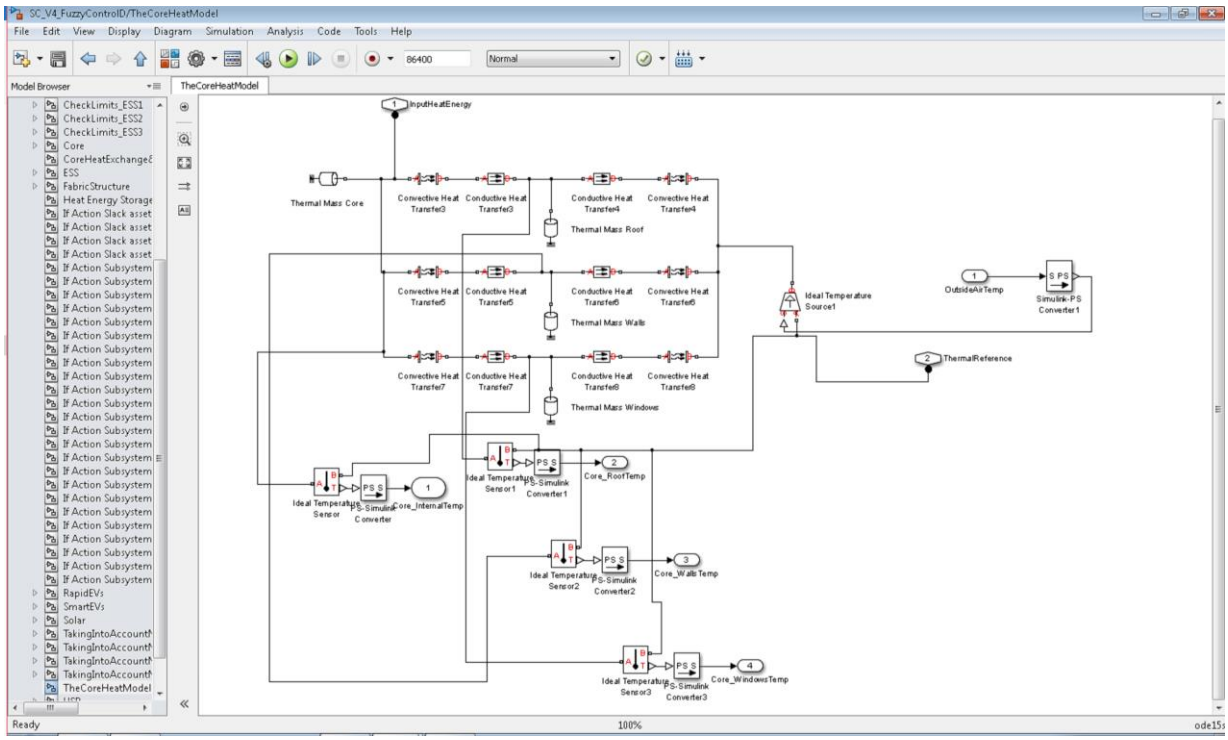

Appendix Figure C-6 MATLAB Simulink building heat model

References

1. *Paris Agreement*. 2015, United Nations: Paris. Available from: http://unfccc.int/files/essential_background/convention/application/pdf/english_paris_agreement.pdf, [Accessed 30/05/2017]

2. *2015 UK greenhouse gas emissions, final figures*. 2017, Department for Business, Energy & Industrial Strategy. Available from: https://www.gov.uk/government/uploads/system/uploads/attachment_data/file/604350/2015_Final_Emissions_statistics.pdf, [Accessed 30/05/2017]

3. *Climate Change Act 2008*. 2008, UK legislation. Available from: http://www.legislation.gov.uk/ukpga/2008/27/pdfs/ukpga_20080027_en.pdf, [Accessed 30/05/2017]

4. *UK plan for tackling roadside nitrogen dioxide concentrations*. 2017, Department for Transport. Available from: https://www.gov.uk/government/uploads/system/uploads/attachment_data/file/633269/air-quality-plan-overview.pdf, [Accessed 31/10/2018]

5. Hill, G., et al. *Monitoring and predicting charging behaviour for electric vehicles*. in *2012 IEEE Intelligent Vehicles Symposium*. 2012. Available from: https://doi.org/10.1109/IVS.2012.6232269.

6. Government, U., *Automated and Electric Vehicles Act 2018*. 2018. Available from: http://www.legislation.gov.uk/ukpga/2018/18/contents/enacted, [Accessed 31/10/2018]

7. *Carbon Footprint of Electricity Generation*. 2011, UK parliamentary office of science and technology. Available from: https://www.parliament.uk/documents/post/postpn_383-carbon-footprint-electricity-generation.pdf, [Accessed 30/05/2017]

8. Boston, A., *Delivering a secure electricity supply on a low carbon pathway*. Energy Policy, 2013. **52**: p. 55-59. Available from: https://doi.org/10.1016/j.enpol.2012.02.004.

9. Schlomer, S., et al., *Annex III: Technology-specific Cost and Performance Parameters*, in *Climate Change 2014: Mitigation of Climate Change*, S. Schlomer, Editor. 2014, Cambridge University Press: Cambridge, United Kingdom and New York, NY, USA. Available from: https://www.ipcc.ch/pdf/assessment-report/ar5/wg3/ipcc_wg3_ar5_annex-iii.pdf, [Accessed

10. *2011 Census Analysis - Comparing Rural and Urban Areas of England and Wales*. 2013, Office for National Statistics. Available from: http://webarchive.nationalarchives.gov.uk/20160105160709/http://www.ons.gov.uk/ons/dcp171776_337939.pdf, [Accessed 30/05/2017]

11. *UK solar photovoltaics deployment data*. 2017; Available from: https://www.gov.uk/government/statistics/solar-photovoltaics-deployment, [Accessed 31/10/2018]

12. *The Electricity Safety, Quality and Continuity Regulations 2002*. 2002, UK statutory instrument. Available from: http://www.legislation.gov.uk/uksi/2002/2665/pdfs/uksi_20022665_en.pdf, [Accessed 30/05/2017]

13. Thomson, M. and D.G. Infield, *Impact of widespread photovoltaics generation on distribution systems.* IET Renewable Power Generation, 2007. **1**(1): p. 33-40. Available from: https://doi.org/10.1049/iet-rpg:20060009.

14. Wang, P., et al., *Integrating Electrical Energy Storage Into Coordinated Voltage Control Schemes for Distribution Networks.* IEEE Transactions on Smart Grid, 2014. **5**(2): p. 1018-1032. Available from: https://doi.org/10.1109/TSG.2013.2292530.

15. *IEEE Guide for Loading Mineral-Oil-Immersed Transformers.* IEEE Std C57.91-1995, 1996. Available from: https://doi.org/10.1109/IEEESTD.1996.79665.

16. Neaimeh, M., et al., *A probabilistic approach to combining smart meter and electric vehicle charging data to investigate distribution network impacts.* Applied Energy, 2015. **157**: p. 688-698. Available from: https://doi.org/10.1016/j.apenergy.2015.01.144.

17. Greenwood, D.M., et al., *A Probabilistic Method Combining Electrical Energy Storage and Real-Time Thermal Ratings to Defer Network Reinforcement.* IEEE Transactions on Sustainable Energy, 2017. **8**(1): p. 374-384. Available from: https://doi.org/10.1109/TSTE.2016.2600320.

18. Barteczko-Hibbert, C., *After Diversity Maximum Demand (ADMD) Report*. 2015, Customer-Led Network Revolution. Available from: http://www.networkrevolution.co.uk/wp-content/uploads/2015/02/After-Diversity-Maximum-Demand-Insight-Report.pdf, [Accessed 30/05/2017]

19. Pierro, M., et al., *Deterministic and Stochastic Approaches for Day-Ahead Solar Power Forecasting.* Journal of Solar Energy Engineering, 2016. **139**(2): p. 021010-1-021010-12. Available from: https://doi.org/10.1115/1.4034823.

20. Foley, A.M., et al., *Current methods and advances in forecasting of wind power generation.* Renewable Energy, 2012. **37**(1): p. 1-8. Available from: http://dx.doi.org/10.1016/j.renene.2011.05.033.

21. Quirós-Tortós, J., L.F. Ochoa, and B. Lees. *A statistical analysis of EV charging behavior in the UK*. in *2015 IEEE PES Innovative Smart Grid Technologies Latin America (ISGT LATAM)*. 2015. Available from: https://doi.org/10.1109/ISGT-LA.2015.7381196.

22. *Ultra Low Emission Vehicles Guide 2016*. 2016, The society of motor manufacturers and traders limited. Available from: https://www.smmt.co.uk/wp-content/uploads/sites/2/ULEV-Report.pdf, [Accessed 30/05/2017]

23. Lasseter, R.H. *MicroGrids*. in *2002 IEEE Power Engineering Society Winter Meeting. Conference Proceedings (Cat. No.02CH37309)*. 2002. Available from: https://doi.org/10.1109/PESW.2002.985003.

24. Ravichandran, A., et al. *The critical role of microgrids in transition to a smarter grid: A technical review*. in *2013 IEEE Transportation Electrification Conference and Expo (ITEC)*. 2013. Available from: https://doi.org/10.1109/ITEC.2013.6573507.

25. Nosratabadi, S.M., R.-A. Hooshmand, and E. Gholipour, *A comprehensive review on microgrid and virtual power plant concepts employed for distributed energy resources scheduling in power systems.* Renewable and Sustainable Energy Reviews, 2017. **67**: p. 341-363. Available from: https://doi.org/10.1016/j.rser.2016.09.025.

26. Huang, S. and D. Infield. *The impact of domestic Plug-in Hybrid Electric Vehicles on power distribution system loads*. in *2010 International Conference on Power System Technology*. 2010. Available from: https://doi.org/10.1109/POWERCON.2010.5666513.

27. Kempton, W. and J. Tomić, *Vehicle-to-grid power implementation: From stabilizing the grid to supporting large-scale renewable energy.* Journal of Power Sources, 2005. **144**(1): p. 280-294. Available from: http://dx.doi.org/10.1016/j.jpowsour.2004.12.022.

28. Yi, J., et al. *Distribution network voltage control using energy storage and demand side response*. in *2012 3rd IEEE PES Innovative Smart Grid Technologies Europe (ISGT Europe)*. 2012. Available from: https://doi.org/10.1109/ISGTEurope.2012.6465666.

29. *Future Potential for DSR in Great Britain*. 2015, Frontier Economics on behalf of the Department of Energy and Climate Change. Available from: https://www.gov.uk/government/uploads/system/uploads/attachment_data

/file/467024/rpt-frontier-DECC_DSR_phase_2_report-rev3-PDF-021015.pdf, [Accessed 31/10/2018]

30. Lidula, N.W.A. and A.D. Rajapakse, *Microgrids research: A review of experimental microgrids and test systems.* Renewable and Sustainable Energy Reviews, 2011. **15**(1): p. 186-202. Available from: http://dx.doi.org/10.1016/j.rser.2010.09.041.

31. *Guidance for developing microgrid projects*. 2016, Highlands and Islands Enterprise. Available from: http://www.hie.co.uk/common/handlers/download-document.ashx?id=47b012c8-34e1-45c5-8e14-e9d5f97cabe5, [Accessed 31/10/2018]

32. Venkataramanan, G. and C. Marnay, *A larger role for microgrids.* IEEE Power and Energy Magazine, 2008. **6**(3): p. 78-82. Available from: https://doi.org/10.1109/MPE.2008.918720.

33. Provance, M., R.G. Donnelly, and E.G. Carayannis, *Institutional influences on business model choice by new ventures in the microgenerated energy industry.* Energy Policy, 2011. **39**(9): p. 5630-5637. Available from: http://dx.doi.org/10.1016/j.enpol.2011.04.031.

34. Cluzel, C. and E. Standen, *Commercial arrangements study: Review of existing commercial arrangements and emerging best practice*. 2013, Customer Led Network Revolution. Available from: http://www.element-energy.co.uk/wordpress/wp-content/uploads/2013/07/CLNR-Commercial-Arrangements-Study_2013.pdf, [Accessed 31/10/2018]

35. Sajjad, I.A., R. Napoli, and G. Chicco. *Future Business Model for Cellular Microgrids*. in *Fourth International Sympossium on Business Modelling and Software Design*. 2014. Available from: https://www.researchgate.net/publication/262817704_Future_Business_Model_For_Cellular_Microgrids.

36. Sanz, J., et al. *Microgrids, a new business model for the energy market*. in *International Conference on Renewable Energys and Power Quality*. 2014. Cordoba, Spain. Available from: https://www.researchgate.net/publication/264287845_Microgrids_a_new_business_model_for_the_energy_market.

37. Hall, S. and K. Roelich, *Business model innovation in electricity supply markets: The role of complex value in the United Kingdom.* Energy Policy, 2016. **92**: p. 286-298. Available from: http://dx.doi.org/10.1016/j.enpol.2016.02.019.

38. Budde Christensen, T., P. Wells, and L. Cipcigan, *Can innovative business models overcome resistance to electric vehicles? Better Place*

and battery electric cars in Denmark. Energy Policy, 2012. **48**(Supplement C): p. 498-505. Available from: https://doi.org/10.1016/j.enpol.2012.05.054.

39. Manandhar, T., et al. *Operational experience of using constraint management methods for connecting distributed generation*. in *23rd International Conference on Electricity Distribution (CIRED)*. 2015. Lyon, France. Available from: http://cired.net/publications/cired2015/papers/CIRED2015_1246_final.pdf.

40. Connor, P.M., et al., *Policy and regulation for smart grids in the United Kingdom.* Renewable and Sustainable Energy Reviews, 2014. **40**(Supplement C): p. 269-286. Available from: https://doi.org/10.1016/j.rser.2014.07.065.

41. Taljaard, R.L., et al. *Standardisation of curtailment analysis and the implications for distribution network operators and generators*. in *CIRED Workshop 2016*. 2016. Helsinki, Finland. Available from: https://doi.org/10.1049/cp.2016.0798.

42. Pudjianto, D., et al. *Investigation of regulatory, commercial, economic and environmental issues in microgrids*. in *2005 International Conference on Future Power Systems*. 2005. Available from: https://doi.org/10.1109/FPS.2005.204223.

43. *Upgrading our energy system: smart systems and flexibility plan*. 2017, Ofgem. Available from: https://www.gov.uk/government/uploads/system/uploads/attachment_data/file/633442/upgrading-our-energy-system-july-2017.pdf, [Accessed 31/10/2018]

44. Olivares, D.E., et al., *Trends in Microgrid Control.* IEEE Transactions on Smart Grid, 2014. **5**(4): p. 1905-1919. Available from: https://doi.org/10.1109/TSG.2013.2295514.

45. Hajimiragha, A.H., et al., *A Robust Optimization Approach for Planning the Transition to Plug-in Hybrid Electric Vehicles.* IEEE Transactions on Power Systems, 2011. **26**(4): p. 2264-2274. Available from: https://doi.org/10.1109/TPWRS.2011.2108322.

46. Dunn, W.L. and J.K. Shultis, *1 - Introduction*, in *Exploring Monte Carlo Methods*. 2012, Elsevier: Amsterdam. p. 1-20. Available from: https://doi.org/10.1016/B978-0-444-51575-9.00001-4.

47. Hong, T., A. Raza, and F.d. León, *Optimal Power Dispatch Under Load Uncertainty Using a Stochastic Approximation Method.* IEEE

Transactions on Power Systems, 2016. **31**(6): p. 4495-4503. Available from: https://doi.org/10.1109/TPWRS.2016.2518205.

48. Uçkun, C., A. Botterud, and J.R. Birge, *An Improved Stochastic Unit Commitment Formulation to Accommodate Wind Uncertainty.* IEEE Transactions on Power Systems, 2016. **31**(4): p. 2507-2517. Available from: https://doi.org/10.1109/TPWRS.2015.2461014.

49. Rostami, M.A. and M. Raoofat, *Optimal operating strategy of virtual power plant considering plug-in hybrid electric vehicles load.* International Transactions on Electrical Energy Systems, 2016. **26**(2): p. 236-252. Available from: https://doi.org/10.1002/etep.2074.

50. Chen, Z., Y. Zhang, and T. Zhang. *An intelligent control approach to home energy management under forecast uncertainties*. in *2015 IEEE 5th International Conference on Power Engineering, Energy and Electrical Drives (POWERENG)*. 2015. Available from: https://doi.org/10.1109/PowerEng.2015.7266395.

51. Soares, J., et al., *A multi-objective model for the day-ahead energy resource scheduling of a smart grid with high penetration of sensitive loads.* Applied Energy, 2016. **162**: p. 1074-1088. Available from: http://dx.doi.org/10.1016/j.apenergy.2015.10.181.

52. Cipcigan, L.M., P. Taylor, and P.F. Lyons, *A dynamic virtual power station model comprising small-scale energy zones.* International Journal of Renewable Energy Technology (IJRET), 2009. **1**(2): p. 173-191. Available from: https://doi.org/10.1504/IJRET.2009.027989.

53. Sharma, I., C.A. Cañizares, and K. Bhattacharya. *Modeling and impacts of smart charging PEVs in residential distribution systems*. in *2012 IEEE Power and Energy Society General Meeting*. 2012. Available from: https://doi.org/10.1109/PESGM.2012.6345131.

54. Yi, J., *Investigation of energy storage system and demand side response for distribution networks*. 2016, Newcastle University. Available from: https://theses.ncl.ac.uk/dspace/bitstream/10443/3374/1/Yi%2C%20J.%202016.pdf, [Accessed

55. Xiong, P. and P. Jirutitijaroen, *Two-stage adjustable robust optimisation for unit commitment under uncertainty.* IET Generation, Transmission & Distribution, 2014. **8**(3): p. 573-582. Available from: https://doi.org/10.1049/iet-gtd.2012.0660.

56. Kim, S.J. and G.B. Giannakis, *Scalable and Robust Demand Response With Mixed-Integer Constraints.* IEEE Transactions on Smart Grid, 2013. **4**(4): p. 2089-2099. Available from: https://doi.org/10.1109/TSG.2013.2257893.

57. Doostizadeh, M., et al., *Energy and Reserve Scheduling Under Wind Power Uncertainty: An Adjustable Interval Approach.* IEEE Transactions on Smart Grid, 2016. **7**(6): p. 2943-2952. Available from: https://doi.org/10.1109/TSG.2016.2572639.

58. Peng, C., et al., *Flexible Robust Optimization Dispatch for Hybrid Wind/Photovoltaic/Hydro/Thermal Power System.* IEEE Transactions on Smart Grid, 2016. **7**(2): p. 751-762. Available from: https://doi.org/10.1109/TSG.2015.2471102.

59. Pirnia, M., et al., *A Novel Affine Arithmetic Method to Solve Optimal Power Flow Problems With Uncertainties.* IEEE Transactions on Power Systems, 2014. **29**(6): p. 2775-2783. Available from: https://doi.org/10.1109/TPWRS.2014.2316114.

60. Castillo, A., et al., *The Unit Commitment Problem With AC Optimal Power Flow Constraints.* IEEE Transactions on Power Systems, 2016. **31**(6): p. 4853-4866. Available from: https://doi.org/10.1109/TPWRS.2015.2511010.

61. Bracco, S., et al., *An Energy Management System for the Savona Campus Smart Polygeneration Microgrid.* IEEE Systems Journal, 2015. **PP**(99): p. 1-11. Available from: https://doi.org/10.1109/JSYST.2015.2419273.

62. Jiang, H., et al. *Robust optimization method for unit commitment with network losses considering wind uncertainties*. in *2012 IEEE Power and Energy Society General Meeting*. 2012. Available from: https://doi.org/10.1109/PESGM.2012.6345295.

63. *Road Use Statistics Great Britain 2016*. 2016, Department for Transport. Available from: https://www.gov.uk/government/uploads/system/uploads/attachment_data/file/514912/road-use-statistics.pdf, [Accessed 31/10/2018]

64. Nissan, *Leaf sales brochure*. 2017. Available from: https://www.nissanusa.com/content/dam/nissan/request-brochure/en/2017/pdf/2017-nissan-leaf-en.pdf, [Accessed 12/07/2017]

65. Mitsubishi, *Outlander PHEV sales brochure*. Available from: http://www.mitsubishi-cars.co.uk/enquiries/brochure/, [Accessed 12/07/2017]

66. Renault, *Zoe sales brochure*. 2017. Available from: https://www.cdn.renault.com/content/dam/Renault/UK/brand-and-editorial/Brochures/Vehicles/zoe-brochure.pdf, [Accessed 12/07/2017]

67. Neaimeh, M., et al., *Analysing the usage and evidencing the importance of fast chargers for the adoption of battery electric vehicles.* Energy

Policy, 2017. **108**: p. 474-486. Available from: http://dx.doi.org/10.1016/j.enpol.2017.06.033.

68. *Strategies for the uptake of electric vehicles and associated infrastructure implications*. 2009, Element Energy on behalf of the Committee on Climate Change. Available from: https://www.theccc.org.uk/archive/aws2/Element_Energy_-_EV_infrastructure_report_for_CCC_2009_final.pdf, [Accessed 31/10/2018]

69. Marmaras, C., E. Xydas, and L. Cipcigan, *Simulation of electric vehicle driver behaviour in road transport and electric power networks.* Transportation Research Part C: Emerging Technologies, 2017. **80**(Supplement C): p. 239-256. Available from: https://doi.org/10.1016/j.trc.2017.05.004.

70. Zenginis, I., et al., *Analysis and quality of service evaluation of a fast charging station for electric vehicles.* Energy, 2016. **112**: p. 669-678. Available from: http://dx.doi.org/10.1016/j.energy.2016.06.066.

71. Bailey, J. and J. Axsen, *Anticipating PEV buyers' acceptance of utility controlled charging.* Transportation Research Part A: Policy and Practice, 2015. **82**: p. 29-46. Available from: http://dx.doi.org/10.1016/j.tra.2015.09.004.

72. Uddin, K., M. Dubarry, and M.B. Glick, *The viability of vehicle-to-grid operations from a battery technology and policy perspective.* Energy Policy, 2018. **113**: p. 342-347. Available from: https://doi.org/10.1016/j.enpol.2017.11.015.

73. Uddin, K., et al., *On the possibility of extending the lifetime of lithium-ion batteries through optimal V2G facilitated by an integrated vehicle and smart-grid system.* Energy, 2017. **133**: p. 710-722. Available from: https://doi.org/10.1016/j.energy.2017.04.116.

74. Dubarry, M., A. Devie, and K. McKenzie, *Durability and reliability of electric vehicle batteries under electric utility grid operations: Bidirectional charging impact analysis.* Journal of Power Sources, 2017. **358**: p. 39-49. Available from: https://doi.org/10.1016/j.jpowsour.2017.05.015.

75. Godina, R., et al., *Smart electric vehicle charging scheduler for overloading prevention of an industry client power distribution transformer.* Applied Energy, 2016. **178**: p. 29-42. Available from: http://dx.doi.org/10.1016/j.apenergy.2016.06.019.

76. Patsios, C., et al., *An integrated approach for the analysis and control of grid connected energy storage systems.* Journal of Energy Storage, 2016. **5**: p. 48-61. Available from: http://dx.doi.org/10.1016/j.est.2015.11.011.

77. Lam, L. and P. Bauer, *Practical Capacity Fading Model for Li-Ion Battery Cells in Electric Vehicles.* IEEE Transactions on Power Electronics, 2013. **28**(12): p. 5910-5918. Available from: https://doi.org/10.1109/TPEL.2012.2235083.

78. Millner, A. *Modeling Lithium Ion battery degradation in electric vehicles*. in *2010 IEEE Conference on Innovative Technologies for an Efficient and Reliable Electricity Supply*. 2010. Available from: https://doi.org/10.1109/CITRES.2010.5619782.

79. Larsen, E., D.K. Chandrashekhara, and J. Ostergard. *Electric Vehicles for Improved Operation of Power Systems with High Wind Power Penetration*. in *2008 IEEE Energy 2030 Conference*. 2008. Available from: https://doi.org/10.1109/ENERGY.2008.4781053.

80. Lunz, B., et al., *Influence of plug-in hybrid electric vehicle charging strategies on charging and battery degradation costs.* Energy Policy, 2012. **46**: p. 511-519. Available from: http://dx.doi.org/10.1016/j.enpol.2012.04.017.

81. Kempton, W. and J. Tomić, *Vehicle-to-grid power fundamentals: Calculating capacity and net revenue.* Journal of Power Sources, 2005. **144**(1): p. 268-279. Available from: http://dx.doi.org/10.1016/j.jpowsour.2004.12.025.

82. Mu, Y., et al., *A Spatial–Temporal model for grid impact analysis of plug-in electric vehicles.* Applied Energy, 2014. **114**: p. 456-465. Available from: http://dx.doi.org/10.1016/j.apenergy.2013.10.006.

83. Pudjianto, D., et al., *Smart control for minimizing distribution network reinforcement cost due to electrification.* Energy Policy, 2013. **52**: p. 76-84. Available from: http://dx.doi.org/10.1016/j.enpol.2012.05.021.

84. Salah, F., et al., *Impact of electric vehicles on distribution substations: A Swiss case study.* Applied Energy, 2015. **137**: p. 88-96. Available from: http://dx.doi.org/10.1016/j.apenergy.2014.09.091.

85. Maitra, A., et al. *Integrating plug-in- electric vehicles with the distribution system*. in *CIRED 2009 - 20th International Conference and Exhibition on Electricity Distribution - Part 1*. 2009. Available from: https://doi.org/10.1049/cp.2009.1127.

86. Putrus, G.A., et al. *Impact of electric vehicles on power distribution networks*. in *2009 IEEE Vehicle Power and Propulsion Conference*. 2009. Available from: https://doi.org/10.1109/VPPC.2009.5289760.

87. Clement-Nyns, K., E. Haesen, and J. Driesen, *The Impact of Charging Plug-In Hybrid Electric Vehicles on a Residential Distribution Grid.* IEEE Transactions on Power Systems, 2010. **25**(1): p. 371-380. Available from: https://doi.org/10.1109/TPWRS.2009.2036481.

88. Lopes, J.A.P., F.J. Soares, and P.M.R. Almeida, *Integration of Electric Vehicles in the Electric Power System.* Proceedings of the IEEE, 2011. **99**(1): p. 168-183. Available from: https://doi.org/10.1109/JPROC.2010.2066250.

89. Sortomme, E., et al., *Coordinated Charging of Plug-In Hybrid Electric Vehicles to Minimize Distribution System Losses.* IEEE Transactions on Smart Grid, 2011. **2**(1): p. 198-205. Available from: https://doi.org/10.1109/TSG.2010.2090913.

90. Richardson, P., D. Flynn, and A. Keane, *Optimal Charging of Electric Vehicles in Low-Voltage Distribution Systems.* IEEE Transactions on Power Systems, 2012. **27**(1): p. 268-279. Available from: https://doi.org/10.1109/TPWRS.2011.2158247.

91. Masoum, M.A.S., P.S. Moses, and S. Hajforoosh. *Distribution transformer stress in smart grid with coordinated charging of Plug-In Electric Vehicles*. in *2012 IEEE PES Innovative Smart Grid Technologies (ISGT)*. 2012. Available from: https://doi.org/10.1109/ISGT.2012.6175685.

92. Papadopoulos, P., et al., *Electric vehicles' impact on british distribution networks.* IET Electrical Systems in Transportation, 2012. **2**(3): p. 91-102. Available from: https://doi.org/10.1049/iet-est.2011.0023.

93. Hoog, J.d., et al., *Optimal Charging of Electric Vehicles Taking Distribution Network Constraints Into Account.* IEEE Transactions on Power Systems, 2015. **30**(1): p. 365-375. Available from: https://doi.org/10.1109/TPWRS.2014.2318293.

94. Al Essa, M. and L. Cipcigan, *Reallocating Charging Loads of Electric Vehicles in Distribution Networks.* Applied Sciences, 2016. **6**(2): p. 53. Available from: https://doi.org/10.3390/app6020053.

95. Papadopoulos, P., et al., *Coordination of the Charging of Electric Vehicles Using a Multi-Agent System.* IEEE Transactions on Smart Grid, 2013. **4**(4): p. 1802-1809. Available from: https://doi.org/10.1109/TSG.2013.2274391.

96. Grau Unda, I., et al., *Management of electric vehicle battery charging in distribution networks with multi-agent systems.* Electric Power Systems Research, 2014. **110**(Supplement C): p. 172-179. Available from: https://doi.org/10.1016/j.epsr.2014.01.014.

97. Xydas, E., C. Marmaras, and L.M. Cipcigan, *A multi-agent based scheduling algorithm for adaptive electric vehicles charging.* Applied Energy, 2016. **177**(Supplement C): p. 354-365. Available from: https://doi.org/10.1016/j.apenergy.2016.05.034.

98. Beaude, O., et al., *Reducing the Impact of EV Charging Operations on the Distribution Network.* IEEE Transactions on Smart Grid, 2016. **7**(6): p. 2666-2679. Available from: https://doi.org/10.1109/TSG.2015.2489564.

99. Xydas, E., et al., *A data-driven approach for characterising the charging demand of electric vehicles: A UK case study.* Applied Energy, 2016. **162**: p. 763-771. Available from: http://dx.doi.org/10.1016/j.apenergy.2015.10.151.

100. Ramos Muñoz, E., et al., *Electric vehicle charging algorithms for coordination of the grid and distribution transformer levels.* Energy, 2016. **113**: p. 930-942. Available from: http://dx.doi.org/10.1016/j.energy.2016.07.122.

101. Vayá, M.G. and G. Andersson. *Centralized and decentralized approaches to smart charging of plug-in Vehicles*. in *2012 IEEE Power and Energy Society General Meeting*. 2012. Available from: https://doi.org/10.1109/PESGM.2012.6344902.

102. López, M.A., et al., *V2G strategies for congestion management in microgrids with high penetration of electric vehicles.* Electric Power Systems Research, 2013. **104**: p. 28-34. Available from: http://dx.doi.org/10.1016/j.epsr.2013.06.005.

103. Tang, D. and P. Wang, *Nodal Impact Assessment and Alleviation of Moving Electric Vehicle Loads: From Traffic Flow to Power Flow.* IEEE Transactions on Power Systems, 2016. **31**(6): p. 4231-4242. Available from: https://doi.org/10.1109/TPWRS.2015.2495254.

104. Heydarian-Forushani, E., M.E.H. Golshan, and M. Shafie-khah, *Flexible interaction of plug-in electric vehicle parking lots for efficient wind integration.* Applied Energy, 2016. **179**: p. 338-349. Available from: http://dx.doi.org/10.1016/j.apenergy.2016.06.145.

105. Shafie-khah, M., et al., *Optimal Behavior of Electric Vehicle Parking Lots as Demand Response Aggregation Agents.* IEEE Transactions on Smart Grid, 2016. **7**(6): p. 2654-2665. Available from: https://doi.org/10.1109/TSG.2015.2496796.

106. Guo, Y., et al., *Two-Stage Economic Operation of Microgrid-Like Electric Vehicle Parking Deck.* IEEE Transactions on Smart Grid, 2016. **7**(3): p. 1703-1712. Available from: https://doi.org/10.1109/TSG.2015.2424912.

107. Ma, T. and O.A. Mohammed, *Optimal Charging of Plug-in Electric Vehicles for a Car-Park Infrastructure.* IEEE Transactions on Industry Applications, 2014. **50**(4): p. 2323-2330. Available from: https://doi.org/10.1109/TIA.2013.2296620.

108. You, P., et al., *Optimal Cooperative Charging Strategy for a Smart Charging Station of Electric Vehicles.* IEEE Transactions on Power Systems, 2016. **31**(4): p. 2946-2956. Available from: https://doi.org/10.1109/TPWRS.2015.2477372.

109. Yazdani-Damavandi, M., et al., *Modeling Operational Behavior of Plug-in Electric Vehicles' Parking Lot in Multienergy Systems.* IEEE Transactions on Smart Grid, 2016. **7**(1): p. 124-135. Available from: https://doi.org/10.1109/TSG.2015.2404892.

110. Lamedica, R., et al., *An energy management software for smart buildings with V2G and BESS.* Sustainable Cities and Society, 2015. **19**: p. 173-183. Available from: http://dx.doi.org/10.1016/j.scs.2015.08.003.

111. Kazemi, M.A., et al., *Optimal siting and sizing of distribution system operator owned EV parking lots.* Applied Energy, 2016. **179**: p. 1176-1184. Available from: http://dx.doi.org/10.1016/j.apenergy.2016.06.125.

112. Quirós-Tortós, J., et al., *Control of EV Charging Points for Thermal and Voltage Management of LV Networks.* IEEE Transactions on Power Systems, 2016. **31**(4): p. 3028-3039. Available from: https://doi.org/10.1109/TPWRS.2015.2468062.

113. *Electric Nation: Customer Information Pack*. Western Power Distribution. Available from: http://www.electricnation.org.uk/wp-content/uploads/2016/09/Electric-Nation-Customer-Information-Brochure.pdf, [Accessed 31/10/2018]

114. *Installation of the UK's first domestic vehicle-to-grid unit for energy storage*. 2017; Available from: https://www.cardiff.ac.uk/news/view/757939-installation-of-the-uks-first-domestic-vehicle-to-grid-unit-for-energy-storage, [Accessed 31/10/2018]

115. *Insight Report: Small and Medium Enterprises (SMEs)*. 2015, Customer-Led Network Revolution. Available from: http://www.networkrevolution.co.uk/project-library/insight-report-insight-report-small-medium-enterprises-smes/, [Accessed 31/10/2018]

116. Ingram, S., S. Probert, and K. Jackson, *The impact of small scale embedded generation on operating parameters of distribution networks*. 2003, PB Power on behalf of the Department for Trade and Industry. Available from: http://webarchive.nationalarchives.gov.uk/20100919181945/http://www.ensg.gov.uk/index.php?article=99, [Accessed 31/10/2018]

117. *PSCAD/EMTDC product website*. Available from: https://hvdc.ca/, [Accessed 31/10/2018]

118. *Users guide: EMTDC transient analysis for PSCAD power system simulation*. 2005, Manitoba HVDC research centre. Available from: https://hvdc.ca/uploads/ck/files/reference_material/EMTDC_User_Guide_v4_3_1.pdf, [Accessed 31/10/2018]

119. Dommel, H.W., *Digital Computer Solution of Electromagnetic Transients in Single-and Multiphase Networks.* IEEE Transactions on Power Apparatus and Systems, 1969. **PAS-88**(4): p. 388-399. Available from: https://doi.org/10.1109/TPAS.1969.292459.

120. *Engineering Recommendation P29: Planning limits for voltage unbalance in the United Kingdom*. 1990, The electricity council. Available from: http://www.nienetworks.co.uk/documents/Security-planning/ER-P29.aspx, [Accessed 31/10/2018]

121. Blythe, P.T., et al., *The north east of England electric vehicle and infrastructure trials*, in *Electric Vehicle Symposium (EVS26)*. 2012: Los Angeles, USA. Available from: http://eprint.ncl.ac.uk/file_store/production/189252/A3619F09-9594-48EC-80FB-A8972135AD9E.pdf, [Accessed

122. Neaimeh, M., et al., *Routing systems to extend the driving range of electric vehicles.* IET Intelligent Transport Systems, 2013. **7**(3): p. 327-336. Available from: https://doi.org/10.1049/iet-its.2013.0122.

123. *National statistics postcode products*. Available from: http://www.ons.gov.uk/ons/guide-method/geography/products/postcode-directories/-nspp-/index.html, [Accessed 31/10/2018]

124. *The Transform Model*. EA Technology. Available from: https://www.eatechnology.com/wp-content/uploads/2017/04/The-Transform-Model-Brochure.pdf, [Accessed 31/10/2018]

125. *Assessing the Impact of Low Carbon Technologies on Great Britain's Power Distribution Networks*. 2012, EA Technology. Available from: https://www.ofgem.gov.uk/sites/default/files/docs/2012/08/ws3-ph2-report.pdf, [Accessed 31/10/2018]

126. Quirós-Tortós, J., *Work Activity 5 "ESPRIT-Enabled Deterministic Impact Studies" - Report for Deliverables 5.1 and 5.2*. 2015, The University Of Manchester. Available from: https://www.researchgate.net/publication/283462005_Work_Activity_5_Esprit-Enabled_Deterministic_Impact_Studies, [Accessed 31/10/2018]

127. *RIIO-ED1: Final determinations for the slow-track electricity distribution companies*. 2014, Ofgem. Available from: https://www.ofgem.gov.uk/sites/default/files/docs/2014/11/riio-ed1_final_determination_expenditure_assessment_0.pdf, [Accessed 31/10/2018]

128. Blythe, P.T., et al., *Rapid Charge Network Activity 6 Study Report*. 2015. Available from: http://rapidchargenetwork.com/public/wax_resources/RCN%20Project%20Study%20Report%20Digital.pdf, [Accessed 31/10/2018]

129. Jenkins, A.M., *Creating virtual energy storage systems from aggregated smart charging electric vehicles*. 2017, IET TV: Glasgow. Available from: https://tv.theiet.org/?videoid=10399, [Accessed 31/10/2018]

130. Jenkins, A.M., et al., *Creating virtual energy storage systems from aggregated smart charging electric vehicles.* CIRED - Open Access Proceedings Journal, 2017. **2017**: p. 1664-1668. Available from: http://digital-library.theiet.org/content/journals/10.1049/oap-cired.2017.0937.

131. Jenkins, A.M., et al. *Optimising virtual power plant response to grid service requests at Newcastle Science Central by coordinating multiple flexible assets*. in *CIRED Workshop 2016*. 2016. Available from: https://doi.org/10.1049/cp.2016.0812.

132. Mosteller, F. and C. Youtz, *Quantifying Probabilistic Expressions.* Statistical Science, 1990. **5**(1): p. 2-12. Available from: http://www.jstor.org/stable/2245869.

133. *National Grid website*. Available from: www.nationalgrid.com, [Accessed 02/09/2015]

134. *Newcastle Science Central website*. Available from: www.newcastlesciencecentral.com, [Accessed 31/10/2018]

135. *Newcastle University: Energy storage test bed is officially switched-on*. 2015; Available from: http://www.ncl.ac.uk/sustainability/news/archivednews/energystoragetestbedisofficiallyswitched-on.html, [Accessed 31/10/2018]

136. Motegi, N., et al., *Introduction to Commercial Building Control Strategies and Techniques for Demand Response*. 2007, Demand Response Research Centre. Available from: http://gaia.lbl.gov/btech/papers/59975.pdf, [Accessed 31/10/2018]

137. Lee, C.C., *Fuzzy logic in control systems: fuzzy logic controller. I.* IEEE Transactions on Systems, Man, and Cybernetics, 1990. **20**(2): p. 404-418. Available from: https://doi.org/10.1109/21.52551.

138. *IPSA Power Software*. Available from: https://www.ipsa-power.com/, [Accessed 31/10/2018]

139. Grigsby, L.L., *Electric power engineering handbook*. 2007, Florida: Taylor & Francis Group.

140. *Generation availability map*. Available from: http://www.northernpowergrid.com/generation-availability-map, [Accessed 01/08/2016]

141. *Insulated Power Cables*. Universal Cable. Available from: http://www.ucable.com.my/images/products/UC%20XLPE%20Catalogue.pdf, [Accessed 31/10/2018]

142. Lanz, B., D. Byrne, and M. Spalding. *Affordable Cable System Reliability and Life Extension Strategy*. in *2016 IEEE Rural Electric Power Conference (REPC)*. 2016. Available from: https://doi.org/10.1109/REPC.2016.16.

143. Liu, R. and S. Boggs, *Cable life and the cost of risk.* IEEE Electrical Insulation Magazine, 2009. **25**(2): p. 13-19. Available from: https://doi.org/10.1109/MEI.2009.4802594.

144. Brandon, N.P., et al., *UK Research needs in grid scale energy storage technologies*. Available from: http://energysuperstore.org/wp-content/uploads/2016/04/IMPJ4129_White_Paper_UK-Research-Needs-in-Grid-Scale-Energy-Storage-Technologies_WEB.pdf, [Accessed 31/10/2018]

145. Alotto, P., M. Guarnieri, and F. Moro, *Redox flow batteries for the storage of renewable energy: A review.* Renewable and Sustainable Energy Reviews, 2014. **29**(Supplement C): p. 325-335. Available from: https://doi.org/10.1016/j.rser.2013.08.001.

146. Bocklisch, T., *Hybrid energy storage approach for renewable energy applications.* Journal of Energy Storage, 2016. **8**(Supplement C): p. 311-319. Available from: https://doi.org/10.1016/j.est.2016.01.004.

147. Jacobson, M.Z., *Fundamentals of atmospheric modeling*. 2 ed. 2005, Cambridge: Cambridge University Press.

148. *UK power spot prices 2016-17*. Available from: www.apxgroup.com/market-results/apx-power-uk/dashboard, [Accessed 21/06/2017]

149. *Linprog linear programming solver* Available from: https://docs.scipy.org/doc/scipy/reference/optimize.linprog-simplex.html, [Accessed 31/10/2018]

150. Dimitris, B. and S. Melvyn, *The Price of Robustness.* Operations Research, 2004. **52**(1): p. 35-53. Available from: https://doi.org/10.1287/opre.1030.0065.

151. *Life expectancy of cables*. 2009; Available from: http://www.basec.org.uk/News/BasecNews/LifeExpectancyofCables, [Accessed 06/04/2017]

152. Allan, A., G. Strbac, and P. Djapic, *Developing the P2/6 Methodology*. 2004, UMIST on behalf of the Department for Trade and Industry. Available from: http://webarchive.nationalarchives.gov.uk/20100919182336/http://www.ensg.gov.uk/assets/methodology.pdf, [Accessed 31/10/2018]

153. *Our Guaranteed Standards of Service*. Northern Power Grid. Available from: https://www.northernpowergrid.com/asset/1/document/1966.pdf, [Accessed 31/10/2018]

154. *Energy consumption in the UK*. 2017, Department for Business, Energy & Industrial Strategy. Available from: https://www.gov.uk/government/uploads/system/uploads/attachment_data/file/633503/ECUK_2017.pdf, [Accessed 31/10/2018]

155. Strbac, G., et al., *Engineering Recommendation P2 Review Workstream 2.7: Alignment of Security of Supply Standard in Distribution Networks with Other Codes and Schemes*. 2015, NERA Economic Consulting, Imperical College & DNV-GL. Available from: http://www.dcode.org.uk/assets/uploads/WS_2.7__Final_Report_clean.pdf, [Accessed 31/10/2018]